Unraveling resistance mechanisms of ESKAPE pathogens with novel natural products and approaches:

Armeniaspirols, Cystobactamids and Myrtucommulones

Dissertation

zur Erlangung des Grades

des Doktors der Naturwissenschaften

der Naturwissenschaftlich-Technischen Fakultät

der Universität des Saarlandes

von

Janetta Magrieta Coetzee

Saarbrücken

2023

Tag des Kolloquiums: 3. April 2024

Prodekan: Prof. Dr. -Ing. Micheal Vielhaber

Berichterstatter: Prof. Dr. Rolf Müller

Prof. Dr. Alexandra K. Kiemer

Vorsitz: Prof. Dr. Uli Kazmaier

Akad. Mitarbeiter: Dr. Maria Lopatniuk

Die vorliegende Arbeit wurde von Juni 2019 bis Mai 2023 unter Anleitung von Herrn Prof. Dr. Rolf Müller an Helmholtz-Institut für Pharmazeutische Forschung Saarland (HIPS) angefertigt.

Acknowledgements

I thank Prof. Dr. Rolf Müller for providing me with this opportunity – this experience changed my life forever. Further, I thank the rest of my committee: Prof. Dr. Alexandra Kiemer and special big thanks to Dr. Jennifer Herrmann for mentorship and opportunities.

I would also like to thank all the collaborators I had the privilege to work with including Evotec and different groups within Saarland University.

I thank Dr. Katarina Cirnski for initially leading and introducing me to the laboratory space and work. I thank Timo Risch, Felix Descher, and Dr. Sari Rasheed for insight, assistance, and enthusiasm in our shared projects. I thank all members of the Helmholtz-Institute for Pharmaceutical Research Saarland (HIPS), especially the Microbial Natural Products (MINS) group for insightful discussions and support.

A big gracious thanks to Dr. Asfandyar Sikandar for taking time to read and correct my thesis and Anastasia Andreas and Dr. Yu-Mi Park for the help in submission process. A special, additional mention to Dr. Asfandyar Sikandar, Dr. Yu-Mi Park, Anastasia Andreas, Jeenu Joy, Dr. Jiaqi Liu and Dr. Sumire Kurasawa for their support and friendship.

I thank my mother, Jeanette Coetzee, for her unwavering emotional support, broad shoulder, and consistent belief in my abilities.

Lastly, a big thanks to my loving partner, Dr. Marcus Baulig, for his love, attention, support, and most importantly his enthusiasm to remember “MIC”, “ciprofloxacin”, and “armeniaspirols”.

Abstract

Antimicrobial resistance poses a serious threat to public health, causing numerous deaths annually. Natural products offer potential for new antimicrobial therapies amidst bacterial resistance. This thesis explores resistance mechanisms of ESKAPE pathogens to three natural products using diverse methods including culture-, molecular-, biochemical-, and bio-informatic-based techniques. Armeniaspirols from *Streptomyces armeniacus* induce membrane depolarization in bacteria. Gram-negative *Escherichia coli* Δ*tolC* exhibits efflux-mediated resistance via mutations up-regulating the ArcAB-TolC homolog efflux pump genes, *mdtNOP*. Cystobactamids, topoisomerase inhibitors, reveal high-level resistance in carbapenem-resistant *Acinetobacter baumannii* due to target mutations and efflux mechanisms. Myrtucommulones-resistant *Staphylococcus aureus* mutants show cross-resistance to vancomycin, daptomycin, and ß-lactams due to response regulator deletions, leading to a VISA-like phenotype. Understanding these mechanisms is vital for developing antimicrobial therapies to combat bacterial resistance. The study's methods and findings offer insights for future drug optimization.

Zusammenfassung

Antimikrobielle Resistenz stellt eine ernsthafte Bedrohung für die öffentliche Gesundheit dar und verursacht jährlich zahlreiche Todesfälle. Naturprodukte bieten ein Potenzial für neue antimikrobielle Therapien angesichts der bakteriellen Resistenz. Diese Dissertation untersucht die Resistenzmechanismen von ESKAPE-Pathogenen gegenüber drei Naturprodukten mithilfe verschiedener Methoden, darunter kultur-, molekular-, biochemisch- und bioinformatisch-basierte Techniken. Armeniaspirole aus *Streptomyces armeniacus* induzieren eine Membrandepolarisation bei Bakterien. Gram-negative *Escherichia coli* Δ*tolC* zeigt effluxvermittelte Resistenz durch Mutationen, die die ArcAB-TolC-Homologe Effluxpumpengene, *mdtNOP*, hochregulieren. Cystobactamide, Topoisomerase-Inhibitoren, zeigen eine hohe Resistenz bei carbapenemresistenten *Acinetobacter baumannii* aufgrund von Zielmutationen und Effluxmechanismen. Myrtucommulone-resistente *Staphylococcus aureus*-Mutanten weisen Kreuzresistenz gegen Vancomycin, Daptomycin und ß-Laktame aufgrund von Deletionen des Antwortregulators auf, was zu einem VISA-ähnlichen Phänotyp führt. Das Verständnis dieser Mechanismen ist entscheidend für die Entwicklung antimikrobieller Therapien zur Bekämpfung bakterieller Resistenz. Die Methoden und Ergebnisse der Studie bieten Einblicke für die zukünftige Optimierung von Medikamenten.

Vorveröffentlichungen der Dissertation

Teile dieser Arbeit wurden vorab mit Genehmigung der Naturwissenschaftlich-Technischen Fakultät III, vertreten durch den Mentor der Arbeit, in folgenden Beiträgen veröffentlicht oder sind derzeit in Vorbereitung zur Veröffentlichung:

Publications

Cirnski, K., Coetzee, J., Herrmann, J., & Müller, R. (2020). Metabolic Profiling to Determine Bactericidal or Bacteriostatic Effects of New Natural Products using Isothermal Microcalorimetry. *Journal of visualized experiments : JoVE*, (164), 10.3791/61703. https://doi.org/10.3791/61703

Zscherp, R., Coetzee, J., Vornweg, J., Grunenberg, J., Herrmann, J., Müller, R., & Klahn, P. (2021). Biomimetic enterobactin analogue mediates iron-uptake and cargo transport into *E. coli* and *P. aeruginosa*. *Chemical science*, *12*(30), 10179–10190. https://doi.org/10.1039/d1sc02084f

Arisetti, N., Fuchs, H. L. S., Coetzee, J., Orozco, M., Ruppelt, D., Bauer, A., Heimann, D., Kuhnert, E., Bhamidimarri, S. P., Bafna, J. A., Hinkelmann, B., Eckel, K., Sieber, S. A., Müller, P. P., Herrmann, J., Müller, R., Winterhalter, M., Steinem, C., & Brönstrup, M. (2021). Total synthesis and mechanism of action of the antibiotic armeniaspirol A. *Chemical science*, *12*(48), 16023–16034. https://doi.org/10.1039/d1sc04290d

Seyfert, C. E., Porten, C., Yuan, B., Deckarm, S., Panter, F., Bader, C. D., Coetzee, J., Deschner, F., Tehrani, K. H. M. E., Higgins, P. G., Seifert, H., Marlovits, T. C., Herrmann, J., & Müller, R. (2023). Darobactins Exhibiting Superior Antibiotic Activity by Cryo-EM Structure Guided Biosynthetic Engineering. *Angewandte Chemie (International ed. in English)*, *62*(2), e202214094. https://doi.org/10.1002/anie.202214094

Contents

List of Figures

Figure S4.2: Percentage (%) cell lysis observed with the addition of myrtucommulone A (**1)** and myrtucommulone F (**2**) with *S. aureus* Newman in TritonX-100 after 24 hours.

Figure S4.3: Scanning electron microscope (SEM) imaging of wild-type *S. aureus* Newman a) in the presence of sub-MIC concentrations of myrtucommulone A (**1)** and myrtucommulone F (**2**) (1 µg/ml for 1; and 0.5 µg/ml for 2) for 4 hours (b and c). Mag: 64.00 K X, EHT: 5.00 kV, WD: 3.3 mm. Scale bar: 100nm.

Figure S4.4: Transmission electron microscope (TEM) imaging of wild-type *S. aureus* Newman a) in the presence of sub-MIC concentrations of myrtucommulone A (**1)** and myrtucommulone F (**2**) (1 µg/ml for 1; and 0.5 µg/ml for 2) for 4 hours (b and c). Scale bar: 500nm (a-d) and 200nm (e-h).

Figure S4.5: Lysine biosynthesis KEGG pathway. Genes highlighted in green were found to be significantly down-regulated in all assessed Myr^R.

List of Tables

Abbreviations

ADP - Adenosine diphosphate

Arm^R - Armeniaspirol-Resistant *E. coli* ΔtolC

ATCC - American Type Culture Collection

ATP - Adenosine triphosphate

CASO – Casein-Soja-Pepton-Agar

CCCP - Carbonyl cyanide m-chlorophenyl hydrazone

CHO-K1 - Chinese hamster ovary cell line

CO_2 - Carbon dioxide

CRAB - Carbapenem-Resistant *Acinetobacter baumanniii*

CTA - Clinical Trial Application

Cys^R - Cystobactamid-Resistant *Acinetobacter baumanniii*

$DIOC_{2(3)}$ - 3,3-dipropylthiacarbocyanine

DNA - Deoxyribonucleic acid

DOC - Deoxycholate

DSMZ - Deutsche Sammlung für Mikroorganismen und Zellkulturen

EMA - European Medicines Agency

EtBr – Ethidium bromide

EU – European Union

FBS - Fetal bovine serum

FDA - Food and Drug Administration

FoR - Frequency of Resistance

HCl - Hydrocloric acid

HPLC-MS - High Performance Liquid Chromatography

HZI - Helmholtz-Zentrum für Infektionsforschung

IC_{50} - Half maximal inhibitory concentration

in vacuo - In vacuum

IND - Investigational New Drug

KEGG - Kyoto Encyclopedia of Genes and Genomes

LPS - Lipopolysaccharide

MALDI-TOF - Matrix-assisted laser desorption/ionization - Time-of-flight analyzer

MATE - Multidrug and toxic compound extrusion

MBC - Minimum bactericidal concentrations

MDR - Multidrug resistant

MFP - Membrane fusion protein

MFS - Major facilitator

MHA - Mueller Hinton Agar

MHBII - Mueller Hinton Broth cation adjusted

MHH - Medizinische Hochschule Hannover

MIC - Minimum Inhibition Concentration

MoR - Mode of Resistance

MPC - Mutation Prevention Concentration

MRSA - Multidrug Resistant *Staphylococcus aureus*

MS – Mass Spectrometry

MSBL - Mass spectrometric β-lactamase

MTT reagent - Thiazolyl blue tetrazolium bromide

Myr^R - Myrtucommulone-Resistant *Staphylococcus aureus*

n.d - Not determined

NBTI - Novel Bacterial Topoisomerase Inhibitors

OD_{600} - Optical density at 600 nm

OMP - Outer membrane protein

*p*ABA - *p*-amino benzoic acid

PACE - Proteobacterial antimicrobial compound efflux

PAßN - Phenylalanine-arginine beta-naphthylamide

PBS - Phosphate buffer solution

PKS/NRPS - Polyketide synthase/non-ribosomal peptide synthetase

PMBN - Polymyxin B nonapeptide

RNA - Ribonucleic acid

RND - Resistance-nodulation-division

SI - Selectivity Index

SMR - Small multidrug resistance

TOF - Time-of-flight

VISA - Vancomycin Intermediate *Staphylococcus aureus*

VRE - Vancomycin Resistant *Enterococci*

Chapter 1: Introduction

1.1. Antibiotics from nature

1.1.1. General Introduction

Unarguably, the introduction of antibiotics for clinical application was a huge breakthrough in the 20th century. Predating this event, different traditional medicines were used across the world in various forms for treatment of societal diseases. Before the development of salvarsan and other anti-infective agents, civilizations made use of nature to treat infections and other diseases (Bennett, 2007). Hence, a common theory developed throughout the world, today called the Doctrine of Signatures. It broadly explains how humans were led to discover the curative nature of plants and food by the physical features resembling the curative value they possess (Bennett, 2007). Even though the theory is not supported by today's knowledge, experimentation with herbal medicines arose from it. The investigation of some examples revealed feasible scientific reasoning that explains why the treatments were successful. For example, *Euphrasia officinalis* L. (eyebright) which was used for the treatment of conjunctivitis solely based on the resemblances to a blood-shot eye (Paduch *et al*., 2014). Today we know that the treatment was successful due to an active compound in *Euphrasia officinalis L*., called aucubin. Aucubin is a natural product that demonstrates anti-inflammatory properties such as tannins and flavonoids (Carlson, 2013; Paduch *et al*., 2014) (Figure 1.1).

a)  b) 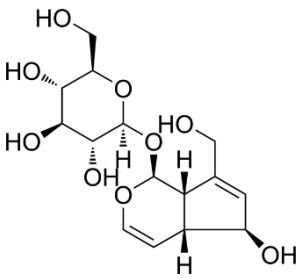

Figure 1.1: a) Visual image of a flower of *Euphrasia officinalis L*. b) Chemical structure of aucubin.

Another example includes a remedy for eye sties described in a 10th century Bald's leechbook (Hutchings *et al*., 2019). The remedy description in Bald's leechbook consisted of the mixture of garlic, wine, and bovine bile that was left in a brass or bronze vessel for several nights before application (Cockayne, 1866). Today, we know that an eye sty is most often caused by a Gram-positive bacteria, such as *Staphylococcus* species. We also know that *Allium* species contains

active antimicrobial compounds used for treatment of *Staphylococcus* infections (Lanzotti V and Bonanomi G, 2013; Hofmann and Eckmann, 2006). Further, bile also has antimicrobial activity and finally, copper prevents bacterial growth and was most probably allowed to seep into the mixture from the copper bowl. The ingredients used were all antimicrobial thus allowing the treatment to be successful (Lanzotti V and Bonanomi G, 2013; Hofmann and Eckmann, 2006).

Besides copper, the antimicrobial nature of the above-mentioned examples are due to secondary metabolites. Secondary metabolites are produced by many organisms including plants, fungi, insects, and bacteria (Ruiz *et al*., 2010). These metabolites are not essential for growth and the class consists of antimicrobial compounds, antitumor agents, pigments, growth hormones, and others (Ruiz *et al*., 2010). Secondary metabolites can function as competitive weapons used against other organisms, metal transporting agents, agents of symbiosis, hormones, differentiation effectors, spore formation agents, and compounds that inhibit or stimulate germination (Demain and Fang, 2000; Ruiz *et al*., 2010). Further, microbial secondary metabolites often have unique structures, and are usually formed during the late growth phase of the producing microorganisms (Ruiz *et al*., 2010). Most antibiotics in current use in the medical and agricultural field are derived from secondary metabolites produced by a group of soil-dwelling bacteria called the actinomycetes (Walsh and Wright, 2005; Aminov, 2010). To produce antimicrobial secondary metabolites, the producing organism needs to be resistant to the secondary metabolite, otherwise it would die due to the production (D'Costa *et al*. 2006). To understand resistance to secondary metabolites, it is important to consider resistance genes, which include self-resistance genes in soil bacteria and genes encoding intrinsic resistance mechanisms present in all or most non-producer environmental bacteria (Peterson and Kaur, 2018). Interestingly, producing organisms such as actinomycetes, *Streptomyces* species, *Bacillus* species, contain multiple mechanisms to ensure complete protection (Brown *et al*., 2017).

With the discovery of penicillin in 1928 and introduction for clinical use in 1940's, resistant strains capable of inactivating penicillin became prevalent and widespread (Fernandes *et al*., 2013). Thus, the general assumption was that bacterial resistance mechanisms developed with the introduction of antibiotics for therapeutic use. However, bacterial penicillinase was identified before the widespread clinical use of penicillin and as exemplified above, resistance mechanisms existed and developed a long time before the introduction of antibiotics into the modern-day society (Davies and Davies, 2010). Other examples of resistance dating back to the pre-antibiotic period include bacteria isolated from permafrost, the gut microbiome of a pre-Columbian Andean mummy from Peru and oral microbiome of four adult human skeletons from a medieval monastery (D'costa *et al*., 2011; Kashuba *et al*., 2017; Santiago-Rodriguez *et al*.,

2015; Warinner *et al*., 2014). All mentioned examples contain bacterial strains with a large number of resistance genes and provides evidence that a large number of antibiotic resistance genes and mechanisms are components of natural microbial populations, and that antibiotic resistance has an ancient origin. Taken aside that antibiotic resistance has ancient origin, an increase of resistance frequency within our society can be linked with the clinical use of antibiotics (Hutchings *et al.*, 2019).

1.1.2. Discovery of Antimicrobial Compounds for Clinical Use

As mentioned previously, nature played a major role in the development of anti-infective agents in the 20th century and even before the start of the antibiotic pipeline, natural healers and alchemists used traditional medicine to treat infections with plants, soil, and other equipment (Harrison *et al.*, 2015; Hutchings *et al.*, 2019). After the discovery of the first synthetic antibiotic in 1910 and the discovery of penicillin, more antibiotics were discovered from actinomycetes, other bacterial species, fungal species and synthetic designed from the chemical scaffolds seen in nature (Figure 1.2). In 1940s, eight antibiotic classes were introduced for clinical use alongside the resistant development of penicillin. In 1950-1960, 20 classes were identified and marketed for use, many of which stemmed from natural products and are still use today (Hutchings *et al.*, 2019). The 1950-1960's are described as the golden era for antibiotic discovery, as preceding this period only nine novel classes were introduced for clinical use.

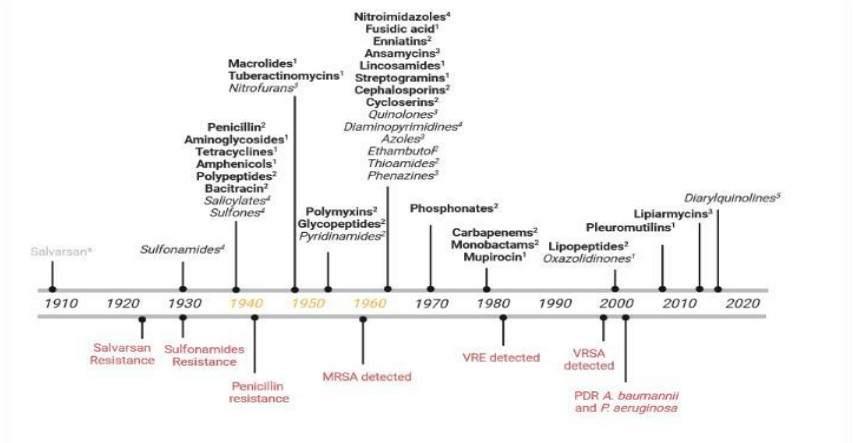

Figure 1.2: Timeline of the introduction of antibiotics classes for clinical use (black) and of resistance identification (red). The golden age of antibiotics (yellow text), Natural products (bold), synthetic compounds (italic), and compounds not in clinical use anymore (grey). The numbers refer to well-described targets of antibiotic classes: [1]Protein synthesis; [2]Cell wall / cell membrane synthesis or disruption; [3]DNA (Deoxyribonucleic acid) / RNA (Ribonucleic acid) synthesis and replication; [4]Folic acid synthesis; [5]ATP synthesis (adapted from Hutchings *et al.*, 2019).

Natural product–based drug discovery continues to be one of the most reliable sources of novel antimicrobial compounds. It has been driven by the investigation of producer micro-organisms, such as *Streptomyces* species (van Santen *et al.*, 2022). Investigation of these micro-organisms and advances in expression in heterologous hosts, purification, identification, and screening methodologies expands the chemistry available for the antibacterial discovery pipeline (Walesch *et al*., 2023). The work of Selman Waksman, Albert Schatz and Elizabeth Bugie on soil-dwelling actinomycetales and their potential to produce antibiotic natural products was the start of the so-called “golden age of antibiotics” (Figure 1.2) (Chopra *et al*., 2002; Waksman *et al.*, 2010).

Following the golden era of discovery, a decline of the discovery rate is seen thus leading to the mainstream approach for the development of new drugs to combat emerging and re-emerging resistance of pathogens as semi-synthetic compounds with improved activity, less sensitivity toward resistance mechanisms, and lower levels of cell toxicity (Chopra *et al*., 2002). Challenges behind natural products chemistry include low reactivity in aromatic amine couplings and solubility problems (Testolin *et al.*, 2020). Despite chemistry difficulties, natural products are still a valuable strategy to pursue in antibacterial drug discovery (Testolin, 2019). Paul Ehrlich introduced the identification and discovery of novel antibiotics by the systematic screening approach. He hypothesized that chemical compounds could be synthesized that would “be able to exert their full action exclusively on the parasite harbored within the organism” which was the start of a large-scale and systematic screening (Silverstein, 2005). In 1904 together with Alfred Bertheim and Sahachiro Hata, they synthesized and screened hundreds of derivatives in syphilis-infected rabbits. The sixth compound in the 600th series tested, thus numbered 606, which cured syphilis-infected rabbits and showed significant promise for the treatment of the venereal disease (Ehrlich and Hata, 1910).

Twenty-two antibiotic classes are currently approved for systemic use by the Food and Drug Administration (FDA, USA) and the European Medicines Agency (EMA). Of these, four classes are derived from synthetic sources, 17 are from natural products, and one class, the nitroheterocycles, has one synthetic compound and one semi-synthetic product. The large impact of natural products as antibiotic scaffolds is clearly highlighted in addition to the 79% of FDA approved antibiotics that are natural products or derivatives of natural products (Werth, 2022). Besides exploring niches and the use of complete synthetic routes, non-traditional strategies that target biological networks and processes as well as combination therapies can contribute to create new antibacterial treatment strategies (Lu and Collins, 2009). Drugs that were designed for a completely different purpose could function as antimicrobials as well as drugs that were only assessed against selective targets can be repurposed. BPH-652, a phosphonosulfonate, was initially used to lower cholesterol by targeting the squalene synthase

was shown to have antimicrobial activity by inhibiting an important enzyme involved in *Staphylococcus aureus* virulence, dehydrosqualene synthase. Therefore, this drug serves as a candidate for multidrug resistant *Staphylococcus aureus* treatment (Gao *et al*., 2017).

1.2. The Problem of Resistance

1.2.1. General Introduction

The process of drug development is a long and costly venture with a poor approval rate (Table 1.1). There are three main steps before a drug can be approved. First, the early research stage that takes from one to seven years of development. Second, the pre-clinical stage that lasts one to two years in general. Lastly, the clinical phase that includes phase one (20-50 people), two (50-500 people), and three (500-50000 people) studies and can last up to seven years (U.S. Department of Health and Human Services, 2016; FDA, 2015; FDA, 2021; FDA, 2022). After a drug passed all the steps and the requirements, and received the final approval the problem of developing drug resistance by selective pressure remains the ultimate challenge. This has been seen in multiple examples, from the start of introducing penicillins to carbapenems (Figure 1.2). There are many factors contributing to the emergence of antibiotic resistance and, as mentioned before, the problems require a complex approach (Figure 1.5) (Chopra *et al*., 2002).

Table 1.1: Stages of drug development to approval. CTA/IND: Clinical Trial Application/ Investigational New Drug – the results from initial testing that include the drug composition and manufacturing. The CTA/IND develops a plan for human testing. NDA: New Drug Application- NDA include all animal and human data, as well as information about how the drug behaves in the body and the manufacturing process. Time (years): average amount of time it takes to successfully develop a drug in years (FDA, 2015; Walesch *et al*., 2023) Cost (Million US Dollars): The mean cost per successful project in 2010 (Paul *et al.*, 2010).

<table>
<tr><td></td><td colspan="2">In vitro and in vivo testing</td><td>Human testing (20-50; 50-500; 500-50000)</td><td>Data review and surveillance after approval</td></tr>
<tr><td></td><td>Early Research</td><td>Pre-clinical</td><td>Clinical</td><td>Approval</td></tr>
<tr><td></td><td>Basic Research</td><td rowspan="4">Good Laboratory and Good Manufacturing Practices (GLP and GMP)</td><td>Phase 1</td><td rowspan="5">Phase 4</td></tr>
<tr><td></td><td>Early discovery</td><td>Phase 2</td></tr>
<tr><td></td><td rowspan="2">hit to lead optimisation</td><td rowspan="2">Phase 3</td></tr>
<tr><td></td><td>Animal testing</td></tr>
<tr><td></td><td>Lead optimisation</td><td>CTA/IND Filing</td><td>NDA Filing</td></tr>
<tr><td>Time (Years)</td><td>1-7</td><td>1-2</td><td>5-7</td><td>1-2</td></tr>
<tr><td>Cost (Million US Dollars)</td><td>10-15</td><td>5</td><td>15;40;150</td><td>50</td></tr>
</table>

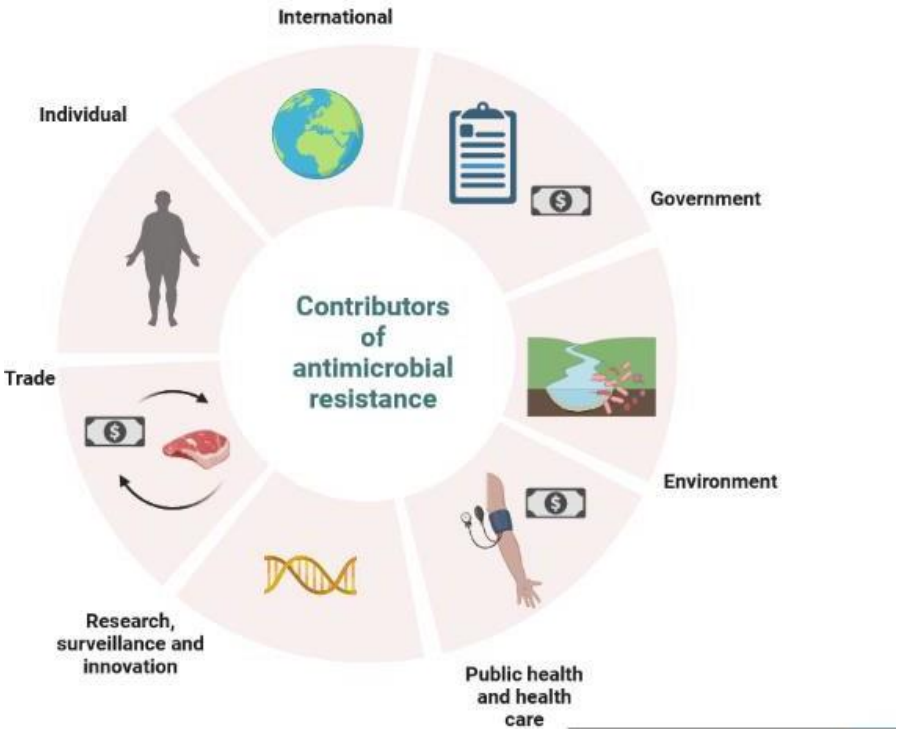

Figure 1.5: Factors that contribute to antibiotic drug resistance. (Adapted from Lambraki *et al*., 2022).

According to WHO (2022) antibiotic resistance occurs when bacteria change in response to the use of medicines. New resistance mechanisms are emerging and spreading to all parts of the world, threatening our ability to treat common infectious diseases. A growing list of infections – such as pneumonia, tuberculosis, blood poisoning, gonorrhoea, and foodborne diseases are becoming more difficult to treat as antibiotics become less effective (WHO, 2022). Magiorakos and co-workers (2011) clarified the definition of a multidrug resistant organism as the "lack of susceptibility to at least one agent in three or more chemical classes of antibiotic (e.g., a β-lactam, an aminoglycoside, a macrolide)". Figure 1.6 clarifies the known mechanisms of resistance in bacteria. *Enterococcus faecium*, *Staphylococcus aureus*, *Klebsiella pneumoniae*, *Acinetobacter baumannii*, *Pseudomonas aeruginosa*, and *Enterobacter* species (also referred to as ESKAPE panel) are most prone to multidrug resistance development and is responsible for healthcare-associated infections as treatment of these pathogens are difficult (WHO, 2022; De Oliveira *et al*., 2020).

Emergence and rise of antimicrobial resistance occur in both Gram-positive and Gram-negative bacteria. However, Gram-negative bacteria require a special mention as discovery for novel drugs are additionally hindered by the lack of knowledge to design molecules that can successfully overcome the barriers imposed by the inner and outer membranes while avoiding efflux-mediated export (Testolin *et al*., 2020). Figure 1.6 described the common

mechanisms of action and observed resistance mechanisms within Gram-positive and Gram-negative bacteria.

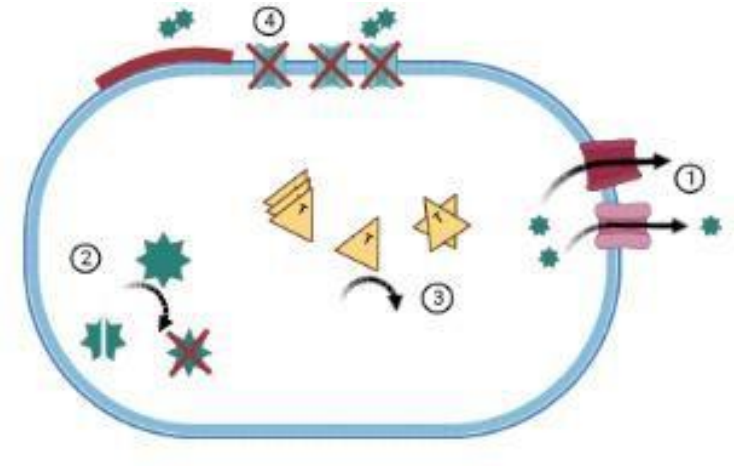

Figure 1.6: Mode of resistance (MoR) of antibiotics – 1: antibiotic efflux; 2: modification and inactivation of drug; 3: target bypass, modification, and protection; 4: reduced membrane permeability (Wright, 2011; Webber and Piddock, 2003; Hoffman, 2001; Blair *et al*., 2015) (adapted from Walesch *et al*., 2023).

Resistance mechanisms are continuously investigated since the unearthing of the enzyme ß-lactamase which was found to be the cause of penicillin resistance (Hutchings *et al.*, 2019). Known mechanisms include over-expression of efflux pumps, modification and inactivation of drugs, target bypass, target modification, target protection, and reduced membrane permeability as seen in Figure 1.6. Most antibacterial compounds need to penetrate the bacterial cell to reach its target. Metabolic changes can restrict outer membrane permeability, thereby preventing the intracellular accumulation of drugs in sufficient concentrations. Restricted permeability can result from the loss of porins that facilitate antibiotic transfer across the outer membrane, and overexpression of outer membrane proteins to prevent antibiotic binding (Lambert, 2002). Alteration of drug targets by modification can be the result of chromosomal mutations that result in a change in amino acid sequence and protein structure that hinder drug binding and thus limiting the anti-bacterial effect (Wright, 2011). Enzymes can also cause modification of drug targets that can be efficient and selective in preventing the employment of a drugs antimicrobial activity (Wright, 2011). Targ*et* alterations also include bacterial cells either over-expressing the drug target to bypass the metabolic pathway originally subject to drug inhibition or by forming new targets that perform similar biochemical functions (Hoffman, 2001). Further, drugs can be modified by enzymes when bacteria gain the capacity

to express enzymes such as β-lactamases or acetyltransferases, phosphotransferases, and nucleotidyltransferases (Blair *et al*., 2015).

1.2.2. Efflux of the drug from the cell

Efflux pumps are bacterial transport proteins that are involved in the translocation of several substances from an intracellular environment to an extracellular environment (Piddock, 2003). The removal of antibiotics from intracellular bacteria, have been extensively studied in various bacteria (Webber and Piddock, 2003). Efflux pumps function to ensure the intracellular drug concentration is limited and unable to reach the bacterial target and exert its antibacterial effect. To date, six super families of efflux pumps have been described based on their structures and coupling energies (Figure 1.7).

The first family is the ATP-binding cassette (ABC) family that utilizes free energy released by ATP hydrolysis to ADP to facilitate the transport of its substrates across a lipid membrane in or out of the cell (Davidson and Chen, 2004; Kim and Hummer, 2012). The second, the small multidrug resistance (SMR) family that is composed of small proteins with four transmembrane α-helical domains (Paulsen *et al*., 1996). Third, the major facilitator (MFS) family that is the largest and most diverse superfamily of secondary transporters known to date (Law *et al*., 2008). It shows a variable number of transmembrane segments, with some members having 12 and others 14 transmembrane regions (Law *et al*., 2008). Fourth, the resistance-nodulation-division (RND) family that are also the most common type of efflux pump in Gram-negative bacteria. This pump can expel a vast range of compounds structurally unrelated molecules, such as dyes, bile salts, detergents, and biocides (Amaral *et al*., 2014; Nishino *et al*., 2021). RND efflux complexes are composed of an outer membrane protein (OMP), an inner membrane protein (RND), and a periplasmic adapter protein (also known as the membrane fusion protein or MFP) that connects the OMP to the RND. The RND protein of the complex is responsible for the efflux using proton motive force (Putman *et al*., 2000). Fifth, the multidrug and toxic compound extrusion (MATE) family. Bacterial MATE transporters have been found to efflux cationic drugs in exchange for protons or sodium ions (Omote *et al*., 2006). Lastly, a recently discovered family, named PACE (proteobacterial antimicrobial compound efflux) (Hassan *et al*., 2015). Members of the PACE family are commonly found encoded within the core genome of a species, suggesting that these efflux pumps are perhaps involved in more than the efflux of biocides (Hassan *et al*., 2015).

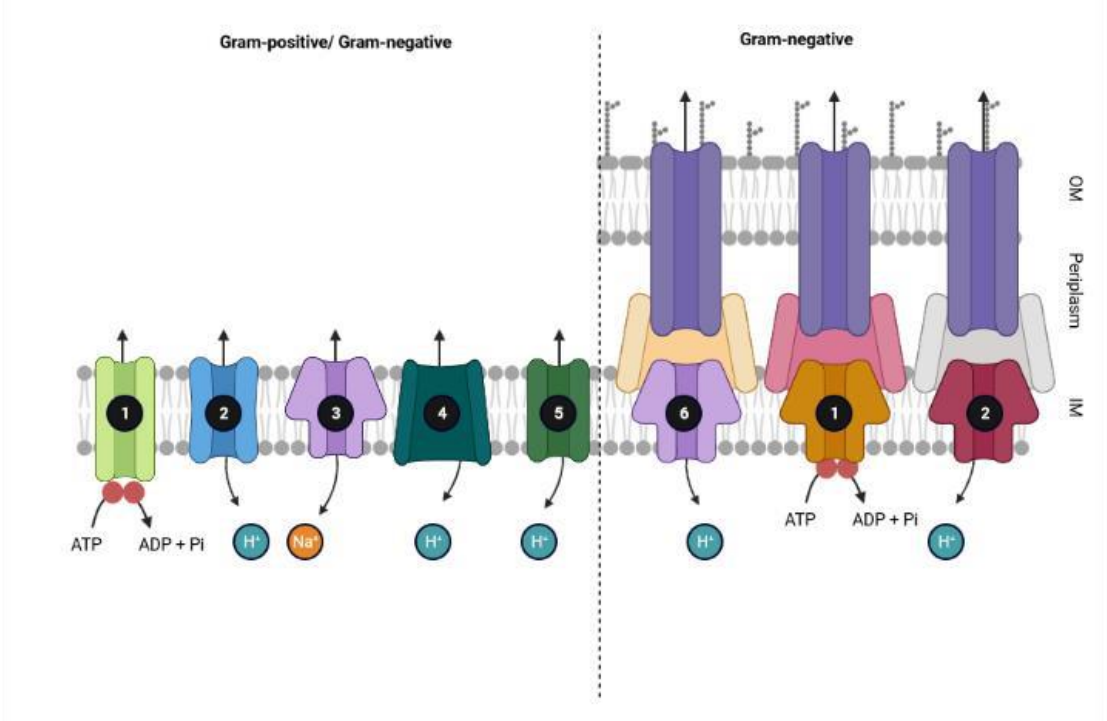

Figure 1.7: Visual representative of six super efflux pump families observed in Gram-positive and Gram-negative bacteria. 1- ABC super family and 2- MFS family is observed with a different composition in Gram-negative bacteria. 3- MATE family, 4- SMR, 5-PACE family and 6- RND family.

Despite the efflux family, most efflux pumps are multidrug transporters that can efficiently pump a wide range of antibiotics (Putman *et al*., 2000; Nishino *et al*., 2009; Kornelsen and Kumar, 2021). However, the over-expression of efflux pumps can have a negative effect on the fitness of bacteria· (Langevin and Dunlop, 2018). Therefore, the regulation of efflux pumps is very important to limit the burden by assessing the benefit of efflux expression to cost (Wen *et al*., 2018). The assessment depends on the surrounding environment, neighboring cells, and the drug concentration. These considerations are all important to enable the maximal growth and survival of the bacterial cells within their ecological niche (Poole, 2008). Transcriptional regulatory proteins regulate the expression levels of efflux pumps and are substrate-dependent (Issa *et al*., 2018). ArcR is a perfect example of a regulator as it forms part of the TetR family and regulates the famous RND efflux pump, ArcAB-TolC (Manjasetty *et al*., 2016). The PACE family efflux pump, AceI, utilize a LysR-type transcriptional regulator, AceR (Bolla *et al*., 2020). The MepA protein, with substrates such as biocides, fluoroquinolones, and tigecycline is regulated by a MarR-type repressor, MepR (Dabul *et al*., 2018). Furthermore, two-component system functions and roles are vast and to no surprise the response regulators effect efflux pump expression in Gram-positive and Gram-negative bacteria (Sun *et al*., 2017; Lin *et al*., 2016; Wu *et al*., 2016; Lin *et al*., 2014; Walker *et al*., 2013).

The primary multidrug resistance efflux pump in *E. coli* is the, well described, AcrAB-TolC. This pump forms part of the RND efflux family and is composed of three proteins spanning from the inner membrane to the outer membrane. AcrA is the protein that connects the periplasmic and the inner membrane, ArcB is the inner membrane transporter that is also responsible to recognize substrates and exports using proton motive force. The TolC protein connects the inner membrane with the outer membrane (Blair *et al*., 2009). Several knock out strains have been created throughout the years such as a knockout mutant of ArcB leads to increase antibiotic activity of compounds (Piddock, 2006; Sulavik, 2001). Further, the ArcAB-TolC has also been shown to play a role in adhesion and invasion in host cells and colonization and persistence in animals (Piddock, 2006). The most intensely studied ABC-transporter in *E. coli* is the MacAB-TolC efflux pump, which actively extrudes substrates including macrolides, polypeptide virulence factors and rough-core lipopolysaccharide (LPS) or similar glycolipids (Jo *et al*., 2017). EmRE is a SMR efflux pump that is observed in in both *E. coli* and *P. aeruginosa*, and that recognizes and mediates the extrusion of toxic polyaromatic compounds (Padariya *et al.*, 2017).

Pseudomonas aeruginosa is notoriously famous for multidrug resistance mostly caused by extensive resistome, low membrane permeability, biofilm formation, and the expression of a large number of efflux pumps (Murry *et al*., 2015; Valot *et al*., 2015; Tuon *et al*., 2022). In total, *P. aeruginosa* has 22 reported efflux pumps. Twelve of the 22 pumps belong to the RND efflux pump family, three to the MFS-type, three ABC-type, two to the SMR-type, one MATE-type, and one PACE-type multidrug efflux pump (De Oliveira *et al*., 2020). MexXY, MexAB-OprM, MexCD-OprJ, and MexEF-OprN bare special mention as they are the four main pumps associated with multidrug resistance (Goncalves *et al*., 2021; Valot *et al*., 2015). The MexXY is the only RND efflux pump without a coding sequence for an outer membrane factor. However, it can form a multidrug efflux pump with OprM from the MexAB-OprM operon and another outer membrane factor called OprA in some strains (Morita *et al*., 2012). Resistance mechanism by means of the MexXY pump are mostly caused by mutations within the MexZ and the two-component regulatory system ParRS repressors (Issa *et al*., 2018; Muller *et al*., 2011; Kawalek *et al*., 2019). The MexAB-OprM is repressed by *mexR*, *nalC*, and *nalD* and resistance by over-expression if the MexAB-OprM is achieved by causing translational disruption (Suresh *et al*., 2018). Nonsense substitutions, non-synonymous substitutions, frameshift mutations and insertions have all been reported to change the repressor protein molecular structure resulting in the over-expression of the pump (Ziha-Zarifi *et al*., 1999; Horna *et al*., 2018; Choudhury *et al*., 2016; Boutoille *et al*., 2004; Ma *et al*., 2021; Suresh *et al*., 2018; Tafti *et al*., 2020). The NfxB is the repressor of the silent or low-level expressed MexCD-OprJ. Nucleotide deletions, missense, and nonsense mutations within the repressor all lead to the over-expression of the MexCD-OprJ (Gomis-font *et al.*, 2021; Jeannot *et al*., 2008). Similar to

MexCD-OprJ, MexEF-OprN is normally inactive or expressed at very low levels. A lysR family repressor, MexT, and a putative oxidoreductase, MexS, under control of the MexEF-OprN (Kohler *et al*., 1999). However, the regulation is not as well understood as other genes such as the *pvc*B, *mvaT* and *ampR* also contribute to the over-expression of this RND multidrug efflux pump (Iftikhar *et al*., 2020; Balasubramanian *et al*. 2012; Westfall *et al*., 2006). Interestingly, the down-regulation of the porin, OprD, is also linked to the overexpression of the MexEF-OprN efflux pump (Kohler *et al*., 1999).

Klebsiella species have several efflux pumps that contribute to multidrug resistance. RND-type efflux systems include AcrAB, OqxAB, EefAB, KexD (Ni *et al*., 2020). Clinical strains of *K. pneumonia* the SMR efflux pump, KpnEF, contributes to resistance to benzalkonium chloride, chlorhexidine, and some other antiseptics (Srinivasan and Rajamohan, 2013). Interestingly, the AcrAB and KpnEF multidrug efflux pumps contribute to reduction in colistin sensitivity. Normally, only LPS and lipid A-associated resistance mechanisms are associate reduced sensitivity (Grogry *et al*., 2021). Imipenem-resistant multidrug-resistance in *Enterobacter aerogenes* and *Klebsiella pneumoniae* has also been reported due to the overexpression if the RND efflux pump, ArcAB-TolC, in combination with a decreased of porin expression (Chevalier *et al*., 2004).

Acinetobacter baumannii has several pumps associated with resistance to a broad range of antibiotics. The main RND efflux pump is the AdeABC, others include AdeDE, AdeFGH, and AdeIJK (Yoon *et al*., 2006). All these efflux pumps have been reported in resistance to aminoglycosides, fluoroquinolones, erythromycin, tetracycline, and chloramphenicol in all bacterial species reported to date (Huang *et al*., 2022). As mentioned, the roles of efflux pumps are not merely the extrusion of compounds but also interaction with the environment and other bacterial cells, substrate binding as well as cellular processes such as motility and virulence of strains. AbaQ is a MFS transporter found in *A baumannii* and Pasqua and co-workers (2021) linked the down regulation of the transporter to a decrease in both virulence and motility. The SMR family in *A. baumannii* include AbeS that transports acriflavine, benzalkonium, and ethidium (Lytvynenko *et al*., 2016) The PACE transporter family was first identified in *A. baumannii.* AceI (Acinetobacter chlorhexidine efflux protein I) contributes to extruding biosynthetic biocides and shares similarities to members of the SMR family in size and secondary structure (Bolla *et al*., 2020; Hassan *et al*., 2018).

Most Gram-positive efflux pumps belong to the MFS, SMR and MATE transporter families (do Socorro Costa *et al*., 2022). However, FarE is a newly described RND pump that was identified from *S. aureus* that confers resistance to fatty acid (Alnaseri *et al*., 2019). There are 10 well described MFS pumps in *S. aureus* that all contribute to resistance biocides, disinfectants, and

other antibiotics (Lekshmi *et al*., 2018). MFS transporters do not only play a role in resistance but has been linked to other biological pathways. For example, promoting host immune response, maintaining cell wall stability, cell adhesion, internalization, and bacterial viability (Pasqua *et al*., 2021). Further mepA is the only MATE efflux described for *S. aureus* and confers low-level resistance to quaternary ammonium compounds, antibiotics such as ciprofloxacin, norfloxacin and the dyes (McAleese *et al*., 2005).

1.2.3. Target bypass, modification, and protection

Development of antimicrobial drugs normally rely on a target within the microbial cell that is vital for survival and growth and that is preferably absent from mammalian cells. One of the best examples of such a target is the peptidoglycan component of the bacterial cell wall (Lambert *et al*., 2005). Despite the target, bacterial cells adapt and form resistance mechanisms to combat the effect of an antimicrobial. Firstly, by target bypass that occurs when the target becomes redundant due to an alternative target that fulfils the function (Wilson *et al*. 2020). An example is the expression of an additional penicillin binding protein, PBP2a, in *S. aureus* MRSA (Multidrug Resistant Staphylococcus aureus) strains by the *mecA* gene (Fergestad *et al*., 2020). The most frequent cause of resistance to the glycopeptide antibiotics in *E. faecium* and *E. faecalis* is the acquisition of one of two related gene clusters, termed VanA and VanB. These gene clusters encode enzymes that produce a modified peptidoglycan precursor terminating in d-Alanyl-d-Lactate (d-Ala-d-Lac) instead of d-Ala-d-Ala. The glycopeptides bind with much lower affinity to d-Ala-d-Lac than to d-Ala-d-Ala (Binda *et al*., 2014).

Secondly, target protection by sterically removing the drug from its target or inducing conformational changes to the target that allow the target to continue functioning albeit in the presence of the drug (Mujwar *et al*., 2019). Mupirocin resistance in *S. aureus* results from point mutations in the target enzyme, isoleucyl-tRNA synthetase, *ileS* (Mujwar *et al*., 2019). Resistance to fusidic acid in *S. aureus* results from alterations in the target that appear in natural mutants and that occurs at low rates in normal staphylococci populations (Turnidge and Collignon, 1999). Target protection can also occur without preventing drug binding. In this situation, the drug reaches the target, but the impact is lessened as exemplified by fusidic acid that inhibits translation by binding to elongation factor G by preventing complex dissociation thus preventing successful translation. However, fusidic acid-resistant *S. aureus* commonly express FusB-type proteins. FusB contains a zinc finger domain promotes dissociation of the bound complex allowing translation to occur successfully by displacing the fusidic acid (Cox at al., 2012).

Lastly, by protecting the target. A well-known example is the methylation of the 16S rRNA by ribosomal methyltransferases that prevents binding of macrolides and lincosamines (Bhujbalrao *et al*., 2018). Another well-explained mechanism is the resistance mechanism for colistin by altering the lipopolysaccharide molecule charge and inhibit interaction between the drug and its target (Elias *et al*., 2021). It should be noted that target protection does not necessary confer high-level resistance. Protection of a target may confer a relatively mild increase in the MIC of the relevant antibiotic; however, in combination with mutation of the target site, very high MICs can be achieved such as in the case of *qnr* gene and quinolone resistance (Ruiz, 2019).

1.2.4. Modification and inactivation of the drug

Bacteria produce several enzymes that can modify or inactivate antibiotics within the cell. The best studied include β-lactamases, macrolide esterase, and aminoglycoside-modifying enzymes (Golkar *et al*., 2018; Jana and Deb 2016). In comparison the efflux pump expression, this mechanism is less likely associated with bacterial fitness cost, as the activity is enzymatic and does not require any alteration to the components of the bacterial cell (Langevin and Dunlop, 2018). Inactivation of a drug can be achieved by degradation or modification. Clear examples of inactivation include hydrolysis of β-lactam antibiotics by β-lactamases at the amide bond of the β-lactam ring (Tooke *et al*., 2019). This mechanism is seen in all Gram-negative and Gram-positive bacteria and has spread globally (Tooke *et al*., 2019). The therapeutic impact of these penicillinases is relatively limited since they do not affect the clinical efficacy of extended spectrum cephalosporins, monobactams, or carbapenems. However, the prevalence of different classes of carbapenem-hydrolyzing enzymes has been increasing globally (Hawkey and Jones, 2009). The first identification of an imported OXA-type carbapenemase in *P. aeruginosa* was reported in 2008, and it was shown to be the same OXA-40 carbapenemase previously described for *A. baumannii* (Sevillano *et al*., 2008). In *A. baumannii*, the insertion sequence IS*Aba*1 is found upstream of the bla_{ampC} gene. The bla_{ampC} gene encodes for AmpC β-lactamase, this the insertion sequence allows for increase of bla_{ampC} gene expression and thus providing resistance to extended-spectrum cephalosporins (Heritier *et al*., 2006).

Aminoglycosides can be modified by acetyltransferases, phosphotransferases or nucleotidyltransferases, modifying the hydroxyl or amino groups of the drug, which in turn substantially reduces the affinity of the drug to the target (Ramirez and Tolmasky, 2010; Thacharodi and Lamont, 2022). These enzymes are categorized based in the chemical modification they mediate. Namely, aminoglycoside phosphoryltransferase enzymes phosphorylate the drug molecule, aminoglycoside acetyltransferase enzymes acetylate the

drug molecule, and aminoglycoside nucleotidyltransferase enzymes adenylate the drug molecule (Ramirez and Tolmasky, 2010). A recent example of a novel aminoglycoside-modifying enzyme is ApmA. ApmA is an acetyltransferase capable of inactivating apramycin, an antibiotic that can currently evade other mechanisms of aminoglycoside resistance (Bordeleau *et al*., 2021). Other examples of drug modification include Tet(X3/X4/X5) hydroxylases enzymes that confer high level resistance by the oxidation of tetracycline and has been reported in *Enterobacterales* and *Acinetobacter* isolates in China (Vázquez-López *et al*., 2020). Esterases that are responsible for modification of macrolides and chloramphenicol acetyltransferase (CAT) enzyme transfers an acetyl group to coenzyme A. In both cases, the modified drugs cannot bind as efficiently to their target on the ribosome thus preventing their activity (Golkar *et al*., 2018; Gu Lui *et al*., 2020).

Gram-positive *S. aureus* also utilize enzymatic inactivation of the antibiotics such as β-lactams, aminoglycosides, macrolides, and oxazolidinones (Darby *et al*., 2022; Chandrakanth *et al*., 2008). Nucleotidyltransferases for lincomycin resistance are encoded by *lnu* genes, for example, *lnu(A)* in *Staphylococcus* species (Feßler *et al*., 2018). While other examples include macrolide phosphotransferases Mph(BM), and Ere(A/B) esterases (Wondrack *et al*., 1996; Schnellmann *et al*., 2006).

1.2.5. Reduced membrane permeability

Most antimicrobial drugs need to cross the bacterial membrane to exert their activity, as their target is located intracellularly (Darby *et al.,* 2022). Gram-negative bacteria have an asymmetric and unique bilayer, with phospholipid being the inner leaflet and outer leaflet studded with lipopolysaccharides and porins (Henderson *et al*., 2016). The double-membrane structure makes the cellular envelope relatively impermeable, providing intrinsic resistance too many antibiotics that work against Gram-positive pathogens (Cox *et al*., 2008). This presents an additional challenge for the development of novel antimicrobials that can penetrate the cell envelope (Lee *et al*., 2013). In addition, alterations to porin protein and changes to phospholipid and fatty acid content can affect the ability of a drug to penetrate the cell and that leads to the emergence of resistance (Darby *et al.,* 2022).

There are two pathways that antibacterial drugs can take to surpass the outer membrane. First, a lipid-mediated pathway for antibiotics such as aminoglycosides (gentamycin, kanamycin), macrolides (erythromycin), rifamycins, novobiocin, fusidic acid and cationic peptides (Darby *et al.,* 2022; Nikaido, 2003). Colistin (polymyxin E) exerts bactericidal activity against most of the Gram-negative pathogens by the disruption and the neutralisation of lipopolysaccharides in the outer membrane (Zhang *et al*., 2000). However, with every mechanism there is a linked mechanism of resistance. The most common resistance mechanism is the modification of LPS

by overexpression and point mutations of the PmrA/PmrB and PhoP/PhoQ two-component systems, and the mgrB gene (Park *et al*., 2011). The second pathway is the general diffusion of hydrophilic antibiotics such as β-lactams, tetracycline, chloramphenicol, and fluoroquinolones (Nikaido, 2003).

Porins are located in the outer membrane. These β-barrel protein channels allow the influx of hydrophilic compounds, including many antibiotics, (<600 kDa) into the cell (Fernández *et al*., 2012). They are categorized based on their function and architecture. There are general nonspecific channels (OmpF and OmpC), substrate-specific channels (PhoE and LamB), and small β-barrel channels (OmpA and OmpX) (Nikaido, 2003). Porins that allow the entry of molecules no larger than 200 Da are present in *Pseudomonas aeruginosa* and *Acinetobacter baumannii* (Chevalier *et al*., 2017). The lack of larger porins result in high impermeable membranes, in particularly for hydrophilic molecules allowing the bacterium to develop resistance to imipenem, meropenem, carbapenems, fluoroquinolones, chloramphenicol, and β-lactam (Zgurskaya and Rybenkov, 2020). Clinical isolates of multidrug-resistant *E. coli* isolates were found with multiple mutations within OmpC that alter the electric charge and affect the permeability of antibiotics such as gentamicin or imipenem (Lou *et al*., 2011). In *P. aeruginosa*, the loss of OprD porins is a commonly reported mechanism of high-level carbapenem resistance (Chevalier *et al*., 2017). This is normally in conjunction with other mechanisms as a study conducted revealed that the loss of no single porin could completely abolish drug entry (Ude *et al*., 2021).

1.3. Techniques for identifying and characterizing bacterial resistance

Due to the variety of known bacterial resistance mechanisms, techniques used to identify resistance and the mechanism must be versatile (Figure 1.8) (Rentschler *et al*., 2021). The frequency of resistance (FoR) is the “frequency at which mutant cells emerge in a bacterial population in the presence of an antibiotic” (Martinez and Baquero, 2000). The development of frequency of resistance is dependent on factors such as the drug used for selections and the concentration of the drug and the bacterium. It is also to keep the correlation between *in vitro* resistance and *in vivo* resistance in mind when investigating the frequency of resistance development (Fung-Tomc, 1990).

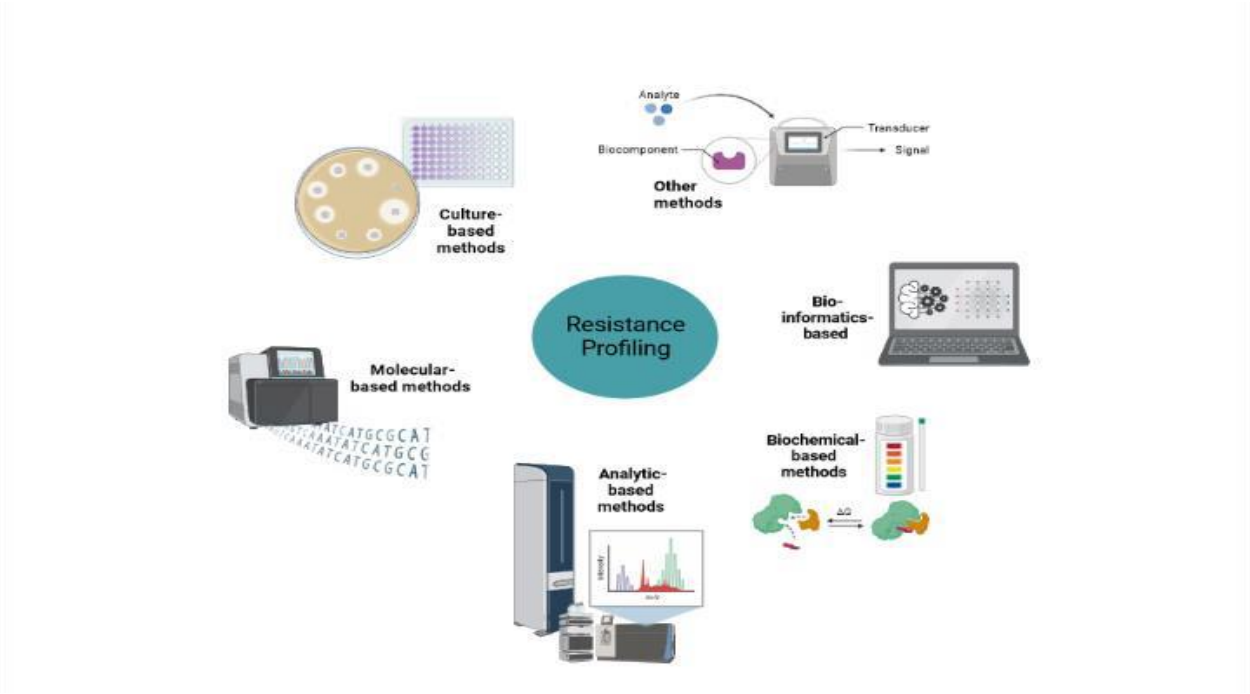

Figure 1.8: Overview of current methods used to investigate resistance and frequency of resistance development. Culture-based approaches (96-well plate broth dilution; agar dilution; disk diffusion), molecular-based, analytic-based, biochemical-based, bio-informatics-based and other methods that include iso-thermal micro-calorimetry, biosensors, protein markers and micro-fluids. (Adapted from Rentschler *et al*., 2021).

1.3.1. Culture-Based Methods

Culture-based methods are considered the golden standard in determining microbial resistance and are used alongside most other techniques such as molecular-based, analytic-based, biochemical-based, and bio-informatics-based tools to identify resistance as well as investigate the resistance mechanism (Maugeri, 2019). Using culture-based methods, susceptibility or resistance is determined by visual examination of bacterial growth in the presence of antimicrobial agents at various concentrations (Jorgensen, 2009). The drawback of these culture-based methods such as 96-well micro-broth dilution, agar dilution, and disk diffusion, and frequency of resistance determination, is bacterial resistance is determined but does not provide further information on the resistance mechanism (Maugeri, 2019). Additionally, long turnaround times, precise data reproducibility and slow-growing or uncultivable pathogens cannot be evaluated are al drawbacks of culture-based methods (van Belkum *et al*., 2020). Despite the drawbacks these methods, they provide end-point results regarding resistance of bacterial strains. The combination of culture-based methods with whole-genome sequencing can aid to undercover the genetic basis of resistance and the mechanism leading toward the observed antimicrobial resistance (Köser *et al*., 2014). This approach reveals how mutations underlie antimicrobial resistance, how are they distributed

across the genome (coding versus noncoding, synonymous versus nonsynonymous mutations) and through time (mutations rise and fix at early or later stages of adaptation) and which target genes contribute to resistance (Dettman *et al*., 2012).

1.3.2. Molecular-Based Methods

Molecular mechanisms of bacterial resistance are studied by polymerase chain reaction (PCR), quantitative RT-PCR, whole-genome sequencing, transcriptome sequencing (RNA-seq), microarray analysis, two-dimensional protein gel electrophoresis, and gene knockout and overexpression studies (Hong *et al.*, 2016). These methods do not only characterize pathogens at the species level but also detect antimicrobial resistance genes (Ota *et al*., 2019). Sequencing allows the complete overview of resistant bacterial genomes and are the best way to investigate the genetic determinants of antimicrobial resistance by the identification of mutations or alterations in specific genes and genome regions that is important in known resistance mechanisms (Diene and Rolain, 2013). These methods focus on amplification of sequences that encode known resistance determinants. Advantages of these methods include the sensitivity and specificity of detection (Tsalik *et al*., 2018; Strommenger *et al*., 2003). These methods are more expensive than culture-based methods. However, in recent years, whole-genome and next-generation sequencing has become increasingly more available and affordable thus feasible to evaluate an entire bacterial genomic DNA sequence; this strategy facilitates confirmation of a bacterial species and identification of potential resistance genes at comparatively lower cost compared to previous years (Li *et al*., 2019). Besides high costs, other drawbacks are that only known resistance mechanism can be determined, complex workflows, experimental pitfalls, experimental biases, and slow turnaround times (Ledeboer and Hodinka *et al*., 2011; Maugeri *et al*., 2019).

RNA-sequencing plays an important role in the discovery of known and novel resistance mechanisms by providing a vast transcriptome (Crofts *et al*., 2017). Comparative studies can compare wild-type strains with treated wild-type strains to help reveal up-and down-regulated genes that could contribute to identifying the mechanism of action by pin-pointing the major contributing genes and proteins (Li *et al*., 2019). Further, these methods can be applied in a comparative study between the wild-type strain and resistant mutants to identify the key expression differences observed which may be caused by the additional resistance observed in the phenotype (Li *et al*., 2019; Crofts *et al*., 2017). Thus, this reveals an important link between the phenotype, genotype, and transcriptome of resistant bacteria (Rabbani *et al*., 2016). A comparative transcriptome analysis with whole-genome sequencing revealed significant transcriptional changes in response of *S. aureus* to the exposure to triple-acting staphylolytic peptidoglycan hydrolase (Yan *et al*., 2022). Computational analyses, including

gene ontology and KEGG (Kyoto Encyclopedia of Genes and Genomes) pathway enrichment, can be employed to further link and identify the observed resistance to cellular pathways. The findings in this work could provide insights into the design of new antimicrobial agents (Yan *et al*., 2022). Schildkraut *et al* (2022) reported the use of RNA-sequencing to reveal a drug specific mechanism of resistance in a mycobacterial strain. RNA-seq analyses of antibiotic resistance mechanisms in *Serratia marcescens* revealed genes that might participate in antimicrobial resistance by participating in folate metabolism or the integrity of cell membranes (Li *et al.*, 2019). Complementarily, techniques such as proteomics- and metabolomics-based methods are becoming more popular and can add more value to the collected data.

1.3.3. Analytic-Based Methods

Mass spectrometry (MS) has become a method of choice for mechanistic elucidation and characterization of small-molecule—protein interactions. According to Charretier and Schrenzel (2016) MS methods can successfully identify antimicrobial resistance caused by horizontal gene transfers or mutations. However, antimicrobial resistance mediated by target mutations remains difficult to detect. The matrix-assisted laser desorption/ionization (MALDI) and the mass time-of-flight (TOF) analyzer (MALDI-TOF) is used to identify bacterial species and recently some efforts have been made toward the use for the detection of antimicrobial resistance patterns. MALDI-TOF functions by ionization by a laser beam that generates singly protonated ions from the sample. The protonated ions are accelerated at a fixed potential and separate based of their mass-to-charge ratio (m/z). The ratio, with MALDI-TOF, is determined by the time required for the ion to travel the length of a flight tube. The output is a characteristic spectrum called peptide mass fingerprint (PMF). The identification is then done by comparing the sample PMF with PMF that is in the database or by comparing the masses of biomarkers of the sample organism with the proteome database. Drawbacks of MALDI-TOF includes expensive equipment and laboratory structure, hampering their wide implementation as *in loco* diagnostic tools, the need for cultivation of a biological specimen, as well as the limitation to identify new resistance mechanism as the application is based on known resistance mechanisms (Patrinos *et al*., 2017).

Vrioni and co-workers (2018) provide a successful use as exemplified by the detection of active carbapenemases, cephalosporinases, and β-lactamases as well as the quantification of bacterial growth in presence of one or more antibiotics. In general, MALDI-TOF can be used as a screening method for the detection of known resistance mechanism (Sharma *et al*., 2020). For example, the detection of β-lactamases by MALDI-TOF lead to a ‘mass spectrometric β-lactamase (MSBL) assay.’ Within this assay, an antibiotic is mixed with a bacterial culture, incubated, centrifuged, and analyzed by MALDI-TOF that results in a mass shift in the non-

hydrolyzed and the hydrolyzed form of the antibiotic confirms the presence or absence of β-lactamase producing bacteria (Kostrzewa *et al*., 2013).

1.3.4. Biochemical-Based Methods

Antimicrobial resistance and susceptibility testing are also performed by determining protein-, enzyme-, antigen-, and metabolite-based molecular signatures and processes using spectrometry techniques, biosensors, and immunoassays (Dabas *et al*., 2017). Biochemical assay provides a shorter turnaround time than molecular-based or culture-based methods. Most of these tests confirm that a detected resistance gene is expressed and phenotypically present. Results are mostly calorimetric end-point readouts. An example is Rapidec Carba NP test is based on detection of in vitro hydrolysis of the β-lactam ring of imipenem by carbapenemases, which results in a color change on a pH-indicator (Nordmann *et al*., 2012). More developed assays are also able to distinguish between different classes of these enzymes (Dortet *et al*., 2012). However, this method also requires a cultivation step and provides no assessment of antibiotic susceptibility (Bogaerts *et al*., 2016) Further, the results are directly dependent on the number of bacterial cells used and has a limited sensitivity to certain lactamases, notably OXA-48 and some metallo-β-lactamases (Wright, 2011; Blair *et al*., 2015; Lambert, 2002).

1.3.5. Bio-informatics-Based Tools

The availability of bioinformatics tools and online accessible databases for antimicrobial resistance detection has increased and the usage has been proven helpful with the use of other above-mentioned methods. According to Hendriksen and co-workers (2019), there are at least 47 freely accessible bioinformatics resources for detection of resistant determinants for DNA or amino acid sequence data developed to date. Examples of such tools include, but are not limited to, CARD, Genefinder, KmerResistance, and ResFinder (Hendriksen *et al*., 2019). All bioinformatics resources differ in terms of the accepted input data, presence, or absence of software, and for the search approach employed it can be based on either mapping or on alignment Hendriksen and co-workers (2019). Therefore, each tool has its strengths and imitations in sensitivity and specificity of detection of resistant determinants. However, the biggest drawback of most of these bioinformatics-based resources are that they are only able to uncover known resistance mechanism that has been proven by other methods. The advancement in whole genome sequencing and the application of online tools for real-time detection of resistance are essential to identify control and prevention strategies to combat the increasing threat of antimicrobial resistance (Hendriksen *et al*., 2019). Accessible tools and DNA sequence data are expanding, which will allow establishing global pathogen surveillance and tracking based on genomics Hendriksen and co-workers (2019). There is, however, a

need for standardization of pipelines and databases as well as phenotypic predictions based on the data. (Hendriksen *et al*., 2019).

1.3.6. Other methods

Micro-fluidic devices have been combined with several different technologies to detect antimicrobial resistance and antimicrobial susceptibility. For example, magnetic nanoparticles linked to antibodies specific for the resistance factor, penicillin-binding protein 2a, were used to detect MRSA that were captured in a micro-fluidic device (Liu *et al*., 2020). Protein markers are capable of direct detection of protein markers of resistance, including the various types of β-lactamases (Chen *et al*., 2020). These tests typically involve specific capture antibodies and detection antibodies conjugated with colloidal gold, and outcomes are evaluated by visual inspection (Chen *et al*., 2020). In order to determine resistance and uncover resistance mechanisms using a single test, a combination of LFIAs and micro-arrays might be employed. Several electrochemical-based test systems have emerged as a more practical and potentially cost-effective (Besant *et al*., 2015). An electrochemical method that facilitated phenotypic profiling of antibiotic-resistant bacteria has been reported. In this approach, bacteria are captured in miniaturized electrode-containing wells and incubated with antimicrobial agents. Bacteria that remain metabolically active can be identified by electrochemically monitoring the reduction in a redox-active reporter molecule (Hannah *et al*., 2020).

Biosensors utilize small test volumes and may provide insight into distinct resistance mechanisms (von Ah *et al*., 2009). The devices measure biological or chemical reactions by generating signals proportional to the concentration of an analyte in the reaction. Exposure to antibiotics causes detectable changes in bacterial membranes, morphology, metabolism, movements, mass, heat production and nucleic acid content. In micro-calorimetry approaches, heat production correlates with the number of cells arising over time (von Ah *et al*., 2009). This approach is applicable to both solid and liquid cultures (Howell *et al*., 2012). Dynamic heat flow patterns have served species identification from urine samples (Bonkat *et al*., 2012). Isothermal micro-calorimetry revealed vancomycin-resistant *Staphylococcus aureus* in <8 hours (Entenza *et al*., 2014). Butini *et al*. (2018) applied isothermal micro-calorimetry to real-time monitoring of microbial viability in biofilms in the presence or absence of antimicrobial compounds. Micro-calorimetric methods, although fast and sensitive, require pure cultures and a high number of bacterial cells. In 2017, the Swedish company SymCel announced an extensive 28-months clinical testing of their micro-calorimeter calScreener™ for antimicrobial susceptibility testing.

1.4. Strategies to overcome or avoid bacterial resistance in drug development

Novel antibacterial drugs are needed to combat antimicrobial resistance at all stages. This includes last-resort therapies, which is a major global public health threat (Alvaro, 2022). The lack of novel drug development aids to the cost of antimicrobial resistance. The cost does not only include that of 1 million human lives lost per year, but also a large financial cost to the healthcare systems and world economy (Williams, 2022; Alvaro 2022). According to the Center for Disease Control (2021), the estimated cost of treatment of one antibiotic resistant microbial infection is 7.6 million US dollars annually. New drug development and encourages further expansion of resistant microbes is hindered by the antibiotic market as most physicians avoid using new, more expensive antibiotics until it is necessary (Arthur, 2022). To combat antibiotic resistance, it is essential for researchers and developers to identify resistance and to understand the mechanisms involved in the development of resistance. To date, some progress can be seen due to the increase of genetic technologies, which enables the investigation of the development of resistance mechanisms on a genome level (Alvaro, 2022). Various research groups have explored the behavior of bacteria in response to specific classes of antibiotics with the help of genetic technologies. The discovery of more effective antibiotics is dependent on understanding the structural basis of antibacterial resistance to design principles that overcome or avoid resistance (Ferreira and Andricopulo, 2014; Reeve *et al*., 2015).

Overcoming resistance of existing antibiotics involves optimizing the first-generation drug to a second-generation drug that is more effective against the resistant organism (Reeve *et al*., 2015). In order to optimize the first-generation drug, it requires time and funds to proper evaluate and develop a more effective second-generation. Therefore, identifying the most commonly observed resistance mechanisms while developing the first-generation compound is important information. This information can be utilized in the structural design of the second-generation drug to ensure that it is less susceptible to the identified resistance. Thus, allowing the second-generation drug to enter clinical trials in a timely manner. A prime example of successful implementation of this strategy is ß-lactams with five consequtive generations as well as the development of tyrosine kinase inhibitors (Huang *et al*., 2012; Wang *et al.*, 2022). To overcome resistance the structure of mutant proteins as well as differences between the wild-type and the resistance mutant is important so that the mutant can be directly targeted. Designing molecules that target the mutated proteins is the most straightforward approach and has been applied in several case studies. For example, improving propargyl-based inhibitors for the trimethoprim-resistant strains of MRSA and the development of several development of tyrosine kinase inhibitors (Huang *et al*., 2012; Wang *et al.*, 2022). In addition to directly

targeting the mutant proteins, identifying compounds that bind to more than one target has proven useful for the development of multitargeting antitubercular drug candidates (Stelitano *et al*., 2020). As previously discussed, resistance can emerge due to mechanisms of resistance other than protein mutations. Thus, targeting the resistance mechanism i.e., efflux pumps or enzymes that chemically inactivate the drug. Such strategies yield drugs for combination therapies, which allows for the development of new drugs. A classic example is the development of inhibitors such as avibactam that is a β-lactamase inhibitor, which inactivates β-lactams by a reversible fast acylation and slow deacylation reaction (Watkins *et al*., 2013). Another example is inhibiting the activity of efflux pumps that can potentially salvage the drug activity by binding to the efflux pump and preventing its functionality (Tong *et al*., 2012).

1.5. Natural products of interest to treat multidrug-resistant bacteria

1.5.1. Armeniaspirols

Armeniaspirols A-C are excellent examples of natural products that are produced by *Streptomyces armeniacus* (Couturier *et al*., 2012). Armeniaspirols have a unique spiro [4.4] non-8-ene scaffold and displays potent antibacterial activities against Gram-positive pathogens including methicillin-sensitive and methicillin-resistant *Staphylococcus aureus*, vancomycin-resistant *Enterococcus faecium* and *Helicobacter pylori* (Arisetti *et al.,* 2021*;* Dufour *et al., 2012;* Jia *et al.,* 2022). Armeniaspirol A leads to membrane depolarization at concentrations in similar range as the observed antibacterial activities (Arisetti *et al.,* 2021; Jia *et al*., 2021). In addition to the protonophore mechanism reported by Arisetti and co-workers (2021), Labana and co-workers (2021) showed that armeniaspirols inhibit the ClpXP and ClpYQ. Along the inhibition of the ClpP, dysregulation of divisome and elongasome key proteins also leads to the inhibition of cell division. Darnowski and co-workers (2023) found that armeniaspirols has a dual mechanism by disrupting the proton membrane force and inhibiting the ATP-dependent proteases ClpXP and ClpYQ resulting in the observed antimicrobial activity.

Jia and colleagues (2021) reported successful *in vivo* treatment of *H. pylori* infection in combination with omeprazole pointing to armeniaspirols as a viable *H. pylori* treatment option. However, the compound also exerts membrane depolarization on mammalian cells, which is a selectivity challenge for future optimization (Arisetti *et al.,* 2021). Armeniaspirol-resistant selection of Gram-positive strains has been unsuccessful which is in line with compounds causing membrane depolarization such as protonophores (Labana *et al*., 2021; Arisetti *et al*., 2021). Despite no activity in Gram-negative strains, Arisetti and co-workers (2021) determined a usable MIC value for *E. Coli Δ*tolC. This *E. coli* strain has a deletion in the TolC, which is a

component in the RND multidrug efflux pump, ArcAB-TolC (Sulavik, 2001). Resistant mutants were selected and indicated a complex efflux-mediated mechanism of resistance by the means of another RND-multidrug efflux pump, MdtNOP. This mechanism was also observed for pyrrolomycin, a natural product containing chlorinated pyrrole moieties (Valderrama *et al*., 2019).

1.5.2. Cystobactamids

Natural products produce a valuable amount of novel antibacterial compounds (Pidot *et al*., 2014). Cystobactamids was initially isolated from the *Cystobacter* species by Müller and co-workers in 2014 by the screening of myxobacterial isolates for novel bioactive compounds and bioactivity-guided fractionation (Baumann *et al.*, 2014). The mechanism of action is by inhibiting bacterial type II a topoisomerase and show little to no cross-resistance to clinically relevant gyrase inhibitors indicating a novel binding site for the same target (Groβ *et al.*, 2021; Hüttel *et al.*, 2017). Cystobactamids consist of tailored *p*ABA, connected by a unique α-methoxy-L-isoasparagine or a β-methoxy-L-asparagine linker moiety (Figure 1.9). The antibacterial activity is determined by the linker and position of the *p*ABA units. Cys 919-1 has a low micromolar activity against *Acinetobacter baumanii*, *Pseudomonas aeruginosa*, *Escherichia coli*, and other pathogens that are classified with high- to critical-priority by the WHO (Tacconelli, 2017; Groß *et al*., 2021). The structure elucidation and total synthesis of cystobactamids was done at approximately the same time as for albicidin, which have completed lead optimization for serious bacterial infections (Behroz *et al.*, 2019; Zborovsky *et al.*, 2021). Albicidin, a PKS/non-ribosomal peptide synthetase product class isolated from *Xanthomonas albilineans*, show structural similarities with cystobactamids (Elgaher *et al.*, 2020) (Figure 1.9). The total synthesis of cystobactamids were established and significant improvements in scalability and activity of novel derivatives cystobactamids are now in the lead optimization phase for multidrug resistant Gram-negative bacterial infections (Elgaher *et al.*, 2020).

a) b)

Figure 1.9: Chemical structures of a) cystobactamid 919-1 and b) albicidin.

1.5.3. Myrtucommulones

Myrtus communis is a shrub that belongs to the Myrtaceae family and is found in the Mediterranean and Western Asia (Messaoud *et al*., 2012). It has been used as traditional

medicine as the leaves were found to be useful in the treatment of digestive, pulmonary, and skin diseases (Nicoletti *et al.*, 2018; Lounasmaa *et al*., 1977). Previous studies resulted in interesting compounds such as phenolic acids, flavonoids, myrtucommulone, and semimyrtucommulone (Messaoud *et al*., 2005; Alipour *et al*., 2014). These compounds also show some antioxidative, anticancer, anti-diabetic, antiviral, antibacterial, antifungal, hepatoprotective and neuroprotective activity (Alipour *et al*., 2014, Appendino *et al*., 2002; Messaoud *et al*., 2012). In the 1970s, the first isolation of a phloroglucinol antibiotic compound was reported (Lounasmaa *et al*., 1977). This compound was named myrtucommulone A (Figure 1.10) showed a broad range of antimicrobial activity against multidrug resistant Gram-positive bacteria (Alipour *et al.*, 2014; Appendino *et al.*, 2002). The antimicrobial activities of phenolic compounds have been ascribed to cell membrane damage (Cox *et al*., 2001). Owlia *et al*., 2010 postulates that the mechanism of action of myrtucommulone A is due to the hydrophobic nature which enable it to permeate and disturb the cytoplasmic membrane.

Transcriptomic studies have been conducted on a another acylphloroglucinol compound, rhodomyrtone, that modulates the expression of proteins and genes involved in cell wall biosynthesis, division, stress responses, antigens, virulence factors, and several metabolic pathways (Visutthi *et al*., 2011). Further investigation on the mechanism of rhodomyrtone revealed the target to be located within the cytoplasm and the resistant phenotype to be caused by the upregulation of the fatty acid efflux pump FarE (Huang *et al*., 2022). Since, no information has been published regarding the mechanism of action myrtucommulones, except that the mechanism is cell wall or membrane related, the assumption is that the mechanism might be similar to that of rhodomyrtone. However, structurally myrtucommulone A and the related myrtucommulones has a hexanoyl residue on the phloroglucinol ring and is characterized by a trimeric, while rhodomyrtone possess a bisfurane fused ring and is a dimeric-monopyrane sub-class of compound (Morkunas *et al*., 2013; Charpentier *et al*., 2017).

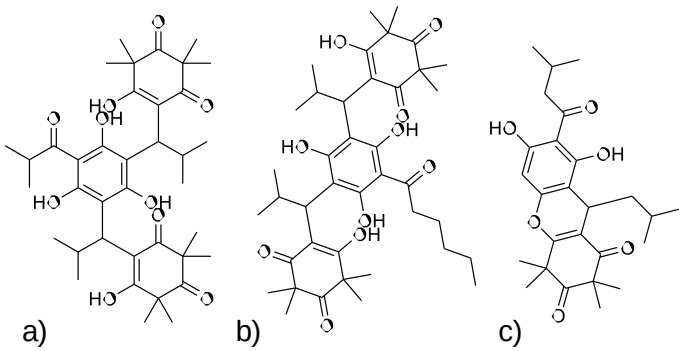

Figure 1.10: Chemical structures of a) myrtucommulone A b) myrtucommulone F and c) rhodomyrtone A.

1.6. Scope of Thesis

As explained, the need for novel antibiotic drugs is growing at a faster pace than discovery of novel compounds, whether chemically or naturally sourced. The usage and application of known drugs on the market gives way for a growing bacterial population that are multidrug resistant. In turn, rendering the use of last resort compounds in clinics. Multidrug resistant infections account for a major cause of death throughout the world. Understanding these mechanisms provide us with a tool to develop antimicrobial compounds that has be ability to overcome the known mechanism of resistance and could therefore aid in treatments of multidrug resistant infections. To elucidate and understand the mechanisms by which bacterial cells use to survive antimicrobial compounds is difficult and complex process that requires several technologies. This thesis aims to elucidate the mode-of-resistances of Gram-negative and Gram-positive pathogens for three novel antibacterial natural products, armeniaspirols, cystobactamids, and myrtucommulones. This was done by utilizing culture-based and biochemical- based assays in combination of whole-genome sequencing and RNA-sequencing to understand the resistant phenotype on a genome and transcriptome level.

1.7. References

Appendino, G., Bianchi, F., Minassi, A., Sterner, O., Ballero, M. and Gibbons, S., 2002. Oligomeric acylphloroglucinols from myrtle (Myrtus communis). Journal of natural products, 65(3), pp.334-338.

Acosta-Gutiérrez, S., Ferrara, L., Pathania, M., Masi, M., Wang, J., Bodrenko, I., Zahn, M., Winterhalter, M., Stavenger, R.A., Pagès, J.M. and Naismith, J.H., 2018. Getting drugs into Gram-negative bacteria: rational rules for permeation through general porins. ACS infectious diseases, 4(10), pp.1487-1498.

Agüero-Chapin, G., Galpert-Cañizares, D., Domínguez-Pérez, D., Marrero-Ponce, Y., Pérez-Machado, G., Teijeira, M. and Antunes, A., 2022. Emerging Computational Approaches for Antimicrobial Peptide Discovery. Antibiotics, 11(7), pp.936.

Alnaseri, H., Kuiack, R.C., Ferguson, K.A., Schneider, J.E., Heinrichs, D.E. and McGavin, M.J., 2019. DNA binding and sensor specificity of FarR, a novel TetR family regulator required for induction of the fatty acid efflux pump FarE in Staphylococcus aureus. Journal of bacteriology, 201(3), pp.e00602-18.

Amaral, L., Martins, A., Spengler, G. and Molnar, J., 2014. Efflux pumps of Gram-negative bacteria: what they do, how they do it, with what and how to deal with them. Frontiers in pharmacology, pp.168.

Aminov, R.I., 2010. A brief history of the antibiotic era: lessons learned and challenges for the future. Frontiers in microbiology, 1, p.134.

Arisetti, N., Fuchs, H.L., Coetzee, J., Orozco, M., Ruppelt, D., Bauer, A., Heimann, D., Kuhnert, E., Bhamidimarri, S.P., Bafna, J.A. and Hinkelmann, B., 2021. Total synthesis and mechanism of action of the antibiotic armeniaspirol A. Chemical Science, 12(48), pp.16023-16034.

Balasubramanian, D., Schneper, L., Merighi, M., Smith, R., Narasimhan, G., Lory, S. and Mathee, K., 2012. The regulatory repertoire of Pseudomonas aeruginosa AmpC ß-lactamase regulator AmpR includes virulence genes. PloS one, 7(3), pp.e34067.

Baumann, S., Herrmann, J., Raju, R., Steinmetz, H., Mohr, K.I., Hüttel, S., Harmrolfs, K., Stadler, M. and Müller, R., 2014. Cystobactamids: myxobacterial topoisomerase inhibitors exhibiting potent antibacterial activity. Angewandte Chemie International Edition, 53(52), pp.14605-14609.

Bennett, B.C., 2007. Doctrine of signatures: an explanation of medicinal plant discovery or dissemination of knowledge?. Economic Botany, 61(3), pp.246-255.

Benveniste, R.A.O.U.L. and Davies, J., 1973. Mechanisms of antibiotic resistance in bacteria. Annual review of biochemistry, 42(1), pp.471-506.

Besant, J.D., Sargent, E.H., and Kelley, S.O., 2015. Rapid electrochemical phenotypic profiling of antibiotic-resistant bacteria. Lab on a Chip, 15(13), pp.2799-2807.

Behroz, I., 2021. Structure-activity Relationship Studies of Albicidin's C-terminal Dipeptide and N-terminal Cinnamoyl Residue (Doctoral dissertation, Technische Universität Berlin).

Bhujbalrao, R., Gavvala, K., Singh, R.K., Singh, J., Boudier, C., Chakrabarti, S., Patwari, G.N., Mély, Y. and Anand, R., 2022. Identification of allosteric hotspots regulating the ribosomal RNA binding by antibiotic resistance-conferring Erm methyltransferases. Journal of Biological Chemistry, 298(8).

Binda, E., Marinelli, F. and Marcone, G.L., 2014. Old and new glycopeptide antibiotics: action and resistance. Antibiotics, 3(4), pp.572-594.

Blair, J.M. and Piddock, L.J., 2009. Structure, function and inhibition of RND efflux pumps in Gram-negative bacteria: an update. Current opinion in microbiology, 12(5), pp.512-519.

Blair, J.M., Webber, M.A., Baylay, A.J., Ogbolu, D.O. and Piddock, L.J., 2015. Molecular mechanisms of antibiotic resistance. Nature reviews microbiology, 13(1), pp.42-51.

Bogaerts, P., Yunus, S., Massart, M., Huang, T.D. and Glupczynski, Y., 2016. Evaluation of the BYG Carba test, a new electrochemical assay for rapid laboratory detection of

carbapenemase-producing Enterobacteriaceae. Journal of clinical microbiology, 54(2), pp.349-358.

Bolla, J.R., Howes, A.C., Fiorentino, F. and Robinson, C.V., 2020. Assembly and regulation of the chlorhexidine-specific efflux pump AceI. Proceedings of the National Academy of Sciences, 117(29), pp.17011-17018.

Bonkat, G., Braissant, O., Widmer, A.F., Frei, R., Rieken, M., Wyler, S., Gasser, T.C., Wirz, D., Daniels, A.U. and Bachmann, A., 2012. Rapid detection of urinary tract pathogens using microcalorimetry: principle, technique and first results. BJU international, 110(6), pp.892-897.

Bordeleau, E., Stogios, P.J., Evdokimova, E., Koteva, K., Savchenko, A. and Wright, G.D., 2021. ApmA is a unique aminoglycoside antibiotic acetyltransferase that inactivates apramycin. Mbio, 12(1), pp.e02705-20.

Boutoille, D., Corvec, S., Caroff, N., Giraudeau, C., Espaze, E., Caillon, J., Plésiat, P. and Reynaud, A., 2004. Detection of an IS21 insertion sequence in the mexR gene of Pseudomonas aeruginosa increasing β-lactam resistance. FEMS Microbiology Letters, 230(1), pp.143-146.

Brown, K., Li, W. and Kaur, P., 2017. Role of aromatic and negatively charged residues of DrrB in multisubstrate specificity conferred by the DrrAB system of Streptomyces peucetius. Biochemistry, 56(13), pp.1921-1931.

Butini, M.E., Gonzalez Moreno, M., Czuban, M., Koliszak, A., Tkhilaishvili, T., Trampuz, A. and Di Luca, M., 2018. Real-time antimicrobial susceptibility assay of planktonic and biofilm bacteria by isothermal microcalorimetry. In Advances in Microbiology, Infectious Diseases and Public Health, 13(19), pp. 61-77.

Carlson, A.W., 1986. Ginseng: America's botanical drug connection to the Orient. Economic Botany, 40, pp.233-249.

Centers for Disease Control and Prevention (CDC). 2021. Partners Estimate Healthcare Cost of Antibiotic-resistant Infections." Apr. 2021.

Charpentier, M. and Jauch, J., 2017. Metal catalysed versus organocatalysed stereoselective synthesis: The concrete case of myrtucommulones. Tetrahedron, 73(47), pp.6614-6623.

Charpentier, X., Polard, P. and Claverys, J.P., 2012. Induction of competence for genetic transformation by antibiotics: convergent evolution of stress responses in distant bacterial species lacking SOS?. Current opinion in microbiology, 15(5), pp.570-576.

Charretier, Y. and Schrenzel, J., 2016. Mass spectrometry methods for predicting antibiotic resistance. PROTEOMICS–Clinical Applications, 10(9-10), pp.964-981.

Chen, C.Y., Clark, C.G., Langner, S., Boyd, D.A., Bharat, A., McCorrister, S.J., McArthur, A.G., Graham, M.R., Westmacott, G.R. and Van Domselaar, G., 2020. Detection of antimicrobial resistance using proteomics and the comprehensive antibiotic resistance database: a case study. PROTEOMICS–Clinical Applications, 14(4), pp.1800182.

Chevalier, S., Bouffartigues, E., Bodilis, J., Maillot, O., Lesouhaitier, O., Feuilloley, M.G., Orange, N., Dufour, A. and Cornelis, P., 2017. Structure, function and regulation of Pseudomonas aeruginosa porins. FEMS microbiology reviews, 41(5), pp.698-722.

Chopra, I., Hesse, L. and O'Neill, A., 2002. Discovery and development of new anti-bacterial drugs. Pharmacochemistry library, 32(1), pp. 213-225.

Choudhury, D., Ghose, A., Chanda, D.D., Talukdar, A.D., Choudhury, M.D., Paul, D., Maurya, A.P., Chakravarty, A. and Bhattacharjee, A., 2016. Correction: Premature termination of MexR leads to overexpression of MexAB-OprM efflux pump in Pseudomonas aeruginosa in a tertiary referral hospital in India. Plos one, 11(3), pp.e0151308.

Cockayne, T.O., 1865. Leechdoms, wortcunning, and starcraft of early England: being a collection of documents, for the most part never before printed, illustrating the history of science in this country before the Norman conquest, 35(2).

Couturier, C., Bauer, A., Rey, A., Schroif-Dufour, C. and Broenstrup, M., 2012. Armeniaspiroles, a new class of antibacterials: antibacterial activities and total synthesis of 5-chloro-Armeniaspirole A. Bioorganic & medicinal chemistry letters, 22(19), pp.6292-6296.

Cox, G., and Wright, G.D., 2013. Intrinsic antibiotic resistance: mechanisms, origins, challenges and solutions. International Journal of Medical Microbiology, 303(6-7), pp.287-292.

Cox, G., Thompson, G.S., Jenkins, H.T., Peske, F., Savelsbergh, A., Rodnina, M.V., Wintermeyer, W., Homans, S.W., Edwards, T.A. and O'Neill, A.J., 2012. Ribosome clearance by FusB-type proteins mediates resistance to the antibiotic fusidic acid. Proceedings of the National Academy of Sciences, 109(6), pp.2102-2107.

Cox, S.D., Mann, C.M., Markham, J.L., Gustafson, J.E., Warmington, J.R. and Wyllie, S.G., 2001. Determining the antimicrobial actions of tea tree oil. Molecules, 6(2), pp.87-91.

Crofts, T.S., Gasparrini, A.J. and Dantas, G., 2017. Next-generation approaches to understand and combat the antibiotic resistome. Nature Reviews Microbiology, 15(7), pp.422-434.

D Alvaro. 2022. Antivioitivv Resistance: advances in Understanding and Drug development. Pharma’s Almanac. Octobe, 11 2022. https://www.pharmasalmanac.com/articles/antibiotic-resistance-advances-in-understanding-and-drug-development. (Accessed: 30 March 2023).

D’Costa, V.M., King, C.E., Kalan, L., Morar, M., Sung, W.W., Schwarz, C., Froese, D., Zazula, G., Calmels, F., Debruyne, R., and Golding, G.B., 2011. Antibiotic resistance is ancient. Nature, 477(7365), pp.457-461.

Dabas, Y., Xess, I., Singh, G., Pandey, M. and Meena, S., 2017. Molecular identification and antifungal susceptibility patterns of clinical dermatophytes following CLSI and EUCAST guidelines. Journal of Fungi, 3(2), p.17.

Dabul, A.N.G., Avaca-Crusca, J.S., Van Tyne, D., Gilmore, M.S., and Camargo, I.L.B.C., 2018. Resistance in in vitro selected Tigecycline-resistant methicillin-resistant Staphylococcus aureus sequence type 5 is driven by mutations in mepR and mepA genes. Microbial Drug Resistance, 24(5), pp.519-526.

Darby, E.M., Trampari, E., Siasat, P., Gaya, M.S., Alav, I., Webber, M.A., and Blair, J.M., 2022. Molecular mechanisms of antibiotic resistance revisited. Nature Reviews Microbiology, pp.1-16.

Darnowski, M.G., Lanosky, T.D., Paquette, A.R. and Boddy, C.N., 2023. Armeniaspirol analogues disrupt the electrical potential (ΔΨ) of the proton motive force. Bioorganic & Medicinal Chemistry Letters, pp.129210.

Davidson, A.L. and Chen, J., 2004. ATP-binding cassette transporters in bacteria. Annual review of biochemistry, 73(1), pp.241-268.

Davies, J. and Davies, D., 2010. Origins and evolution of antibiotic resistance. Microbiology and molecular biology reviews, 74(3), pp.417-433.

D'Costa, V.M., McGrann, K.M., Hughes, D.W. and Wright, G.D., 2006. Sampling the antibiotic resistome. Science, 311(5759), pp.374-377.

De Oliveira, D.M., Forde, B.M., Kidd, T.J., Harris, P.N., Schembri, M.A., Beatson, S.A., Paterson, D.L. and Walker, M.J., 2020. Antimicrobial resistance in ESKAPE pathogens. Clinical microbiology reviews, 33(3), pp.e00181-19.

Demain, A.L. and Fang, A., 2000. The natural functions of secondary metabolites. History of modern biotechnology I, pp.1-39.

Dettman, J.R., Rodrigue, N., Melnyk, A.H., Wong, A., Bailey, S.F. and Kassen, R., 2012. Evolutionary insight from whole-genome sequencing of experimentally evolved microbes. Molecular ecology, 21(9), pp.2058-2077.

Diene, S.M. and Rolain, J.M., 2013. Investigation of antibiotic resistance in the genomic era of multidrug-resistant Gram-negative bacilli, especially Enterobacteriaceae, Pseudomonas and Acinetobacter. Expert Review of Anti-infective Therapy, 11(3), pp.277-296.

do Socorro Costa, M., da Silva, A.R.P., Araújo, N.J.S., Barbosa Filho, J.M., Tavares, J.F., de Freitas, T.S., Junior, F.N.P., de Sousa, E.O., Maia, F.P.A., de Vasconcelos, J.E.L. and Pinheiro, J.C.A., 2022. Evaluation of the antibacterial and inhibitory activity of NorA and MepA efflux pumps from Staphylococcus aureus by diosgenin. Life Sciences, 308(1), pp.120978.

Dortet, L., Poirel, L. and Nordmann, P., 2012. Rapid identification of carbapenemase types in Enterobacteriaceae and Pseudomonas spp. by using a biochemical test. Antimicrobial agents and chemotherapy, 56(12), pp.6437-6440.

Dufour, C., Wink, J., Kurz, M., Kogler, H., Olivan, H., Sablé, S., Heyse, W., Gerlitz, M., Toti, L., Nußer, A. and Rey, A., 2012. Isolation and Structural Elucidation of Armeniaspirols A–C: Potent Antibiotics against Gram-Positive Pathogens. Chemistry–A European Journal, 18(50), pp.16123-16128.

Ehrlich, P. and Halta, S., 1910. Die experimentelle chemotherapie der Spirillosen (Vol. 8). Berlin: Julius Springer.

Elgaher, W.A., Hamed, M.M., Baumann, S., Herrmann, J., Siebenbürger, L., Krull, J., Cirnski, K., Kirschning, A., Brönstrup, M., Müller, R. and Hartmann, R.W., 2020. Cystobactamid 507: concise synthesis, mode of action, and optimization toward more potent antibiotics. Chemistry–A European Journal, 26(32), pp.7219-7225.

Elias, R., Duarte, A. and Perdigão, J., 2021. A molecular perspective on colistin and Klebsiella pneumoniae: Mode of action, resistance genetics, and phenotypic susceptibility. Diagnostics, 11(7), p.1165.

Entenza, J.M., Betrisey, B., Manuel, O., Giddey, M., Sakwinska, O., Laurent, F. and Bizzini, A., 2014. Rapid detection of Staphylococcus aureus strains with reduced susceptibility to vancomycin by isothermal microcalorimetry. Journal of clinical microbiology, 52(1), pp.180-186.

Fergestad, M.E., Stamsås, G.A., Morales Angeles, D., Salehian, Z., Wasteson, Y. and Kjos, M., 2020. Penicillin-binding protein PBP2a provides variable levels of protection toward different β-lactams in Staphylococcus aureus RN4220. Microbiologyopen, 9(8), pp.e1057.

Fernandes, R., Amador, P. and Prudêncio, C., 2013. β-Lactams: chemical structure, mode of action and mechanisms of resistance. Reviews and Research in Medical Microbiology, 24(1), pp.7-17.

Fernández, L. and Hancock, R.E., 2013. Adaptive and mutational resistance: role of porins and efflux pumps in drug resistance. Clinical Microbiology Reviews, 26(1), pp.163.

Feßler, A.T., Wang, Y., Wu, C. and Schwarz, S., 2018. Mobile lincosamide resistance genes in staphylococci. Plasmid, 99, pp.22-31.

Food and Drug Administration (FDA). 2015. Novel Drugs 2015: Summary. http://wayback.archive-it.org/7993/20161022195939/http://www.fda.gov/downloads/Drugs/DevelopmentApprovalProcess/DrugInnovation/UCM481709.pdf. (Accessed: 28 February 2023).

Food and Drug Administration (FDA). 2021. Advancing health trough innovation: new drug therapy approvals 2021. https://www.fda.gov/media/155227/download. (Accessed: 28 February 2023).

Food and Drug Administration (FDA). 2022. New drugs at FDA: CDER's new molecular entities and new therapeutic biological products. https://www.fda.gov/drugs/development-approval-process-drugs/new-drugs-fda-cders-new-molecular-entities-and-new-therapeutic-biological-products. (Accessed: 28 February 2023).

Fung-Tomc, J.C., 1990. Correlation of in vitro and in vivo resistance development to antimicrobial agents. Antimicrobic Newsletter, 7(3), pp.17-24.

Gao P, Davies J, Kao RYT. 2017. Dehydrosqualene Desaturase as a Novel Target for Anti-Virulence Therapy against Staphylococcus aureus. mBio.8(5), pp.e01224-17.

Gogry, F.A., Siddiqui, M.T., Sultan, I., and Haq, Q.M.R., 2021. Current update on intrinsic and acquired colistin resistance mechanisms in bacteria. Frontiers in medicine, 8(1), pp.677720.

Golkar, T., Zieliński, M. and Berghuis, A.M., 2018. Look and outlook on enzyme-mediated macrolide resistance. Frontiers in microbiology, 9(1), pp.1942.

Gomis-Font, M.A., Pitart, C., del Barrio-Tofiño, E., Zboromyrska, Y., Cortes-Lara, S., Mulet, X., Marco, F., Vila, J., López-Causapé, C. and Oliver, A., 2021. Emergence of Resistance to Novel Cephalosporin–β-lactamase Inhibitor Combinations through the Modification of the Pseudomonas aeruginosa MexCD-OprJ Efflux Pump. Antimicrobial Agents and Chemotherapy, 65(8), pp.e00089-21.

Gonçalves, T. and Vasconcelos, U., 2021. Colour me blue: the history and the biotechnological potential of pyocyanin. Molecules, 26(4), pp.927.

Gu Liu, C., Green, S.I., Min, L., Clark, J.R., Salazar, K.C., Terwilliger, A.L., Kaplan, H.B., Trautner, B.W., Ramig, R.F. and Maresso, A.W., 2020. Phage-antibiotic synergy is driven by a unique combination of antibacterial mechanism of action and stoichiometry. MBio, 11(4), pp.e01462-20.

Hannah, S., Dobrea, A., Lasserre, P., Blair, E.O., Alcorn, D., Hoskisson, P.A. and Corrigan, D.K., 2020. Development of a rapid, antimicrobial susceptibility test for E. coli based on low-cost, screen-printed electrodes. Biosensors, 10(11), pp.153.

Harrison, F., Roberts, A.E., Gabrilska, R., Rumbaugh, K.P., Lee, C., and Diggle, S.P., 2015. A 1,000-year-old antimicrobial remedy with antistaphylococcal activity. MBio, 6(4), pp.e01129-15.

Hassan, K.A., Liu, Q., Elbourne, L.D., Ahmad, I., Sharples, D., Naidu, V., Chan, C.L., Li, L., Harborne, S.P., Pokhrel, A. and Postis, V.L., 2018. Pacing across the membrane: the novel PACE family of efflux pumps is widespread in Gram-negative pathogens. Research in microbiology, 169(7-8), pp.450-454.

Hassan, K.A., Liu, Q., Henderson, P.J. and Paulsen, I.T., 2015. Homologs of the Acinetobacter baumannii AceI transporter represent a new family of bacterial multidrug efflux systems. MBio, 6(1), pp.e01982-14.

Hawkey, P.M. and Jones, A.M., 2009. The changing epidemiology of resistance. Journal of antimicrobial chemotherapy, 64(suppl_1), pp.i3-i10.

Henderson, J.C., Zimmerman, S.M., Crofts, A.A., Boll, J.M., Kuhns, L.G., Herrera, C.M. and Trent, M.S., 2016. The power of asymmetry: architecture and assembly of the Gram-negative outer membrane lipid bilayer. Annual review of microbiology, 70, pp.255-278.

Hendriksen, R.S., Bortolaia, V., Tate, H., Tyson, G.H., Aarestrup, F.M. and McDermott, P.F., 2019. Using genomics to track global antimicrobial resistance. Frontiers in public health, 7, p.242.

Heritier, C., Poirel, L. and Nordmann, P., 2006. Cephalosporinase over-expression resulting from insertion of ISAba1 in Acinetobacter baumannii. Clinical microbiology and infection, 12(2), pp.123-130.

Hoffman, S.B., 2001. Mechanisms of antibiotic resistance. Compendium, 23(5), pp.464-473.

Hofmann, A.F. and Eckmann, L., 2006. How bile acids confer gut mucosal protection against bacteria. Proceedings of the National Academy of Sciences, 103(12), pp.4333-4334.

Hong, J., Hu, J. and Ke, F., 2016. Experimental induction of bacterial resistance to the antimicrobial peptide tachyplesin I and investigation of the resistance mechanisms. Antimicrobial agents and chemotherapy, 60(10), pp.6067-6075.

Hopwood, D.A., 2007. Streptomyces in nature and medicine: the antibiotic makers. Oxford University Press.

Horna, G., López, M., Guerra, H., Saénz, Y. and Ruiz, J., 2018. Interplay between MexAB-OprM and MexEF-OprN in clinical isolates of Pseudomonas aeruginosa. Scientific reports, 8(1), pp.1-11.

Housseini B Issa, K., Phan, G. and Broutin, I., 2018. Functional mechanism of the efflux pumps transcription regulators from Pseudomonas aeruginosa based on 3D structures. Frontiers in molecular biosciences, 5, p.57.

Howell, M., Wirz, D., Daniels, A.U. and Braissant, O., 2012. Application of a microcalorimetric method for determining drug susceptibility in mycobacterium species. Journal of clinical microbiology, 50(1), pp.16-20.

Huang, W.S., Metcalf, C.A., Sundaramoorthi, R., Wang, Y., Zou, D., Thomas, R.M., Zhu, X., Cai, L., Wen, D., Liu, S. and Romero, J., 2010. Discovery of 3-[2-(imidazo [1, 2-b] pyridazin-3-yl) ethynyl]-4-methyl-N-{4-[(4-methylpiperazin-1-yl) methyl]-3-(trifluoromethyl) phenyl} benzamide (AP24534), a potent, orally active pan-inhibitor of breakpoint cluster region-abelson (BCR-ABL) kinase including the T315I gatekeeper mutant. Journal of medicinal chemistry, 53(12), pp.4701-4719.

Hughes, C.C. and Fenical, W., 2010. Antibacterials from the sea. Chemistry–A European Journal, 16(42), pp.12512-12525.

Hutchings, M.I., Truman, A.W. and Wilkinson, B., 2019. Antibiotics: past, present and future. Current opinion in microbiology, 51, pp.72-80.

Hüttel, S., Testolin, G., Herrmann, J., Planke, T., Gille, F., Moreno, M., Stadler, M., Broenstrup, M., Kirschning, A. and Müller, R., 2017. Discovery and Total synthesis of natural cystobactamid derivatives with superior activity against Gram-negative pathogens. Angewandte Chemie International Edition, 56(41), pp.12760-12764.

Iftikhar, A., Asif, A., Manzoor, A., Azeem, M., Sarwar, G., Rashid, N. and Qaisar, U., 2020. Mutation in pvcABCD operon of Pseudomonas aeruginosa modulates MexEF-OprN efflux system and hence resistance to chloramphenicol and ciprofloxacin. Microbial pathogenesis, 149, p.104491.

Jana, S., and Deb, J.K., 2006. Molecular understanding of aminoglycoside action and resistance. Applied microbiology and biotechnology, 70, pp.140-150.

Jeannot, K., Elsen, S., Köhler, T., Attree, I., Van Delden, C. and Plésiat, P., 2008. Resistance and virulence of Pseudomonas aeruginosa clinical strains overproducing the MexCD-OprJ efflux pump. Antimicrobial agents and chemotherapy, 52(7), pp.2455-2462.

Jia, J., Zhang, C., Liu, Y., Huang, Y., Bai, Y., Hang, X., Zeng, L., Zhu, D. and Bi, H., 2022. Armeniaspirol A: a novel anti-Helicobacter pylori agent. Microbial Biotechnology, 15(2), pp.442-454.

Jo, I., Hong, S., Lee, M., Song, S., Kim, J.S., Mitra, A.K., Hyun, J., Lee, K. and Ha, N.C., 2017. Stoichiometry and mechanistic implications of the MacAB-TolC tripartite efflux pump. Biochemical and biophysical research communications, 494(3-4), pp.668-673.

Kashuba, E., Dmitriev, A.A., Kamal, S.M., Melefors, O., Griva, G., Römling, U., Ernberg, I., Kashuba, V. and Brouchkov, A., 2017. Ancient permafrost staphylococci carry antibiotic resistance genes. Microbial ecology in health and disease, 28(1), pp.1345574.

Kawalek, A., Modrzejewska, M., Zieniuk, B., Bartosik, A.A. and Jagura-Burdzy, G., 2019. Interaction of ArmZ with the DNA-binding domain of MexZ induces expression of mexXY multidrug efflux pump genes and antimicrobial resistance in Pseudomonas aeruginosa. Antimicrobial Agents and Chemotherapy, 63(12), pp.e01199-19.

Kelmani Chandrakanth, R., Raju, S. and Patil, S.A., 2008. Aminoglycoside-resistance mechanisms in multidrug-resistant Staphylococcus aureus clinical isolates. Current Microbiology, 56, pp.558-562.

Kim, Y.C. and Hummer, G., 2012. Proton-pumping mechanism of cytochrome c oxidase: A kinetic master-equation approach. Biochimica et Biophysica Acta (BBA)-Bioenergetics, 1817(4), pp.526-536. Law, C.J., Maloney, P.C., and Wang, D.N., 2008. Ins and outs of major facilitator superfamily antiporters. Annu. Rev. Microbiol., 62, pp.289-305.

Köhler, T., Epp, S.F., Curty, L.K. and Pechère, J.C., 1999. Characterization of MexT, the regulator of the MexE-MexF-OprN multidrug efflux system of Pseudomonas aeruginosa. Journal of bacteriology, 181(20), pp.6300-6305.

Kornelsen, V. and Kumar, A., 2021. Update on multidrug resistance efflux pumps in Acinetobacter spp. Antimicrobial Agents and Chemotherapy, 65(7), pp.e00514-21. Langevin, A.M. and Dunlop, M.J., 2018. Stress introduction rate alters the benefit of AcrAB-TolC efflux pumps. Journal of bacteriology, 200(1), pp.e00525-17.

Köser, C.U., Ellington, M.J. and Peacock, S.J., 2014. Whole-genome sequencing to control antimicrobial resistance. Trends in Genetics, 30(9), pp.401-407.

Kostrzewa, M., Sparbier, K., Maier, T. and Schubert, S., 2013. MALDI-TOF MS: an upcoming tool for rapid detection of antibiotic resistance in microorganisms. PROTEOMICS–Clinical Applications, 7(11-12), pp.767-778.

Labana, P., Dornan, M.H., Lafrenière, M., Czarny, T.L., Brown, E.D., Pezacki, J.P. and Boddy, C.N., 2021. Armeniaspirols inhibit the AAA+ proteases ClpXP and ClpYQ leading to cell division arrest in Gram-positive bacteria. Cell Chemical Biology, 28(12), pp.1703-1715.

Lambert, P., 2002. Mechanisms of antibiotic resistance in Pseudomonas aeruginosa. Journal of the royal society of medicine, 95(41), pp.22.

Lambert, P.A., 2005. Bacterial resistance to antibiotics: modified target sites. Advanced drug delivery reviews, 57(10), pp.1471-1485.

Lanzotti, V., Bonanomi, G. and Scala, F., 2013. What makes Allium species effective against pathogenic microbes?. Phytochemistry reviews, 12(1), pp.751-772.

Ledeboer, N.A. and Hodinka, R.L., 2011. Molecular detection of resistance determinants. Journal of Clinical Microbiology, 49(9_Supplement), pp.S20-S24.

Lekshmi, M., Ammini, P., Adjei, J., Sanford, L.M., Shrestha, U., Kumar, S., and Varela, M.F., 2018. Modulation of antimicrobial efflux pumps of the major facilitator superfamily in Staphylococcus aureus. AIMS microbiology, 4(1), pp.1.

Li, Z., Xu, M., Wei, H., Wang, L. and Deng, M., 2019. RNA-seq analyses of antibiotic resistance mechanisms in Serratia marcescens. Molecular Medicine Reports, 20(1), pp.745-754.

Lin, F.Y., Liu, C.I., Liu, Y.L., Zhang, Y., Wang, K., Jeng, W.Y., Ko, T.P., Cao, R., Wang, A.H.J. and Oldfield, E., 2010. Mechanism of action and inhibition of dehydrosqualene synthase. Proceedings of the National Academy of Sciences, 107(50), pp.21337-21342.

Lin, M.F., Lin, Y.Y. and Lan, C.Y., 2015. The role of the two-component system BaeSR in disposing chemicals through regulating transporter systems in Acinetobacter baumannii. PLoS One, 10(7), pp.e0132843.

Lin, Y.T., Huang, Y.W., Liou, R.S., Chang, Y.C. and Yang, T.C., 2014. MacABCsm, an ABC-type tripartite efflux pump of Stenotrophomonas maltophilia involved in drug resistance, oxidative and envelope stress tolerances and biofilm formation. Journal of Antimicrobial Chemotherapy, 69(12), pp.3221-3226.

Liu, Y., Lehnert, T. and Gijs, M.A., 2020. Fast antimicrobial susceptibility testing on Escherichia coli by metabolic heat nanocalorimetry. Lab on a Chip, 20(17), pp.3144-3157.

Lou, H., Chen, M., Black, S.S., Bushell, S.R., Ceccarelli, M., Mach, T., Beis, K., Low, A.S., Bamford, V.A., Booth, I.R. and Bayley, H., 2011. Altered antibiotic transport in OmpC mutants isolated from a series of clinical strains of multi-drug resistant E. coli. PloS one, 6(10), p.e25825.

Lounasmaa, M., Puri, H.S. and Widén, C.J., 1977. Phloroglucinol derivatives of Callistemon lanceolatus leaves. Phytochemistry (UK).

Lu, T.K. and Collins, J.J., 2009. Engineered bacteriophage targeting gene networks as adjuvants for antibiotic therapy. Proceedings of the National Academy of Sciences, 106(12), pp.4629-4634.

Lytvynenko, I., Brill, S., Oswald, C., and Pos, K.M., 2016. Molecular basis of polyspecificity of the small multidrug resistance efflux pump AbeS from Acinetobacter baumannii. Journal of Molecular Biology, 428(3), pp.644-657.

Ma, Z., Xu, C., Zhang, X., Wang, D., Pan, X., Liu, H., Zhu, G., Bai, F., Cheng, Z., Wu, W. and Jin, Y., 2021. A MexR mutation which confers aztreonam resistance to Pseudomonas aeruginosa. Frontiers in Microbiology, 12, p.659808.

MacNeil, I.A., Tiong, C.L., Minor, C., August, P.R., Grossman, T.H., Loiacono, K.A., Lynch, B.A., Phillips, T., Narula, S., Sundaramoorthi, R. and Tyler, A., 2001. Expression and isolation of antimicrobial small molecules from soil DNA libraries. Journal of molecular microbiology and biotechnology, 3(2), pp.301-308.

Magiorakos AP, Srinivasan A, Carey RB, Carmeli Y, Falagas ME, Giske CG, Harbarth S, Hindler JF, Kahlmeter G, Olsson-Liljequist B, Paterson DL, Rice LB, Stelling J, Struelens MJ, Vatopoulos A, Weber JT, Monnet DL. 2012. Multidrug-resistant, extensively drug-resistant and pandrug-resistant bacteria: an international expert proposal for interim standard definitions for acquired resistance. Clinical Microbiological Infection. 18(3), pp.268-81.

Mak, S., Xu, Y. and Nodwell, J.R., 2014. The expression of antibiotic resistance genes in antibiotic-producing bacteria. Molecular microbiology, 93(3), pp.391-402.

Makovitzki, A., Avrahami, D. and Shai, Y., 2006. Ultrashort antibacterial and antifungal lipopeptides. Proceedings of the National Academy of Sciences, 103(43), pp.15997-16002.

Manjasetty, B.A., Halavaty, A.S., Luan, C.H., Osipiuk, J., Mulligan, R., Kwon, K., Anderson, W.F. and Joachimiak, A., 2016. Loop-to-helix transition in the structure of multidrug regulator AcrR at the entrance of the drug-binding cavity. Journal of structural biology, 194(1), pp.18-28.

Martinez JL, Baquero F. Mutation frequencies and antibiotic resistance. Antimicrob Agents Chemother. 2000 Jul;44(7):1771-7. doi: 10.1128/AAC.44.7.1771-1777.2000. PMID: 10858329; PMCID: PMC89960

Maugeri, G., Lychko, I., Sobral, R. and Roque, A.C., 2019. Identification and antibiotic-susceptibility profiling of infectious bacterial agents: a review of current and future trends. Biotechnology journal, 14(1), pp.1700750.

McAleese, F., Petersen, P., Ruzin, A., Dunman, P.M., Murphy, E., Projan, S.J. and Bradford, P.A., 2005. A novel MATE family efflux pump contributes to the reduced susceptibility of laboratory-derived Staphylococcus aureus mutants to tigecycline. Antimicrobial agents and chemotherapy, 49(5), pp.1865-1871.

McPhillie, M.J., Cain, R.M., Narramore, S., Fishwick, C.W. and Simmons, K.J., 2015. Computational methods to identify new antibacterial targets. Chemical Biology & Drug Design, 85(1), pp.22-29.

Messaoud, C., Zaouali, Y., Salah, A.B., Khoudja, M.L. and Boussaid, M., 2005. Myrtus communis in Tunisia: variability of the essential oil composition in natural populations. Flavour and Fragrance Journal, 20(6), pp.577-582.

Messaoud, C., Laabidi, A. and Boussaid, M., 2012. Myrtus communis L. infusions: the effect of infusion time on phytochemical composition, antioxidant, and antimicrobial activities. Journal of food science, 77(9), pp.C941-C947.

Morita, Y., Tomida, J. and Kawamura, Y., 2012. Primary mechanisms mediating aminoglycoside resistance in the multidrug-resistant Pseudomonas aeruginosa clinical isolate PA7. Microbiology, 158(4), pp.1071-1083.

Mujwar, S., Deshmukh, R., Harwansh, R.K., Gupta, J.K. and Gour, A., 2019. Drug repurposing approach for developing novel therapy against mupirocin-resistant Staphylococcus aureus. Assay and drug development technologies, 17(7), pp.298-309.

Muller, C., Plésiat, P. and Jeannot, K., 2011. A two-component regulatory system interconnects resistance to polymyxins, aminoglycosides, fluoroquinolones, and β-lactams in Pseudomonas aeruginosa. Antimicrobial agents and chemotherapy, 55(3), pp.1211-1221.

Murray, B.E., 1992. Beta-lactamase-producing enterococci. Antimicrobial agents and chemotherapy, 36(11), pp.2355-2359.

Murray, J.L., Kwon, T., Marcotte, E.M. and Whiteley, M., 2015. Intrinsic antimicrobial resistance determinants in the superbug Pseudomonas aeruginosa. MBio, 6(6), pp.e01603-15.

Ni, R.T., Onishi, M., Mizusawa, M., Kitagawa, R., Kishino, T., Matsubara, F., Tsuchiya, T., Kuroda, T. and Ogawa, W., 2020. The role of RND-type efflux pumps in multidrug-resistant mutants of Klebsiella pneumoniae. Scientific reports, 10(1), pp.1-10.

Nicoletti, R., Salvatore, M.M., Ferranti, P. and Andolfi, A., 2018. Structures and bioactive properties of myrtucommulones and related acylphloroglucinols from Myrtaceae. Molecules, 23(12), p.3370.

Nikaido, H., 2003. Molecular basis of bacterial outer membrane permeability revisited. Microbiology and molecular biology reviews, 67(4), pp.593-656.

Nishino, K., Nikaido, E. and Yamaguchi, A., 2009. Regulation and physiological function of multidrug efflux pumps in Escherichia coli and Salmonella. Biochimica et Biophysica Acta (BBA)-Proteins and Proteomics, 1794(5), pp.834-843.

Nordmann, P., Poirel, L. and Dortet, L., 2012. Rapid detection of carbapenemase-producing Enterobacteriaceae.

Omote, H., Hiasa, M., Matsumoto, T., Otsuka, M. and Moriyama, Y., 2006. The MATE proteins as fundamental transporters of metabolic and xenobiotic organic cations. Trends in pharmacological sciences, 27(11), pp.587-593.

Ota, Y., Furuhashi, K., Nanba, T., Yamanaka, K., Ishikawa, J., Nagura, O., Hamada, E. and Maekawa, M., 2019. A rapid and simple detection method for phenotypic antimicrobial resistance in Escherichia coli by loop-mediated isothermal amplification. Journal of Medical Microbiology, 68(2), pp.169-177.

Owlia, P., Najafabadi, L.M., Nadoshan, S.M., Rasooli, I. and Saderi, H., 2010. Effects of sub-minimal inhibitory concentrations of some essential oils on virulence factors of Pseudomonas aeruginosa. Journal of Essential Oil Bearing Plants, 13(4), pp.465-476.

Padariya, M., Kalathiya, U. and Baginski, M., 2018. Structural and dynamic insights on the EmrE protein with TPP+ and related substrates through molecular dynamics simulations. Chemistry and physics of lipids, 212, pp.1-11.

Paduch, R., Woźniak, A., Niedziela, P. and Rejdak, R., 2014. Assessment of eyebright (Euphrasia officinalis L.) extract activity in relation to human corneal cells using in vitro tests. Balkan medical journal, 2014(1), pp.29-36.

Park, Y.K., Choi, J.Y., Shin, D., and Ko, K.S., 2011. Correlation between overexpression and amino acid substitution of the PmrAB locus and colistin resistance in Acinetobacter baumannii. International journal of antimicrobial agents, 37(6), pp.525-530.

Pasqua, M., Bonaccorsi di Patti, M.C., Fanelli, G., Utsumi, R., Eguchi, Y., Trirocco, R., Prosseda, G., Grossi, M. and Colonna, B., 2021. Host-Bacterial pathogen communication: the Wily role of the multidrug efflux pumps of the MFS family. Frontiers in Molecular Biosciences, 8, pp.723274.

Patrinos, G.P. and Ansorge, W. eds., 2009. Molecular diagnostics. Academic Press.

Paul, S.M., Mytelka, D.S., Dunwiddie, C.T., Persinger, C.C., Munos, B.H., Lindborg, S.R., and Schacht, A.L., 2010. How to improve R&D productivity: the pharmaceutical industry's grand challenge. Nature reviews Drug discovery, 9(3), pp.203-214.

Paulsen, I.T., Skurray, R.A., Tam, R., Saier Jr, M.H., Turner, R.J., Weiner, J.H., Goldberg, E.B. and Grinius, L.L., 1996. The SMR family: a novel family of multidrug efflux proteins involved with the efflux of lipophilic drugs. Molecular microbiology, 19(6), pp.1167-1175.

Payne, D.J., Gwynn, M.N., Holmes, D.J. and Pompliano, D.L., 2007. Drugs for bad bugs: confronting the challenges of antibacterial discovery. Nature reviews Drug discovery, 6(1), pp.29-40.

Peterson, A., Aas, S. and Wasserman, D., 2018. Selected Abstracts From the 2018 International Neuroethics Society Annual Meeting, *AJOB Neuroscience* 9(4), pp. W1-W21.

Piddock, L.J., 2006. Clinically relevant chromosomally encoded multidrug resistance efflux pumps in bacteria. Clinical microbiology reviews, 19(2), pp.382-402.

Pidot, S.J., Coyne, S., Kloss, F. and Hertweck, C., 2014. Antibiotics from neglected bacterial sources. International Journal of Medical Microbiology, 304(1), pp.14-22.

Poole, K., 2008. Bacterial multidrug efflux pumps serve other functions. Microbe-American Society for Microbiology, 3(4), p.179.

Prija, F. and Prasad, R., 2017. DrrC protein of Streptomyces peucetius removes daunorubicin from intercalated dnrI promoter. Microbiological Research, 202, pp.30-35.

Putman, M., van Veen, H.W. and Konings, W.N., 2000. Molecular properties of bacterial multidrug transporters. Microbiology and molecular biology reviews, 64(4), pp.672-693.

Rabbani, B., Nakaoka, H., Akhondzadeh, S., Tekin, M. and Mahdieh, N., 2016. Next generation sequencing: implications in personalized medicine and pharmacogenomics. Molecular biosystems, 12(6), pp.1818-1830.

Rahman, H., Austin, B., Mitchell, W.J., Morris, P.C., Jamieson, D.J., Adams, D.R., Spragg, A.M. and Schweizer, M., 2010. Novel anti-infective compounds from marine bacteria. Marine drugs, 8(3), pp.498-518.

Ramirez, M.S. and Tolmasky, M.E., 2010. Aminoglycoside modifying enzymes. Drug resistance updates, 13(6), pp.151-171.

Reeve, S.M., Gainza, P., Frey, K.M., Georgiev, I., Donald, B.R. and Anderson, A.C., 2015. Protein design algorithms predict viable resistance to an experimental antifolate. Proceedings of the National Academy of Sciences, 112(3), pp.749-754.

Reller, L.B., Weinstein, M., Jorgensen, J.H. and Ferraro, M.J., 2009. Antimicrobial susceptibility testing: a review of general principles and contemporary practices. Clinical infectious diseases, 49(11), pp.1749-1755.

Rentschler, S., Kaiser, L. and Deigner, H.P., 2021. Emerging options for the diagnosis of bacterial infections and the characterization of antimicrobial resistance. International Journal of Molecular Sciences, 22(1), p.456.

Ruiz, B., Chávez, A., Forero, A., García-Huante, Y., Romero, A., Sánchez, M., Rocha, D., Sánchez, B., Rodríguez-Sanoja, R., Sánchez, S. and Langley, E., 2010. Production of microbial secondary metabolites: regulation by the carbon source. Critical reviews in microbiology, 36(2), pp.146-167.

Ruiz, J., 2019. Transferable mechanisms of quinolone resistance from 1998 onward. Clinical microbiology reviews, 32(4), pp.e00007-19.

Santiago-Rodriguez, T.M., Fornaciari, G., Luciani, S., Dowd, S.E., Toranzos, G.A., Marota, I. and Cano, R.J., 2015. Gut microbiome of an 11th century AD pre-Columbian Andean mummy. PloS one, 10(9), pp.e0138135.

Schildkraut, J.A., Coolen, J.P., Burbaud, S., Sangen, J.J., Kwint, M.P., Floto, R.A., op den Camp, H.J., Te Brake, L.H., Wertheim, H.F., Neveling, K. and Hoefsloot, W., 2022. RNA Sequencing Elucidates Drug-Specific Mechanisms of Antibiotic Tolerance and Resistance in Mycobacterium abscessus. Antimicrobial Agents and Chemotherapy, 66(1), pp.e01509-21.

Schnellmann, C., Gerber, V., Rossano, A., Jaquier, V., Panchaud, Y., Doherr, M.G., Thomann, A., Straub, R. and Perreten, V., 2006. Presence of new mecA and mph (C) variants conferring antibiotic resistance in Staphylococcus spp. isolated from the skin of horses before and after clinic admission. Journal of Clinical Microbiology, 44(12), pp.4444-4454.

Sevillano, E., Gallego, L. and Garcia-Lobo, J.M., 2009. First detection of the OXA-40 carbapenemase in P. aeruginosa isolates, located on a plasmid also found in A. baumannii. Pathologie Biologie, 57(6), pp.493-495.

Sharma, M., Singhal, L., Gautam, V. and Ray, P., 2020. Distribution of carbapenemase genes in clinical isolates of Acinetobacter baumannii & a comparison of MALDI-TOF mass spectrometry-based detection of carbapenemase production with other phenotypic methods. The Indian Journal of Medical Research, 151(6), p.585.

Sharpe, A.N. and Jackson, A.K., 1972. Stomaching: a new concept in bacteriological sample preparation. Applied microbiology, 24(2), pp.175-178.

Silverstein, A.M., 2005. Paul Ehrlich, archives and the history of immunology. Nature immunology, 6(7), pp.639-639.

Soria-Mercado, I.E., Prieto-Davo, A., Jensen, P.R. and Fenical, W., 2005. Antibiotic terpenoid chloro-dihydroquinones from a new marine actinomycete. Journal of natural products, 68(6), pp.904-910.

Srinivasan, V.B. and Rajamohan, G., 2013. KpnEF, a new member of the Klebsiella pneumoniae cell envelope stress response regulon, is an SMR-type efflux pump involved in broad-spectrum antimicrobial resistance. Antimicrobial agents and chemotherapy, 57(9), pp.4449-4462.

Stelitano, G., Sammartino, J.C. and Chiarelli, L.R., 2020. Multitargeting compounds: a promising strategy to overcome multi-drug resistant tuberculosis. Molecules, 25(5), p.1239.

Strommenger, B., Kettlitz, C., Werner, G. and Witte, W., 2003. Multiplex PCR assay for simultaneous detection of nine clinically relevant antibiotic resistance genes in Staphylococcus aureus. Journal of clinical microbiology, 41(9), pp.4089-4094.

Sulavik, M.C., Houseweart, C., Cramer, C., Jiwani, N., Murgolo, N., Greene, J., DiDomenico, B., Shaw, K.J., Miller, G.H., Hare, R. and Shimer, G., 2001. Antibiotic susceptibility profiles of Escherichia coli strains lacking multidrug efflux pump genes. Antimicrobial agents and chemotherapy, 45(4), pp.1126-1136.

Sun, J.R., Chiang, Y.S., Shang, H.S., Perng, C.L., Yang, Y.S. and Chiueh, T.S., 2017. Phenotype microarray analysis of the AdeRS two-component system in Acinetobacter baumannii. European Journal of Clinical Microbiology & Infectious Diseases, 36(12), pp.2343-2353.

Suresh, M., Nithya, N., Jayasree, P.R., Vimal, K.P. and Manish Kumar, P.R., 2018. Mutational analyses of regulatory genes, mexR, nalC, nalD and mexZ of mexAB-oprM and mexXY operons, in efflux pump hyperexpressing multidrug-resistant clinical isolates of Pseudomonas aeruginosa. World Journal of Microbiology and Biotechnology, 34, pp.1-11.

Tacconelli, E., 2017. Global Priority List of Antibiotic-Resistant Bacteria to Guide Research, Discovery, and Development.

Tafti, F.A., Eslami, G., Zandi, H. and Barzegar, K., 2020. Mutations in nalc gene of Mex AB-OprM efflux pump in carbapenem resistant Pseudomonas aeruginosa isolated from burn wounds in Yazd, Iran. Iranian Journal of Microbiology, 12(1), pp.32.

Testolin, G., 2019. Structural optimization and photopharmacological studies of the cystobactamids class of natural products.

Testolin, G., Cirnski, K., Rox, K., Prochnow, H., Fetz, V., Grandclaudon, C., Mollner, T., Baiyoumy, A., Ritter, A., Leitner, C. and Krull, J., 2020. Synthetic studies of cystobactamids as antibiotics and bacterial imaging carriers lead to compounds with high in vivo efficacy. Chemical Science, 11(5), pp.1316-1334.

Thacharodi, A. and Lamont, I.L., 2022. Aminoglycoside-Modifying Enzymes Are Sufficient to Make Pseudomonas aeruginosa Clinically Resistant to Key Antibiotics. Antibiotics, 11(7), p.884.

Tooke, C.L., Hinchliffe, P., Bragginton, E.C., Colenso, C.K., Hirvonen, V.H., Takebayashi, Y. and Spencer, J., 2019. β-Lactamases and β-Lactamase Inhibitors in the 21st Century. Journal of molecular biology, 431(18), pp.3472-3500.

Tossi, A., Sandri, L. and Giangaspero, A., 2000. Amphipathic, α-helical antimicrobial peptides. Peptide Science, 55(1), pp.4-30.

Tsalik, E.L., Bonomo, R.A. and Fowler Jr, V.G., 2018. New molecular diagnostic approaches to bacterial infections and antibacterial resistance. Annual review of medicine, 69, pp.379-394.

Tuon, F.F., Dantas, L.R., Suss, P.H. and Tasca Ribeiro, V.S., 2022. Pathogenesis of the Pseudomonas aeruginosa biofilm: A review. Pathogens, 11(3), p.300.

Turnidge, J. and Collignon, P., 1999. Resistance to fusidic acid. International Journal of Antimicrobial Agents, 12(1), pp.S35-S44.

U.S. Department of Health and Human Services. 2016. New Drugs at FDA: CDER's new molecular entities and new therapeutic biological products. http://wayback.archive-it.org/7993/20161022052126/http://www.fda.gov/Drugs/DevelopmentApprovalProcess/DrugInnovation/default.htm. (Accessed: 28 February 2023).

Ude, J., Tripathi, V., Buyck, J.M., Söderholm, S., Cunrath, O., Fanous, J., Claudi, B., Egli, A., Schleberger, C., Hiller, S. and Bumann, D., 2021. Outer membrane permeability: Antimicrobials and diverse nutrients bypass porins in Pseudomonas aeruginosa. Proceedings of the National Academy of Sciences, 118(31), p.e2107644118.

Uzoh, A., 2022. ANTIBIOTIC RESISTANCE IN THE MEMBER STATES OF THE EUROPEAN UNION.

Valderrama, K., Pradel, E., Firsov, A.M., Drobecq, H., Bauderlique-le Roy, H., Villemagne, B., Antonenko, Y.N. and Hartkoorn, R.C., 2019. Pyrrolomycins are potent natural protonophores. Antimicrobial agents and chemotherapy, 63(10), pp.e01450-19.

Valot, B., Guyeux, C., Rolland, J.Y., Mazouzi, K., Bertrand, X. and Hocquet, D., 2015. What it takes to be a Pseudomonas aeruginosa? The core genome of the opportunistic pathogen updated. PloS one, 10(5), p.e0126468.

van Belkum, A., Burnham, C.A.D., Rossen, J.W., Mallard, F., Rochas, O. and Dunne Jr, W.M., 2020. Innovative and rapid antimicrobial susceptibility testing systems. Nature Reviews Microbiology, 18(5), pp.299-311.

van Santen, J.A., Poynton, E.F., Iskakova, D., McMann, E., Alsup, T.A., Clark, T.N., Fergusson, C.H., Fewer, D.P., Hughes, A.H., McCadden, C.A. and Parra, J., 2022. The Natural Products Atlas 2.0: A database of microbially-derived natural products. Nucleic acids research, 50(D1), pp.D1317-D1323.

Vázquez-López, R., Solano-Gálvez, S.G., Juárez Vignon-Whaley, J.J., Abello Vaamonde, J.A., Padró Alonzo, L.A., Rivera Reséndiz, A., Muleiro Álvarez, M., Vega López, E.N., Franyuti-Kelly, G., Álvarez-Hernández, D.A. and Moncaleano Guzmán, V., 2020. Acinetobacter baumannii resistance: a real challenge for clinicians. Antibiotics, 9(4), p.205.

Visutthi, M., Srimanote, P. and Voravuthikunchai, S.P., 2011. Responses in the expression of extracellular proteins in methicillin-resistant Staphylococcus aureus treated with rhodomyrtone. The Journal of Microbiology, 49, pp.956-964. Huang, L., Wu, C., Gao, H., Xu, C., Dai, M., Huang, L., Hao, H., Wang, X. and Cheng, G., 2022. Bacterial multidrug efflux pumps at the frontline of antimicrobial resistance: An overview. Antibiotics, 11(4), p.520.

von Ah, U., Wirz, D., and Daniels, A.U., 2009. Isothermal micro calorimetry–a new method for MIC determinations: results for 12 antibiotics and reference strains of E. coli and S. aureus. BMC microbiology, 9(1), pp.1-14.

Vrioni, G., Tsiamis, C., Oikonomidis, G., Theodoridou, K., Kapsimali, V. and Tsakris, A., 2018. MALDI-TOF mass spectrometry technology for detecting biomarkers of antimicrobial resistance: current achievements and future perspectives. Annals of translational medicine, 6(12).

Waksman, S.A., Schatz, A., and Reynolds, D.M., 2010. Production of antibiotic substances by actinomycetes. Annals of the New York Academy of Sciences, 1213(1), p.112.

Walesch, S., Birkelbach, J., Jézéquel, G., Haeckl, F.J., Hegemann, J.D., Hesterkamp, T., Hirsch, A.K., Hammann, P. and Müller, R., 2023. Fighting antibiotic resistance—strategies and (pre) clinical developments to find new antibacterials. EMBO reports, 24(1), p.e56033.

Walker, J.N., Crosby, H.A., Spaulding, A.R., Salgado-Pabón, W., Malone, C.L., Rosenthal, C.B., Schlievert, P.M., Boyd, J.M. and Horswill, A.R., 2013. The Staphylococcus aureus ArlRS

two-component system is a novel regulator of agglutination and pathogenesis. PLoS pathogens, 9(12), p.e1003819.

Walsh, C. and Wright, G., 2005. Introduction: antibiotic resistance. Chemical reviews, 105(2), pp.391-394.

Wang, E., Mi, X., Thompson, M.C., Montoya, S., Notti, R.Q., Afaghani, J., Durham, B.H., Penson, A., Witkowski, M.T., Lu, S.X. and Bourcier, J., 2022. Mechanisms of resistance to noncovalent Bruton's tyrosine kinase inhibitors. New England Journal of Medicine, 386(8), pp.735-743.

Warinner, C., Rodrigues, J.F.M., Vyas, R., Trachsel, C., Shved, N., Grossmann, J., Radini, A., Hancock, Y., Tito, R.Y., Fiddyment, S. and Speller, C., 2014. Pathogens and host immunity in the ancient human oral cavity. Nature genetics, 46(4), pp.336-344.

Watkins, R.R., Papp-Wallace, K.M., Drawz, S.M. and Bonomo, R.A., 2013. Novel β-lactamase inhibitors: a therapeutic hope against the scourge of multidrug resistance. Frontiers in microbiology, 4, p.392. Thong, W.L., Zhang, Y., Zhuo, Y., Robins, K.J., Fyans, J.K., Herbert, A.J., Law, B.J. and Micklefield, J., 2021. Gene editing enables rapid engineering of complex antibiotic assembly lines. Nature Communications, 12(1), p.6872.

Webber, M.A. and Piddock, L.J.V., 2003. The importance of efflux pumps in bacterial antibiotic resistance. Journal of antimicrobial chemotherapy, 51(1), pp.9-11.

Wen, X., Langevin, A.M. and Dunlop, M.J., 2018. Antibiotic export by efflux pumps affects growth of neighboring bacteria. Scientific Reports, 8(1), p.15120.

Werth, B. J. 2022. Overview of antibacterial drugs. https://www.merckmanuals.com/professional/infectious-diseases/bacteria-and-antibacterial-drugs/overview-of-antibacterial-drugs. (Accessed: 30 January 2023).

Westfall, L.W., Carty, N.L., Layland, N., Kuan, P., Colmer-Hamood, J.A., and Hamood, A.N., 2006. mvaT mutation modifies the expression of the Pseudomonas aeruginosa multidrug efflux operon mexEF-oprN. FEMS microbiology letters, 255(2), pp.247-254.

Williams, T. 2021. Drug-resistant Infections Led to $1.9 Billion in Health Care Costs, More Than 10,000 Deaths Among Older Adults in One Year. Infectious Diseases Society of America. 7 Oct. 2021.

Wilson, D.N., Hauryliuk, V., Atkinson, G.C. and O'Neill, A.J., 2020. Target protection as a key antibiotic resistance mechanism. Nature Reviews Microbiology, 18(11), pp.637-648.

Wondrack, L., Massa, M., Yang, B.V. and Sutcliffe, J., 1996. Clinical strain of Staphylococcus aureus inactivates and causes efflux of macrolides. Antimicrobial Agents and Chemotherapy, 40(4), pp.992-998.

World Health Organization, 2022. 2021 antibacterial agents in clinical and preclinical development: an overview and analysis.

Wright, G.D., 2010. Q&A: Antibiotic resistance: where does it come from and what can we do about it?. BMC biology, 8, pp.1-6.

Wright, G.D., 2011. Molecular mechanisms of antibiotic resistance. Chemical communications, 47(14), pp.4055-4061.

Wu, C.J., Huang, Y.W., Lin, Y.T., Ning, H.C. and Yang, T.C., 2016. Inactivation of SmeSyRy two-component regulatory system inversely regulates the expression of SmeYZ and SmeDEF efflux pumps in Stenotrophomonas maltophilia. PLoS One, 11(8), p.e0160943.

Xu, Y., Willems, A., Au-Yeung, C., Tahlan, K. and Nodwell, J.R., 2012. A two-step mechanism for the activation of actinorhodin export and resistance in Streptomyces coelicolor. MBio, 3(5), pp.e00191-12.

Yan, X., Xie, Y., Li, C., Donovan, D.M., Gehring, A., Irwin, P. and He, Y., 2022. Comparative transcriptome analysis reveals differentially expressed genes related to antimicrobial properties of lysostaphin in Staphylococcus aureus. Antibiotics, 11(2), p.125.

Yoon, E.J., Balloy, V., Fiette, L., Chignard, M., Courvalin, P. and Grillot-Courvalin, C., 2016. Contribution of the Ade resistance-nodulation-cell division-type efflux pumps to fitness and pathogenesis of Acinetobacter baumannii. MBio, 7(3), pp.e00697-16.

Zborovsky, L., Kleebauer, L., Seidel, M., Kostenko, A., von Eckardstein, L., Gombert, F.O., Weston, J. and Süssmuth, R.D., 2021. Improvement of the antimicrobial potency, pharmacokinetic and pharmacodynamic properties of albicidin by incorporation of nitrogen atoms. Chemical science, 12(43), pp.14606-14617.

Zgurskaya, H.I. and Rybenkov, V.V., 2020. Permeability barriers of Gram-negative pathogens. Annals of the New York Academy of Sciences, 1459(1), pp.5-18.

Zhang, L., Dhillon, P., Yan, H., Farmer, S., and Hancock, R.E., 2000. Interactions of bacterial cationic peptide antibiotics with outer and cytoplasmic membranes of Pseudomonas aeruginosa. Antimicrobial agents and chemotherapy, 44(12), pp.3317-3321.

Ziha-Zarifi, I., Llanes, C., Köhler, T., Pechere, J.C. and Plesiat, P., 1999. In vivo emergence of multidrug-resistant mutants of Pseudomonas aeruginosa overexpressing the active efflux system MexA-MexB-OprM. Antimicrobial Agents and Chemotherapy, 43(2), pp.287-291.

Chapter 2: Transcriptome analysis of armeniaspirol-resistant *E. coli* characterizes an efflux-mediated mechanism of resistance

2.1. Abstract

Armeniaspirols are polyketide compounds and within this study, isolated armeniaspirol-resistant *Escherichia coli* mutants (Arm^R) confirmed and characterized the main resistance mechanism and identified the two major mutations responsible for the resistance mechanism. In addition, a plausible link can be seen between the resistance in Arm^R and other protonophores such as indole as both interfere with the membrane potential of bacterial cells. The main mechanism of Gram-negative *E. coli* strains is efflux-mediated and caused by two different mutations leading to the up-regulation of the putative MdtNOP efflux pump. One, large gene deletions that altered the expression of MdtOP gene and the other a single point mutation within the *mdtO* gene which allowed for the over expression of the *mdtP* gene. The transcriptome profiles of the genotypically unique Arm^R were assessed and linked to the found gene mutations. The overall transcriptome assessment confirmed the role of the putative MdtNOP efflux pump by the over expression of the outer membrane channel gene, *mdtP*. In addition, transcriptomic analysis provided information regarding overall resistance contributors such as acid resistance, propionate metabolism and phage shock operon within all Arm^R which might aid in the understanding of protonophore resistance.

2.2. Introduction

Natural products have provided a major foundation for the development of antibiotic drugs thus far and novel compound classes are discovered continuously (Atanasov *et al*., 2021). Armeniaspirols belong to such a compound class. The strain *Streptomyces armeniacus* DSM-19369 produce three derivatives when cultivated on a malt-containing medium (Dufour *et al.*, 2012) (Figure 2.1). Armeniaspirol (A, B and C) are polyketide antibiotics, the biosynthesis was partially described by Fu and co-workers (2019), and their total synthesis was described by Arisetti and co-workers (2021). Dufour and co-workers (2012) first determined that armeniaspirols display moderate to high *in vitro* activity against Gram-positive pathogens such as methicillin-resistant *Staphylococcus aureus* (MRSA) and vancomycin-resistant *Enterococcus faecium* (VRE).

It was determined that armeniaspirols inhibit the bacterial divisome through direct inhibition of the ClpYQ and ClpXP proteases in *Bacillus subtilis* and other clinically relevant pathogens (Labana *et al*., 2021; Darnowinski *et al*., 2022). However, reported *in vitro* inhibitory

concentrations were significantly higher than the concentrations required to achieving bacterial killing. Thus, Arisetti and co-workers (2021) studied an additional mechanism of action that is independent from protease inhibition and reported that armeniaspirols mainly act through a membrane-directed effect, which is typically seen for protonophores. This is in line with their fast onset of action and lack of resistance development in Gram-positive bacteria such as *S. aureus* (Dufour *et al*., 2012; Labana *et al*., 2021; Arisetti *et al*., 2021). In agreement to Arisetti al co-workers (2021), armeniaspirol A showed *in vitro* and *in vivo* activity to *Helicobacter pylori* strains by the disruption of bacterial cell membranes (Jia *et al*., 2022). Recently, Darnowinski *et al*., 2023 proved that armeniaspirols have a dual mechanism of proton motor force disruption and the inhibition of ClpYQ and ClpXP proteases that result in the observed antibacterial activity. A dual mechanism with a proton motor force disruption can also be observed at high concentrations in *B. subtillus* in another natural product, chelocardin. Interestingly, the main mechanism of *E. coli* and *Klebsiella pneumonia* against chelocardin treatment is also efflux-mediated (Darnowinski *et al*., 2023; Stepanek *et al*., 2016; Hennessen *et al*., 2020; Chabbert and Scavizzi, 1976).

Despite inactivity against wild-type strains of Gram-negative *Pseudomonas aeruginosa* and *E. coli* descibed by Dufour and co-workers (2012), Arisetti and colleagues (2021) found that armeniaspirols are active against *E. coli* when the outer membrane transmembrane domain of the AcrAB-TolC-efflux resistance-nodulation-division (RND) efflux pump is removed (Δ*tolC*). Arisetti and co-workers (2021) further investigated cultivated and investigated the genome of Arm^R that revealed several mutations within *mdtO* gene, which encodes for a component of another putative RND efflux system, MdtNOP, which possibly compensates for the loss of function of AcrAB-TolC. The MdtNOP (synonyms include YjcRQP and SdsRQP) multidrug efflux pump is a putative pump that has been reported to be involved in the resistance to sulfa drugs (Shimanda *et al*., 2009).

The regulation of this putative efflux has not been well described but evidence points towards LeuO, a LysR transcription factor being a regulator. The LeuO was also reported to regulate the multidrug efflux pump, ArcEF. The deletion of the *mdtP* resulted in resistance to several sulfur drugs as well as acriflavin, puromycin, and tetraphenylarsonium chloride (Sulavik *et al*., 2001; Shimada, 2009). Both *mdtO* and *mdtN* are located within the inner membrane. The MdtO is an uncharacterized protein however, a deletion of *mdtO* resulted in sensitivity to sulfur drugs (Shimada, 2009). The MdtN is described as the fusion protein of the MdtNOP efflux pump.

Due to the occurrence of the putative MdtNOP pump linked with resistance in the previous study, we analyzed selected Arm^R and assessed differences in gene expression by transcriptomics. This provided a large overview and a link between the genome, the transcriptome, and the cellular phenotypes of the Arm^R. Three Arm^R had different genotypes

however, all Arm^R shared the most upregulated gene, *mdtP*, with an average up-regulation of 6.7-fold as well as *ymgC* and a biofilm/acid-resistance regulator, *ariR* (*ymcB*) and with an average upregulation of 5.9 and 5-fold, respectively. These findings highlight the importance of *mdtP* within the putative MdtNOP efflux system as well as the role of the putative MdtNOP efflux system in armeniaspirol-resistance in *E. coli*. Further, the transcriptome provides previous unknown information that links the putative multidrug efflux pump with additional means of resistance that include acid-resistance, persister formation, and propionate metabolism.

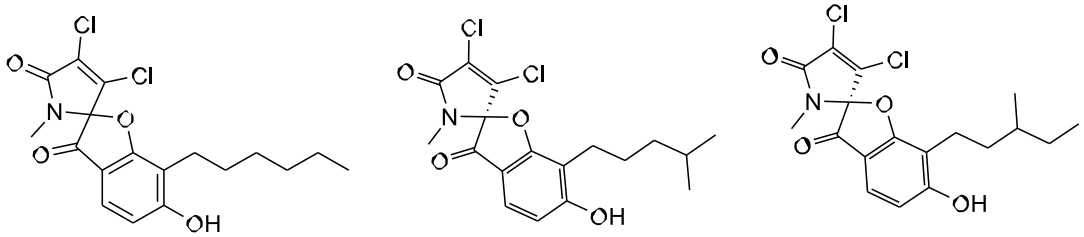

Figure 2.1: Structures of a) armeniaspirol A , b) armeniaspirol B, and c) armeniaspirol C.

2.3. Results

High level Arm^R selection and a low-level frequency of resistance

Arm^R from *E. coli* K12 Δ*tolC* strain (Donner *et al*., 2017) was obtained by means of spontaneous resistance development during the determination of frequency of resistance for armeniaspirol A and armeniaspirol B at 4x MIC (8 µg/mL). We determined the frequency to be 2.5×10^{-8} and 1.25×10^{-8} for armeniaspirol A and armeniaspirol B, respectively. The selected Arm^R had a shift in MIC of ≥32-fold compared to the *E. coli* K12 Δ*tolC* strain with a MIC of 2 µg/mL (Table S2.1).

Whole genome sequencing of Arm^R reveals efflux related and unrelated mutations

A total of 18 Arm^R were selected and sequenced. 50% of Arm^R has mutations that affect the MdtNOP efflux pump while the other 50% of Arm^R has mutations that seem unrelated to the MdtNOP efflux pump (Table 2.1; Table S2.2). Mutations affecting the MdtNOP efflux pump include several point mutations within *mdtO* (component of MdtNOP efflux system) (S2K; S2R; A3K; A3T; L4I; N5G; S6T; L7E; L7V; P8K; L9C; Q654H) as well as large gene deletions that include the *mdtN* (component of MdtNOP efflux system) (*ΔalsRBACEK-yjcS-ytcA-mdtN*). Genes that are seemingly unrelated to the MdtNOP efflux pump are point mutations of *prfB* (peptide chain release factor two) (T173S), intergenic region between *csrA* (Carbon storage regulator A) and *serV* (tRNA serine): (-289C>T), intergenic region upstream of *cvpA* (colicin V production accessory protein) (-70C>T), *FdoG* (formate dehydrogenase-O) (Y145F; N114K) and *plsB* (membrane-bound glycerol-3-phosphate acyltransferase).

Table 2.1: Genotypes of all Arm^R mapped to *E. coli* K12 reference strain (accession no. CP009273.1).

Strain	Genotype
E. coli Δ tolC	*E. coli ΔtolC*
Arm^{R}1	*E. coli ΔtolC; mdtO:* S2K; A3T; L4I; N5G; S6T; L7E; L9C; *prfB:* T173S
Arm^{R}2	*E. coli ΔtolC; mdtO:* S2K; A3K; L4I; N5G; P8K; L9C; *prfB:* T173S
Arm^{R}3	*E. coli ΔtolC; mdtO:* S2R; P8K; L9C; *prfB:* T173S
Arm^{R}4	*E. coli ΔtolC; mdtO:* S2R; N5S; L7V; P8K; L9C; *prfB:* T173S
Arm^{R}5	*E. coli ΔtolC; mdtO:* S2K; A3K; L4I; N5G; S6K; L7E; P8K; L9C; *prfB:* T173S
Arm^{R}6	*E. coli ΔtolC; mdtO:* S2K; A3T; L4I; N5G; S6K; L7E; P8K; L9C; *prfB:* T173S
Arm^{R}7	*E. coli ΔtolC; serV:* -289C>T
Arm^{R}8	*E. coli ΔtolC; serV:* -289C>T
Arm^{R}9	*E. coli ΔtolC; serV:* -289C>T
Arm^{R}10	*E. coli ΔtolC; serV:* -289C>T
Arm^{R}11	*E. coli ΔtolC; serV:* -289C>T
Arm^{R}12	*E. coli ΔtolC; serV:* -289C>T
Arm^{R}13	*E. coli ΔtolC; serV:* -289C>T
Arm^{R}14	*E. coli ΔtolC; cvpA:* -70C>T*; FdoG:* N144K
Arm^{R}15	*E. coli ΔtolC; cvpA:* -70C>T*; FdoG:* N144K*; plsB:* A204P; R207G
Arm^{R}16	*E. coli ΔtolC; ΔalsRBACEK-yjcS-ytcA-mdtN*
Arm^{R}17	*E. coli ΔtolC; ΔalsRBACEK-yjcS-ytcA-mdtN; cvpA:* -70C>T*; FdoG:* Y145F
Arm^{R}18	*E. coli ΔtolC; mdtO:* Q654H*; plsB:* A204P; V206F; R207G; D215G

Arm^R reveals cross-resistance to family compound resistant mutant

No cross-resistance was observed for gentamycin, kanamycin, tetracycline, chloramphenicol, erythromycin, linezolid, and spectinomycin (Table S2.2). However, armeniaspirols share a common mechanism of action with compounds that contain chlorinated pyrrole moieties and therefore assessed armeniaspirol A and armeniaspirol B against a pyrrolomycin-resistant *E. coli* Δ*tolC* strain that was described by Valderrama and co-workers (2020). Here, full cross-resistance (>64 µg/mL) was observed for armeniaspirol A and armeniaspirol B against the pyrrolomycin-resistant *E. coli* Δ*tolC* strain (*E. coli* Δ*tolC* Δ*alsRBACEK-yjcS-ytcA-mdtN*) with large gene deletions that effect the MdtNOP efflux system.

Transcriptomic assessments of Arm^R reveals efflux related and unrelated response

Fully resistant Arm^R were selected to further investigate the MdtNOP efflux pump related mechanism by the transcriptome assessment of Arm^{R}16, Arm^{R}17 and Arm^{R}18. These three Arm^R, not only have two different mutations that affect the MdtNOP efflux pump but also

contains MdtNOP unrelated gene mutations (Table 2.1; Table S2.2). The variation within the gene mutations observed within the Arm^R are diverse, however, the determined MIC of all Arm^R were determined to be >64 µg/mL (Table S2.1). The transcriptome profiles of all three Arm^R showed 41 up-regulated genes and 101 down-regulated genes with a p-value of ≤0.001 and fold-change of ≤-2; ≥2. Overlaying all three transcriptome profiles revealed 13 shared up-regulated genes and 15 shared down-regulated genes (Figure 2.3; Table S2.3). The shared upregulated genes found in all Arm^R was *mdtP* (multidrug resistance outer membrane protein), followed by *ymgC* and *ariR* (*ymgB*) (Figure 2.2; Table S2.3). Further transcriptome analysis revealed a significant difference as Arm^{R}18 has significantly less down-regulate genes compared to Arm^{R}16 and Arm^{R}17 (Figure 2.3).

The GO term enrichment assessment of the shared up-regulated genes resulted in “Propionate catabolic process”, “Propionate metabolic process”, “phage shock” and “Tricarboxylic acid cycle” GO term enrichment. Further, STRING cluster analysis revealed “Phage shock” and “Propionate catabolic” clusters were enriched (Figure 2.4). The KEGG pathway analysis confirmed the enrichment as the “Propanoate metabolism” pathway was significantly enriched (Figure 2.5).

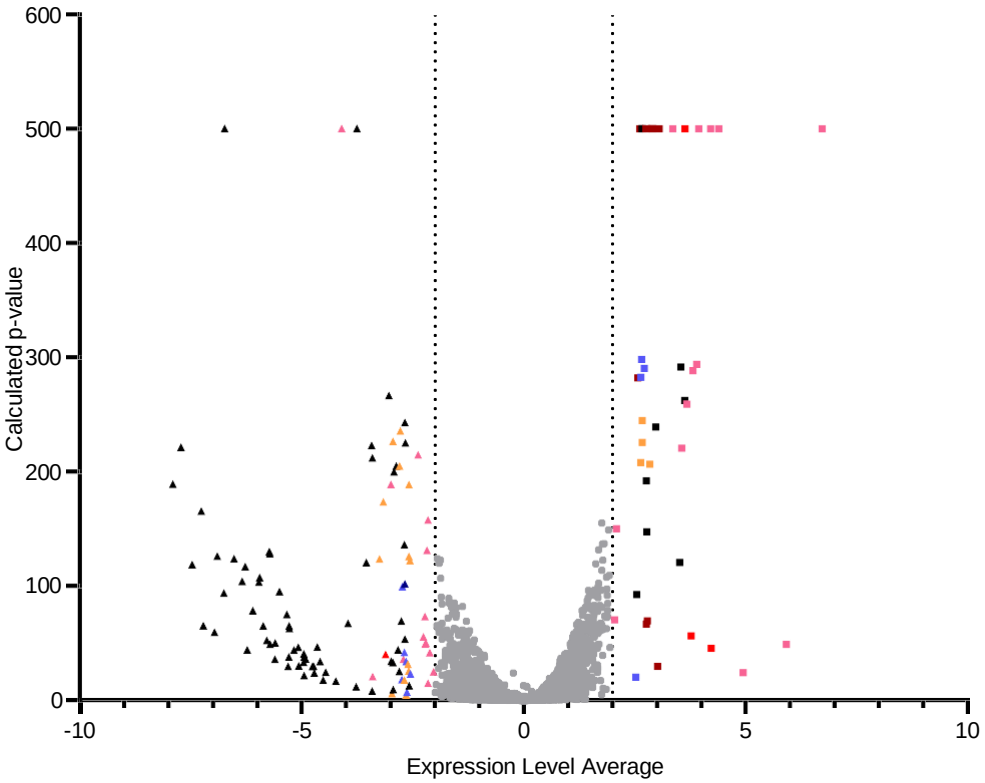

Figure 2.2: Volcano plot of DEGs that were up- and down-regulated in all Arm^R (pink: all Arm^R, orange: Arm^{R}16, blue: Arm^{R}17, dark red: Arm^{R}18, bright red: Arm^{R}1 and Arm^{R}3, black: Arm^{R}16 and Arm^{R}17, triangles: down-regulated genes, squares: up-regulated genes, grey circles: does qualify the fold-change ≤-2; ≥2 and p-value ≤0.001 criteria).

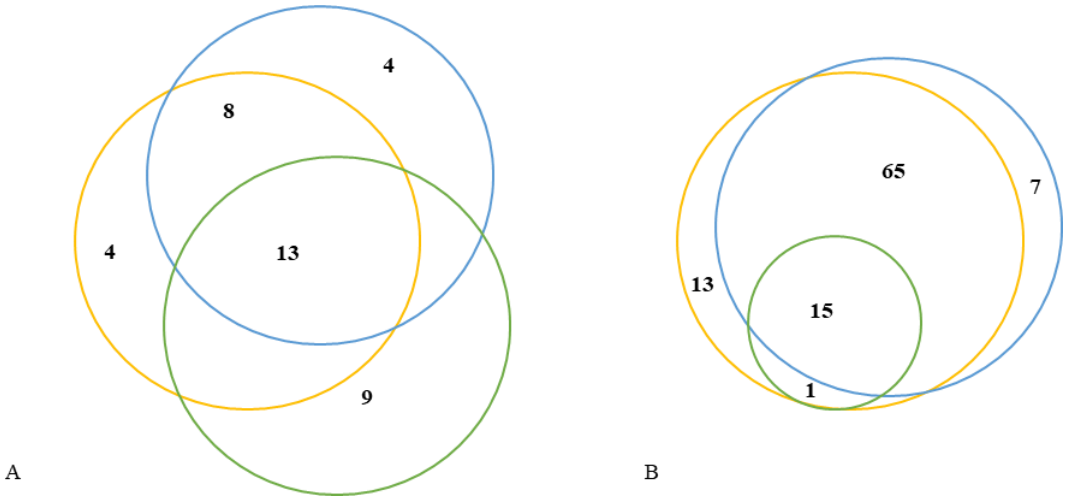

Figure 2.3: (A) Up-regulated and (B) down-regulated DEGs shared between all Arm^R strains (fold-change ≤-2; ≥2 and p-value ≤0.001) (DeepVenn, 2020, Hulsen *et al*., 200). Yellow: Arm^{R}16, Blue: Arm^{R}17 and Green: Arm^{R}18.

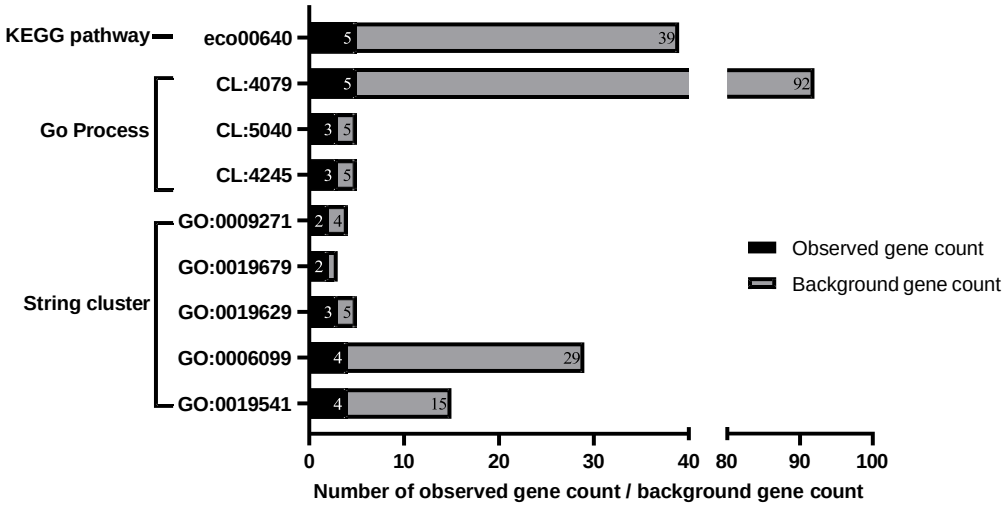

Figure 2.4: Significant enriched String cluster, GO Process, and KEGG pathways of shared up-regulated DEGs of all Arm^R (≤-2; ≥2; p-value <0.001). (GO: 0019541 - Propionate metabolic process; GO: 0006099- Tricarboxylic acid cycle; GO: 0019629- Propionate catabolic process, 2-methylcitrate cycle; GO: 0019679- Propionate metabolic process, methylcitrate cycle; GO: 0009271- Phage shock; CL: 4245- Propionate catabolic process, and 2-methylcitrate synthase activity; CL: 5040- Phage shock, and pspc domain; CL: 4079- Carbon metabolism, and propionate metabolic process; eco00640- Propanoate metabolism).

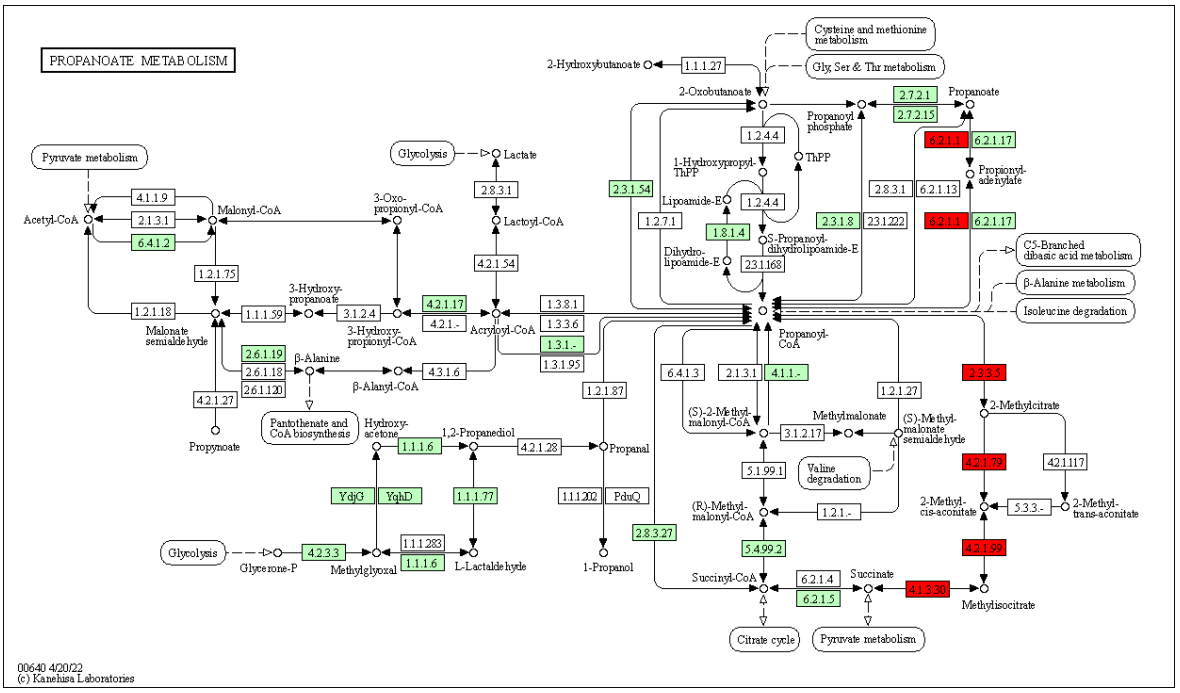

Figure 2.5: KEGG Propanoate metabolism pathway (eco00640). Red: up-regulated in all ArmR (≤-2; ≥2 and p-value ≤0.001). (6.2.1.1 – acs, 2.3.3.5 – prpC, 4.3.1.79 – prpD, 4.2.1.99 – acnB, 4.1.3.30 – prpB). (Kanehisa *et al*., 2023).

2.4. Discussion and Conclusion

Armeniaspirol-resistant mutants were obtained by means of spontaneous resistance at 4x MIC (8 µg/mL) development, which resulted in a low frequency of resistance. This is in line with mechanisms that alter the proton motive force of bacterial membranes as in the case of armeniaspirols that cause membrane depolarization in Gram-positive and Gram-negative strains (Arisetti *et al*., 2021). According to Feng and co-workers (2015), this mechanism results in a low level of resistance development. The genome analysis of Arm^R resulted in 50% of strains with gene mutations that are related to the MdtNOP efflux pump while 50% seem to be unrelated to the efflux pump. Further investigation is needed to understand the resistance caused by the single nucleotide mutation in the intergenic region downstream of the *csrA* gene and upstream of *serV*, which was present in 33% of the Arm^R. However, for this study purpose, further investigation was done on MdtNOP related gene mutations by means of next-generation sequening to get a clear understanding of the resistant phenotype.

Point mutations within the *mdtO* gene are the most common mutations related to the MdtNOP efflux pump while Arm^{R}16 and Arm^{R}17 contains a large gene deletion that could be similar to the observed resistance mechanism of the pyrrolomycin-resistant *E. coli* Δ*tolC* mutant (Valderrama *et al*., 2019). Armeniaspirols belongs to a large family of natural products that all contain chlorinated pyrrole moieties, which share a proposed common mechanism of action

and resistance as proposed by Arisetti and co-workers (2021). Cross-resistance is observed for armeniaspirol A and B against a pyrrolomycin-resistant *E. coli* Δ*tolC* mutant where an 8855-bp deletion of nine genes resulted in the overexpression of MdtOP to compensate for the loss of Δ*tolC* within the *E. coli* Δ*tolC* strains (Valderrama *et al*., 2019). This confirms the importance of the MdtNOP efflux pump in *E. coli* Δ*tolC* resistance to armeniaspirols.

Whole genome sequencing of three Arm^R selected for transcriptomics revealed large deletion of 8,635 base pairs (3561446-3591507 bp) of nine individual genes [*mdtN* (multidrug resistance protein), *ytcA* (hypothetical protein), *yjcS* (linear primary-alkylsulfatase)], and the D-allose operon *alsRBACEK*) in Arm^R16 and Arm^R17. The genotypes of Arm^R16 and Arm^R17 are similar to pyrrolomycin-resistant *E. coli* Δ*tolC* mutants reported by Valderrama and co-workers (2019) (accession no. CP009273.1), where a large deletion allows for the overexpression of *mdtOP* and possibly compensates the loss of function of AcrAB-TolC in the *E. coli* Δ*tolC* strain, conferring resistance to armeniaspirols. Referring to the transcriptome profiles, Arm^R16 and Arm^R17 have a large number of down-regulated genes (data not shown). All of those genes are in near proximity to the 8635 bp deletion. It is therefore likely that the deletion of the 9 genes influenced the genes and operons such as *rpoB*, *yjdP*, *phnCDEFGHIJKLMNOP*, *crfC*, *yjcZ*, *proP*, *pmrR*, *basSR*, *eptA*, *adiCYI*, *melRAB*, *fumB*, *yjdF*, *dcuBRS*, *yjdIJ*, *ghoS* and *lysU* listed in significant down-regulated genes of Arm^R16 and Arm^R17 (data not shown).

In addition to the 8,635 base pairs (3561446-3591507 bp) deletion, Arm^R17 carries a mutation in the intergenic region within the promotor range of *cvpA* (Colicin V production protein) (-70bpC->T) as well as a single point mutation (Y145F) in *fdoG* (Formate dehydrogenase-O) (Table 2.1). The *cvpA* gene plays an important role in cell envelope homeostasis and contributes to deoxycholate (DOC) resistance (Warr *et al*., 2021). Deoxycholate enters bacterial cells by passive diffusion as well as porins and causes damage to the cell envelope and DNA, alterations in redox state, generation of protein folding stress and in turn disrupt membrane potential (Urdabeta and Casadesüs, 2017). The occurrence of *cvpA* across diverse bacterial phyla, including in species which are never exposed to DOC, suggests that *cvpA* function is not only restricted to responding to DOC stress and could possibly be triggered by the change in membrane potential caused by armeniaspirols. Arm^R17 did not show any significant upregulation of *cvpA* and additional biochemical studies to elucidate the mechanistic bases of *cvpA* function and regulation is needed. Arm^R17 also did not show any significant up- or down-regulation of the *fdoG* gene (data not shown). Formate dehydrogenase-O is an electron transfer element in the glucose metabolism. It promotes oxidative stress tolerance and survival in stationary phase (Iwadate *et al*., 2017). Further, the transcriptome of Arm^R16 and Arm^R17 both revealed an upregulation of the *mdtO* with an average upregulation of 3.63-fold (data not shown). The *mdtN* is drastically down- regulated in Arm^R16 and Arm^R17 due to

the gene being part of the large deletion of 8635 bp. In comparison, no up-regulation of the *mdtO* was observed in Arm^{R}18. Arm^{R}18 did not reveal a deletion but a single point mutation (*Q654H*) in the *mdtO* gene and therefore the *mdtN* was not significantly down-regulated as in the case of Arm^{R}16 and Arm^{R}17. In addition to the single point mutation in the *mdtO* gene, four point mutations (A204P; V206F; R207G; D215G) were observed in the *plsB* (membrane-bound glycerol-3-phosphate acyltransferase) gene (Table S2.2). As mentioned, the *mdtO* is a homolog of ArcB in the ArcAB-tolC efflux pump in *Escherichia coli* and MexB in the MexAB-oprM in *Pseudomonas aeruginosa* and contributes to puromycin, acriflavine, tetraphenylarsonium chloride and sulfur drugs (Sulavik *et al*., 2001; Shimada, 2009). The route of efflux dependent resistance is a feasible argument; however, the role of *plsB* is still elusive and not understood. The *plsB* is responsible to catalyze the first step in the phospholipid biosynthesis and plays a role in persister cell formation as well as the Stringent response as it is a proposed target of (p)ppGpp. Inhibition occurs during the production of (p)ppGpp which interferes with membrane-associated steps in peptidoglycan biosynthesis, which can allow for resistance (Larson *et al*., 1980; Poole *et al*., 2012). The interaction between *plsB*, persister cell formation, Stringent response and armeniaspirol-resistance requires further investigation.

When visualizing the up-regulated genes in the three independent transcriptome profiles, a small number of variations are seen (Figure 2.2; Figure 2.3). However, a significant difference for the transcriptome data of Arm^{R}18 is apparent as Arm^{R}18 has significantly less down-regulate genes compared to Arm^{R}16 and Arm^{R}17. This observation might be attributed to the absence of the large deletion mutation that was found within Arm^{R}16 and Arm^{R}17 (Table 2.1). It is noteworthy to mention that despite the difference of down-regulated genes between the Arm^R, the main upregulated gene found in all Arm^R was *mdtP*, (multidrug resistance outer membrane protein) followed by *ymgC* and *ariR*(*ymgB*) genes that both form part of the biofilm formation and maintenance and acid-resistance (Lee *et al*., 2007). Interesting, the *ariR* gene was renamed when Lee and co-workers (2007) identified the function of ymgBC is to regulate acid resistance by indole. Indole is a protonophore, similar to armeniaspirols, which might explain the up-regulation in the Arm^R. Further supporting this, Jia and co-workers (2022) showed that armeniaspirols inhibit biofilm formation and kills biofilms of *H. pylori* in a dose-dependent manner.

Genes that were significantly up-regulated and involved within the propionate metabolism are the *prpBCD* genes that are normally up-regulated during adenylate cyclase in response to low glucose. This response creates cAMP which activates Crp leading to up-regulation of enzymes such as acetyl CoA synthase (*acs*), the ATP synthase complex, genes involved in the TCA cycle, the glyoxylate cycle, glycolysis, gluconeogenesis, the pentose phosphate pathway, the methylglyoxyl pathway, propionate metabolism (*prpBCD*) and galactitol degradation (*gatDZY*)

reactions (Franchini *et al*., 2015). Understanding why the propionate metabolism is upregulated within the Arm^R might be associated with the membrane depolarization effect observed in armeniaspirol treated cells. An increase of propionate metabolism has been reported to be associated with drug tolerance to unrelated classes of antibiotics as well as protonophores, such as monensin, by altering propionyl-CoA metabolism (Russell *et al*., 1989; Morehead and Dawson, 1992; Hicks *et al*.; 2018). Further, Shen *et al* (2017) showed that protonophores such as monensin and nisin increase propionate production through the succinate pathway, which seems plausible within armeniaspirol-resistance according to the shared up-regulation of the genes (Table S2.3). The precise reasoning of why bacteria that produce more propionate is more resistant to ionophores has not yet been identified; however, the link between armeniaspirol-resistance and the propionate metabolism is of definite interest as the genes encoding for propionyl-CoA metabolism are seen to be up-regulated in all three Arm^R independent of the genotype mutations observed (Figure 2.2; Table S2.3).

Further, the pspABCD (phage shock protein) operon that is up-regulated allows for cell membrane repair under external pressure such as exposure to an antibacterial or chemical compound that disrupts normal cell membrane function (Joly *et al*., 2010; Guo *et al*., 2019) (Table S2.3). *E. coli* persister cells are induced by indole, a protonophore, also induces *pspA* operon expression (Darwin *et al*., 2013). The complete link between the phage shock operon and persister formation has not been fully investigated. However, since armeniaspirols are protonophores, the upregulation of the phage shock operon might be link to persister formation, which may contribute to the observed resistance of Arm^R (Arisetti *et al*., 2021).

Within this study, we were able obtain Arm^R strains, determine cross-resistance to similar natural product family compound and confirm the main resistance mechanism of Gram-negative *E. coli* strains to be efflux-mediated. We were able to distinguish between two major mutations within the putative MdtNOP efflux pump. One, a large gene deletion that altered the expression of *mdtOP* and the other a single point mutation within the *mdtO* gene which allowed for the over expression of the *mdtP*. In addition to the mutations that affect the MdtNOP pump, another mutation was observed in one Arm^R, in the promotor region of *cvpA* that is linked to protonophore resistance. Four single point mutations were also observed within *plsB* that is linked to persister cell formation and stringent response resistances. The transcriptome profiles of the genotypically unique Arm^R were then assessed and linked the found gene mutations. Further, the overall transcriptome assessments of all three Arm^R confirmed the role of the putative MdtNOP efflux pump by the over expression of the outer membrane channel, *mdtP*. The transcriptome also provided information regarding additional resistance contributors such as acid resistance, propionate metabolism and phage shock operon which can be further investigated.

2.5. References

Arisetti, N., Fuchs, H.L., Coetzee, J., Orozco, M., Ruppelt, D., Bauer, A., Heimann, D., Kuhnert, E., Bhamidimarri, S.P., Bafna, J.A. and Hinkelmann, B., 2021. Total synthesis and mechanism of action of the antibiotic armeniaspirol A. Chemical Science, 12(48), pp.16023-16034.

Atanasov, A.G., Zotchev, S.B., Dirsch, V.M. and Supuran, C.T., 2021. Natural products in drug discovery: advances and opportunities. Nature reviews Drug discovery, 20(3), pp.200-216.

Chabbert, Y.A. and Scavizzi, M.R., 1976. Chelocardin-inducible resistance in Escherichia coli bearing R plasmids. Antimicrobial agents and chemotherapy, 9(1), pp.36-41.

Darnowski, M.G., Lanosky, T.D., Labana, P., Brazeau-Henrie, J.T., Calvert, N.D., Dornan, M.H., Natola, C., Paquette, A.R., Shuhendler, A.J. and Boddy, C.N., 2022. Armeniaspirol analogues with more potent Gram-positive antibiotic activity show enhanced inhibition of the ATP-dependent proteases ClpXP and ClpYQ. RSC Medicinal Chemistry, 13(4), pp.436-444.

Darnowski, M.G., Lanosky, T.D., Paquette, A.R. and Boddy, C.N., 2023. Armeniaspirol analogues disrupt the electrical potential (ΔΨ) of the proton motive force. Bioorganic & Medicinal Chemistry Letters, p.129210.

Darwin, A.J., 2013. Stress relief during host infection: the phage shock protein response supports bacterial virulence in various ways. PLoS pathogens, 9(7), p.e1003388.

Donner, J., Reck, M., Bunk, B., Jarek, M., App, C.B., Meier-Kolthoff, J.P., Overmann, J., Müller, R., Kirschning, A. and Wagner-Döbler, I., 2017. The biofilm inhibitor carolacton enters Gram-negative cells: studies using a TolC-deficient strain of Escherichia coli. Msphere, 2(5), pp.e00375-17.

Dufour, C., Wink, J., Kurz, M., Kogler, H., Olivan, H., Sablé, S., Heyse, W., Gerlitz, M., Toti, L., Nußer, A. and Rey, A., 2012. Isolation and Structural Elucidation of Armeniaspirols A–C: Potent Antibiotics against Gram-Positive Pathogens. Chemistry–A European Journal, 18(50), pp.16123-16128.

Feng, X., Zhu, W., Schurig-Briccio, L.A., Lindert, S., Shoen, C., Hitchings, R., Li, J., Wang, Y., Baig, N., Zhou, T., and Kim, B.K., 2015. Antiinfectives targeting enzymes and the proton motive force. Proceedings of the National Academy of Sciences, 112(51), pp.E7073-E7082.

Franchini, A.G., Ihssen, J. and Egli, T., 2015. Effect of global regulators RpoS and cyclic-AMP/CRP on the catabolome and transcriptome of Escherichia coli K12 during carbon-and energy-limited growth. PLoS One, 10(7), p.e0133793.

Fu, C., Xie, F., Hoffmann, J., Wang, Q., Bauer, A., Brönstrup, M., Mahmud, T. and Müller, R., 2019. Armeniaspirol antibiotic biosynthesis: chlorination and oxidative dechlorination steps affording spiro [4.4] non-8-ene. ChemBioChem, 20(6), pp.764-769.

Guo, H., Suzuki, T., and Rubinstein, J.L., 2019. Structure of a bacterial ATP synthase. Elife, 8, p.e43128.

Hennessen, F., Miethke, M., Zaburannyi, N., Loose, M., Lukežič, T., Bernecker, S., Hüttel, S., Jansen, R., Schmiedel, J., Fritzenwanker, M. and Imirzalioglu, C., 2020. Amidochelocardin overcomes resistance mechanisms exerted on tetracyclines and natural chelocardin. Antibiotics, 9(9), p.619.

Hicks, N.D., Yang, J., Zhang, X., Zhao, B., Grad, Y.H., Liu, L., Ou, X., Chang, Z., Xia, H., Zhou, Y. and Wang, S., 2018. Clinically prevalent mutations in Mycobacterium tuberculosis alter propionate metabolism and mediate multidrug tolerance. Nature microbiology, 3(9), pp.1032-1042.

Hulsen, T., de Vlieg, J. and Alkema, W., 2008. BioVenn–a web application for the comparison and visualization of biological lists using area-proportional Venn diaGrams. BMC genomics, 9(1), pp.1-6.

Iwadate, Y., Funabasama, N., Kato, J., 2017. Involvement of formate dehydrogenases in stationary phase oxidative stress tolerance in Escherichia coli. FEMS Microbiology Letters, 364(20), fnx193

Jia, J., Zhang, C., Liu, Y., Huang, Y., Bai, Y., Hang, X., Zeng, L., Zhu, D. and Bi, H., 2022. Armeniaspirol A: a novel anti-Helicobacter pylori agent. Microbial Biotechnology, 15(2), pp.442-454.

Joly, N., Engl, C., Jovanovic, G., Huvet, M., Toni, T., Sheng, X., Stumpf, M.P. and Buck, M., 2010. Managing membrane stress: the phage shock protein (Psp) response, from molecular mechanisms to physiology. FEMS microbiology reviews, 34(5), pp.797-827.

Kanehisa, M., Furumichi, M., Sato, Y., Kawashima, M. and Ishiguro-Watanabe, M., 2023. KEGG for taxonomy-based analysis of pathways and genomes. Nucleic Acids Research, 51(D1), pp.D587-D592.

Labana, P., Dornan, M.H., Lafrenière, M., Czarny, T.L., Brown, E.D., Pezacki, J.P. and Boddy, C.N., 2021. Armeniaspirols inhibit the AAA+ proteases ClpXP and ClpYQ leading to cell division arrest in Gram-positive bacteria. Cell Chemical Biology, 28(12), pp.1703-1715.

Larson, T.J., Lightner, V.A., Green, P.R., Modrich, P., and Bell, R.M., 1980. Membrane phospholipid synthesis in Escherichia coli. Identification of the sn-glycerol-3-phosphate acyltransferase polypeptide as the plsB gene product. Journal of Biological Chemistry, 255(19), pp.9421-9426.

Lee, J., Page, R., García-Contreras, R., Palermino, J.M., Zhang, X.S., Doshi, O., Wood, T.K. and Peti, W., 2007. Structure and function of the Escherichia coli protein YmgB: a protein

critical for biofilm formation and acid-resistance. Journal of molecular biology, 373(1), pp.11-26.

Morehead, M.C., and Dawson, K.A., 1992. Some growth and metabolic characteristics of monensin-sensitive and monensin-resistant strains of Prevotella (Bacteroides) ruminicola. Applied and environmental microbiology, 58(5), pp.1617-1623.

Poole, K., 2012. Bacterial stress responses as determinants of antimicrobial resistance. Journal of Antimicrobial Chemotherapy, 67(9), pp.2069-2089.

Russell, J.B. and Strobel, H., 1989. Effect of ionophores on ruminal fermentation. Applied and environmental microbiology, 55(1), pp.1-6.

Shimada, T., Yamamoto, K. and Ishihama, A., 2009. Involvement of the leucine response transcription factor LeuO in regulation of the genes for sulfa drug efflux. Journal of bacteriology, 191(14), pp.4562-4571.

Shen, J., Liu, Z., Yu, Z. and Zhu, W., 2017. Monensin and nisin affect rumen fermentation and microbiota differently in vitro. Frontiers in microbiology, 8, p.1111.

Stepanek, J.J., Lukežič, T., Teichert, I., Petković, H. and Bandow, J.E., 2016. Dual mechanism of action of the atypical tetracycline chelocardin. Biochimica et Biophysica Acta (BBA)-Proteins and Proteomics, 1864(6), pp.645-654.

Sulavik, M.C., Houseweart, C., Cramer, C., Jiwani, N., Murgolo, N., Greene, J., DiDomenico, B., Shaw, K.J., Miller, G.H., Hare, R. and Shimer, G., 2001. Antibiotic susceptibility profiles of Escherichia coli strains lacking multidrug efflux pump genes. Antimicrobial agents and chemotherapy, 45(4), pp.1126-1136.

Urdaneta, V. and Casadesús, J., 2017. Interactions between bacteria and bile salts in the gastrointestinal and hepatobiliary tracts. Frontiers in medicine, 4, p.163.

Valderrama, K., Pradel, E., Firsov, A.M., Drobecq, H., Bauderlique-le Roy, H., Villemagne, B., Antonenko, Y.N. and Hartkoorn, R.C., 2019. Pyrrolomycins are potent natural protonophores. Antimicrobial agents and chemotherapy, 63(10), pp.e01450-19.

Warr, A.R., Giorgio, R.T. and Waldor, M.K., 2021. Genetic analysis of the role of the conserved inner membrane protein CvpA in enterohemorrhagic Escherichia coli resistance to deoxycholate. Journal of Bacteriology, 203(6), pp.e00661-20.

2.6. Supplemental Figures and Tables

Table S2.1: Minimum inhibition concentration (µg/mL) of Arm^R assessed for armeniaspirol A, armeniaspirol B, gentamycin, kanamycin, tetracycline, chloramphenicol, erythromycin, linezolid, and spectinomycin.

Strain	A	B	GM	KAN	TET	CHL	ERY	LIN	SPEC
E. coli ΔtolC	2	2	1	2	0.5	1	2	8	8
Arm^R1	>64	>64	0.5	1	0.5	1	2	4	8
Arm^R2	>64	>64	0.5	2	0.5	1	2	4	8
Arm^R3	>64	>64	0.5	2	0.5	1	2	4	8
Arm^R4	>64	>64	0.5	2	0.5	1	2	4	8
Arm^R5	>64	>64	0.5	2	0.5	2	2	4	8
Arm^R6	>64	>64	1	2	0.5	1	2	8	8
Arm^R7	>64	>64	0.5	2	0.5	1	2	4	8
Arm^R8	>64	>64	1	2	0.5	1	2	8	8
Arm^R9	>64	>64	0.5	2	0.5	1	2	8	8
Arm^R10	>64	>64	0.5	2	0.5	2	2	8	8
Arm^R11	>64	>64	0.5	2	0.5	2	2	8	8
Arm^R12	>64	>64	0.5	2	0.5	2	2	8	8
Arm^R13	>64	>64	0.5	2	0.5	2	2	8	8
Arm^R14	>64	>64	0.5	2	0.5	2	2	8	8
Arm^R15	>64	>64	0.5	2	0.5	2	2	8	8
Arm^R16	>64	>64	0.5	2	0.5	2	2	8	8
Arm^R17	>64	>64	0.5	2	0.5	2	2	8	8
Arm^R18	>64	>64	0.5	2	0.5	2	2	8	8

A: Armenaispirol A, B: Armeniaspirol B, GM: Gentamycin, KAN: Kanamycin, TET: Tetracycline, CHL: Chloramphenicol, ERY: Erythromycin, LIN: Linezolid, and SPEC: Spectinomycin

Table S2.2: Gene mutations of all Arm^R mapped to *E. coli* K12 reference strain (accession no. CP009273.1).

Strain	Mutations affecting MdtNOP (RND Efflux)	Intergenic region upstream of *serV* (tRNA-serine)	prfB (Peptide chain release factor)	Intergenic region upstream of and *cvpA* (Colicin V production)	*FdoG* (Formate dehydrogenase-O)	*plsB* (Membrane-bound glycerol-3-phosphate acyltransferase)
E. coli ΔtolC	-	-	-	-	-	-
Arm^{R}1	*mdtO:* S2K; A3T, L4I; N5G; S6T; L7E; L9C	-	T173S		-	-
Arm^{R}2	*mdtO:* S2K; A3K, L4I; N5G; P8K; L9C	-	T173S		-	-
Arm^{R}3	*mdtO:* S2R; P8K; L9C	-	T173S		-	-
Arm^{R}4	*mdtO:* S2R; N5S; L7V; P8K; L9C	-	T173S		-	-
Arm^{R}5	*mdtO:* S2K; A3K L4I; N5G; S6K; L7E; P8K; L9C	-	T173S		-	-
Arm^{R}6	*mdtO:* S2K; A3T L4I; N5G; S6K; L7E; P8K; L9C	-	T173S	-	-	-
Arm^{R}7	-	G>A (Position: 1067334)	-	-	-	-
Arm^{R}8	-	G>A (Position: 1067334)	-	-	-	-
Arm^{R}9	-	G>A (Position: 1067334)	-	-	-	-
Arm^{R}10	-	G>A (Position: 1067334)	-	-	-	-
Arm^{R}11	-	G>A (Position: 1067334)	-	-	-	-

Arm^{R}12	-	G>A (Position: 1067334)	-	-	-	-
Arm^{R}13	-	G>A (Position: 1067334)	-	-	-	-
Arm^{R}14	-	-	-	*- 70>T*	N144K	-
Arm^{R}15	-	-	-	-	-	A204P; R207G
Arm^{R}16	*ΔalsRBACEK-yjcS-ytcA-mdtN*	-	-	-	-	-
Arm^{R}17	*ΔalsRBACEK-yjcS-ytcA-mdtN*	-	-	*c. 70C->T*	*Y145F*	-
Arm^{R}18	*mdtO: Q654H*	-	-	-	-	*A204P; V206F; R207G; D215G*

Table S2.3: List of up-and down-regulated DEGs shared between Arm^R strains (p-value ≤0.001 and fold-change of ≥2; ≤-2).

Gene Name	STRING Database Annotation	Calculated p-value	Average Level of Expression	Average level of Confidence	Average p-value
ansB	Periplasmic l-asparaginase 2; Belongs to the asparaginase 1 family	500	-4.10	1000	0
nudI	Pyrimidine deoxynucleotide diphosphatase nudi; Catalyzes the hydrolysis of nucleoside triphosphates, with a preference for pyrimidine deoxynucleoside triphosphates (dUTP, dTTP and dCTP)	20.56	-3.40	83.91	2.79E-21
pgaA	Exports the biofilm adhesin polysaccharide poly-beta-1,6-N- acetyl-D-glucosamine (PGA) across the outer membrane. The PGA transported seems to be partially N-deacetylated since N-deacetylation of PGA by PgaB is needed for PGA export through the PgaA porin	188.81	-3.00	215.33	1.6E-189
hypothetical protein	predicted membrane protein	35.85	-2.70	39.15	1.42E-36
Glycerol-3-phosphate responsive antiterminator	Uncharacterized protein YgcP; Putative anti-terminator regulatory protein	101.58	-2.67	110.27	2.6E-102
ompW	Outer membrane protein w; Acts as a receptor for colicin S4	214.55	-2.37	246.79	2.8E-215
ferredoxin-like protein FixX	Putative 4fe-4s ferredoxin-type protein; Could be part of an electron transfer system required for anaerobic carnitine reduction. Could be a 3Fe-4S cluster-containing protein	55.29	-2.25	65.58	5.08E-56
gatB	Galactitol-specific pts enzyme iib component; The phosphoenolpyruvate-dependent sugar phosphotransferase system (PTS), a major carbohydrate active transport system, catalyzes the phosphorylation of incoming sugar substrates concomitant with their	73.12	-2.22	129.56	7.77E-74

	translocation across the cell membrane. The enzyme II complex composed of GatA, GatB and GatC is involved in galactitol transport. It can also use D-glucitol				
hypothetical protein	DUF1202 family putative secreted protein; Uncharacterized protein YggM; Putative alpha helix chain	49.17	-2.22	53.66	6.77E-50
ferredoxin-type protein	Ferredoxin-type protein, role in electron transfer to periplasmic nitrate reductase napa; Could be involved in the maturation of NapA, the catalytic subunit of the periplasmic nitrate reductase before its export into the periplasm. Is not involved in the electron transfer from menaquinol or ubiquinol to the periplasmic nitrate reductase	49.79	-2.20	88.60	1.64E-50
yhbU	U32 peptidase family protein; Required for O (2)-independent ubiquinone (coenzyme Q) biosynthesis. Together with UbiV, is essential for the C6-hydroxylation reaction in the oxygen-independent ubiquinone biosynthesis pathway	130.96	-2.18	155.21	1.1E-131
DNA binding domain, excisionase family	Not Annotated by String-DB	157.53	-2.15	173.30	3E-158
mrpA	ygiL - Putative fimbrial-like adhesin protein; Putative fimbrial-like protein	14.75	-2.15	18.64	1.78E-15
hypothetical protein	E14 prophage; uncharacterized protein YmfE; Uncharacterized protein YmfE; Phage or Prophage Related	41.61	-2.11	52.98	2.46E-42
vancomycin high temperature exclusion protein	Not Annotated by String-DB	24.86	-2.03	29.17	1.39E-25
lsrC	Autoinducer-2 ABC transporter membrane subunit LsrC	70.52	2.05	103.66	3.01E-71
aceK	Isocitrate dehydrogenase kinase/phosphatase	150.30	2.0	207.28	5.1E-151
astC	Succinylornithine transaminase, plp-dependent; Catalyzes the transamination of N (2)-succinylornithine and alpha-ketoglutarate into N (2)-succinylglutamate semialdehyde and glutamate. Can also function as an acetylornithine aminotransferase	500	3.36	1000	0
prpC	2-methylcitrate synthase; Involved in the catabolism of short chain fatty acids (SCFA) via the tricarboxylic acid (TCA) (acetyl degradation route) and via the 2-methylcitrate cycle I (propionate degradation route). Catalyzes the Claisen condensation of propionyl-CoA and oxaloacetate (OAA) to yield 2-methylcitrate (2-MC) and CoA. Also catalyzes the condensation of oxaloacetate with acetyl-CoA to yield citrate but with a lower specificity	220.66	3.56	487.67	2.2E-221
pspB	Psp operon transcription co-activator; The phage shock protein (psp) operon (pspABCDE) may play a significant role in the competition for survival under nutrient- or energy-limited	259.22	3.68	752.21	6E-260

	conditions. PspB participates in transcription regulation				
prpD	2-methylcitrate dehydratase; Involved in the catabolism of short chain fatty acids (SCFA) via the tricarboxylic acid (TCA) (acetyl degradation route) and via the 2-methylcitrate cycle I (propionate degradation route). Catalyzes the dehydration of 2-methylcitrate (2-MC) to yield the cis isomer of 2- methyl-aconitate. It is also able to catalyze the dehydration of citrate and the hydration of cis-aconitate at a lower rate. Due to its broad substrate specificity, it is responsible for the residual aconitase activity of the acnAB-null mutant	288.30	3.81	761.82	5E-289
pspD	Peripheral inner membrane phage-shock protein; The phage shock protein (psp) operon (pspABCDE) may play a significant role in the competition for survival under nutrient- or energy-limited conditions	294	3.90	763.73	1E-294
pspC	Psp operon transcription co-activator; The phage shock protein (psp) operon (pspABCDE) may play a significant role in the competition for survival under nutrient- or energy-limited conditions. PspC participates in transcription regulation	500	3.94	1000	0
acs	Propionyl-coa synthetase; Catalyzes the synthesis of propionyl-CoA from propionate and CoA. Also converts acetate to acetyl-CoA but with a lower specific activity (By similarity)	500	4.21	1000	0
prpB	2-methylisocitrate lyase; Involved in the catabolism of short chain fatty acids (SCFA) via the 2-methylcitrate cycle I (propionate degradation route). Catalyzes the thermodynamically favored C-C bond cleavage of (2R,3S)-2- methylisocitrate to yield pyruvate and succinate via an alpha-carboxy-carbanion intermediate	500	4.40	1000	0
ariR	Probable rcsb/c two-component-system connector, global regulator of biofilm formation and acid-resistance; A connector protein for RcsB/C regulation of biofilm and acid-resistance, providing additional signal input into the two- component signaling pathway. May serve to stimulate biofilm maturation, via the Rcs phosphorelay. Regulates expression of genes involved in acid-resistance and biofilm formation, including the RcsB/C two-component system. May be a non-specific DNA-binding protein that binds genes and/or intergenic regions via a geometric recognition.	24.25	4.95	118.16	5.6E-25
hypothetical protein	ymgC	48.90	5.92	167.27	1.26E-49
mdtP	Putative multidrug efflux pump outer membrane channel; Could be involved in resistance to puromycin, acriflavine and tetraphenylarsonium chloride	500	6.73	1000	0

Chapter 3: Unraveling the cross-resistance patterns and transcriptome of *A. baumannii* reveals target mutations and efflux-mediated mechanism of resistance for cystobactamids

3.1. Abstract

Acinetobacter baumannii is classified as a priority pathogen and a global problem. There is no clear “standard of care” antibiotic for carbapenem-resistant *Acinetobacter baumannii* infections and thus, combination therapy with colistin and polymyxins is most efficient and commonly used. Bacterial topoisomerase II inhibitors, Cystobactamids, are potential candidates for treatment of carbapenem-resistant *Acinetobacter baumannii* infections. Cystobactamids was originally isolated from a soil dwelling micro-organism, *Cystobacter* spiecies and has a promising susceptibility profile that can be compared to colistin and other topoisomerase inhibitors. Within this study, several cystobactamid derivatives were assessed by means of minimum inhibition concentration against several *A. baumannii* strains and the IC_{50} (Half maximal inhibitory concentration) of these derivatives were determined against bacterial topoisomerase II and topoisomerase IV. In addition, cystobactamid-resistant *A. baumannii* mutants (Cys^R) were cultivated and assessed. Cross-resistance was determined against clinically relevant drugs such as ciprofloxacin, colistin, zoliflodacin, gepotdacin, levofloxacin and moxifloxicin. Little to no cross-resistance was observed. Moreover, the genomic DNA of 30 resistant Cys^R were sequenced and revealed *gyrA* (gyrase A) and *gyrB* (gyrase A) mutations occur in 53% of the Cys^R. These mutations are scattered and not in a specific binding site nor do they overlap with known binding sites of ciprofloxacin, zoliflodacin or moxifloxacin. Interestingly, a gene mutation within *ybdL* (PLP-dependent aminotransferase) is the second most occurring mutation that occurs in 27% of the Cys^R. Transcriptomic analysis was done on four resistant mutant strains containing the *ybdL* mutation and revealed the up-regulation of MepA, a MATE efflux pump that is known to extrude fluoroquinolones and the neighbor gene of *ybdL*. It is plausible to assume that the genomic mutation in *ybdL* leads to the over-expression of MepA efflux pump, resulting in the observed resistance. However, further in-depth investigation is needed to confirm these findings.

3.2. Introduction

Acinetobacter genus of Gram-negative bacteria was first isolated from soil by a Dutch microbiologist, Beijernick in the 20th century (Beijerinck, 1911). *Acinetobacter baumannii* forms part of the *Acinetobacter* genus and is on the priority pathogen list for research and development of new antibiotics (Tacconelli, 2017). This list comprises of several pathogens

that poses a threat to public health by causing severe and invasive infections linked with high mortality rates (Tacconelli *et al*., 2018). *A. baumannii* cause infections of the respiratory tract, bloodstream, and commonly in skin wound infections (Kyriakidis *et al*., 2021). Of greater concern is multidrug-resistant *A. baumannii* that is rapidly emerging due to the high degree of resistance to antibiotics and multiple classes of antimicrobial agents (Whiteway *et al*., 2022). Resistant development within *Acinetobacter* is similar to *Pseudomonas* species, however unlike *Pseudomonas* species*, Acinetobacter* has not yet been as intensely studied (Lupo *et al*., 2018). The most common resistance mechanisms include antimicrobial-inactivating enzymes, protection of bacterial targets, reducing the membrane permeability, and increasing efflux of the antibiotic (Blair *et al*., 2015). A clear and well-described example for antimicrobial-inactivating enzyme in *A. baumannii* is carbapenemase, which is currently one in the major concerns regarding antimicrobial resistance in several species due to the broad range of cross-resistance to other antibiotic classes (Tacconelli *et al*., 2018). Carbapenem was the treatment of multidrug resistant *A. baumannii*. However, this led to a severe increase of carbapenem-resistance *A. baumannii* (CRAB) (Fournier *et al*., 2020).

Cystobactamids forms a novel compound class originally isolated from *Cystobacter* species that display pronounced activity against Gram-positive and Gram-negative bacteria including *A. baumannii* (Baumann *et al*., 2014). This compound class is biosynthesised by a nonribosomal peptide synthesis (NRPS) pathway with an unusual assembly with a central linker flanked by substituted *p*ABA (*para*-amino benzoic acid) units (Baumann *et al*., 2014). The mechanism of action is by the inhibition of topoisomerase II as well as induction of DNA double-strand breaks and induction of the SOS response (Baumann *et al*., 2014; Groß *et al*., 2021). Here, we investigated the possible application of cystobactamids for the treatment of *A. baumannii*. Several derivatives were assessed on *A. baumannii* strains, including CRAB and clinical isolates. We investigated the genotypes of Cys^R and provide an overview of the resistance profiles based on cross-resistance and the resistant mutation genotypes. In addition, we investigated the transcriptomic change of Cys^R with the second most occurring gene mutation in *ybdL* that leads to a resistant phenotype.

3.3. Results

Susceptibility Profiling and Synergy of cystobactamid derivatives

To assess the susceptibility of cystobactamids on *A. baumannii*, minimum inhibition concentrations (MIC) were assessed on a selected panel of strains that included lab strains, multidrug-resistant clinical isolates including CRAB strains. The strains were assessed against eight cystobactamid derivatives that were part of a larger project to optimize cystobactamids. The strains were also assessed against clinically relevant antibiotics such as ciprofloxacin, colistin, zoliflodacin, gepotdacin, levofloxacin and moxifloxicin (Table 3.1; Table 3.2). It is

apparent that the overall susceptibility profile of colistin is the most impressive; however, cystobactamids derivatives **5** and **8** provide a comparable profile. Overall, the cystobactamid derivates **3**, **5**, **6**, **7**, and **8** showed a susceptibility profile that surpasses the profiles of ciprofloxacin, zoliflodacin, gepotidacin, levofloxacin, moxifloxacin. The IC_{50} values of *A. baumannii* DNA gyrase and decantation assay revealed a higher inhibition than ciprofloxacin or zoliflodacin. Further, cystobactamids shows a higher level of inhibition of *A. baumannii* topoisomerase IV compared to DNA gyrase (Table 3.3.). Table S3.1 reveals the observed synergy between selected cystobactamid derivatives and colistin in *A. baumannii* DSM-30008.

Table 3.1: Minimum inhibition concentration of selected *A. baumannii* strains against selective cystobactamid derivatives and current clinically important antibiotics.

Strain	1	2	3	4	5	6	7	8	CIP	COL	ZOL	GEP	LEV	MOX
DSM-30007	0.5	8	0.5	0.03	0.06	0.13	0.03	0.01	0.8	0.13	8	16-32	2	1
DSM-30008	1	1	0.5	0.06	0.13	0.25	0.06	0.13	0.1	0.13	4	8	0.13	0.06
CIP-105742	0.3	0.06	0.03	0.03	0.03	0.03	0.01	0.03	0.1	0.13	2	4	0.06	0.03
BAA-1710	8	64	0.5	0.06	0.25	0.25	0.5	0.25	6.4	0.3	4	16	16	8
CIP-107292	>64	64	1	4	0.5	0.5	0.5	1	6.4	0.13	16	16	8	16
R835	64	64	0.5	2	0.13	0.5	0.5	1	6.4	0.13	8	16	8	4

CIP- ciprofloxacin; COL-colistin; ZOL-zoliflodacin; GEP-gepotidacin; LEV-levofloxacin; MOX- moxifloxacin

Table 3.2: Minimum inhibition concentration of selected *A. baumannii* CRAB clinical isolates strains against a cystobactamid derivative and current clinical important antibiotics.

Strain	5	6	7	8	CIP	COL	ZOL	LEV	MOX
038 OXA-23	≤0.03	0.025	≤0.03	0.01	6.4	0.125	8	16	16
045 OXA-58	≤0.03	0.025	≤0.03	0.05	6.4	0.125	8	8	8
046 OXA-40	≤0.03	0.0125	≤0.03	0.025	6.4	0.125	2	4	8
070 NDM-1	≤0.03	0.2	≤0.03	0.025	64	0.06	8	4	4
054 OXA-51-ISAba1	≤0.03	0.05	≤0.03	0.2	64	0.125	8	64	64
NCTC 13301 (OXA-23)	≤0.03	0.2	≤0.03	0.125	64	0.5	8	32	32

CIP- ciprofloxacin; COL-colistin; ZOL-zoliflodacin; LEV-levofloxacin; MOX- moxifloxacin

Table 3.3: The determined IC_{50} values for cystobactamid derivates as well as ciprofloxacin in Gyrase Supercoiling Assay and Topoisomerase IV Decatenation Assay.

Compound	*A. baumannii* DNA Gyrase Supercoiling Assay IC_{50} (µM)	*A. baumannii* DNA Topoisomerase IV Decatenation Assay IC_{50} (µM)
Ciprofloxacin	1.7	2.7
Levofloxacin	9.24	1.48
1	0.47	0.17
2	0.57	0.11
3	1.1	0.19
4	1.58	0.44
5	3.8	0.12
6	4.6	0.31
7	1.3	0.12
8	0.25	0.18

Resistant development, whole genome sequencing, and homology

Several Cys^R were selected from spontaneous resistance development when determing the frequency of resistance at 4x MIC, 8x MIC and 16x MIC to cystobactamid derivatives that were all in the range of ≤ $9x10^{-8}$. The Cys^R were assessed by MIC shift and cross-resistance to selected reference antibiotics. Whole genome DNA isolation was done for 30 selected Cys^R after which Illumina sequencing was done and the reads were mapped to the appropriate genome reference and analyzed in Geneious software (Geneious Prime® 2023.0.1 Build 2022-11-28). Whole genome sequencing revealed *gyrA* (gyrase A) and *gyrB* (gyrase A) mutations in 53% of the 30 selected Cys^R (Figure 3.1). The gyrase mutations are also mostly single point mutations that lead to the exchange of arginine amino acids within the C-terminal region of gyrase (Table S3.4). Furthermore, the mutations are scattered and not in a specific binding site nor overlapping with known binding sites of ciprofloxacin, zoliflodacin and moxifloxacin (Figure 3.2). Interestingly, a gene mutation within *ybdL* (PLP-dependent aminotransferase) is the second most occurring mutation that occurs in 27% of the resistant Cys^R (Figure 3.1).

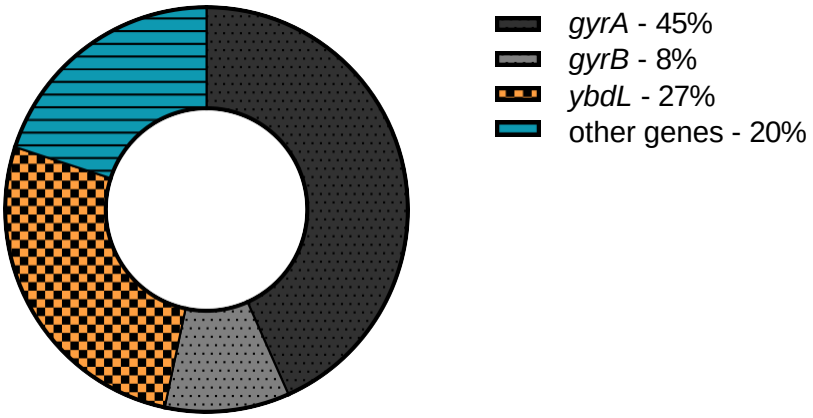

Figure 3.1: Diagram representing the percentage of gene occurrence in 30 selected Cys^R.

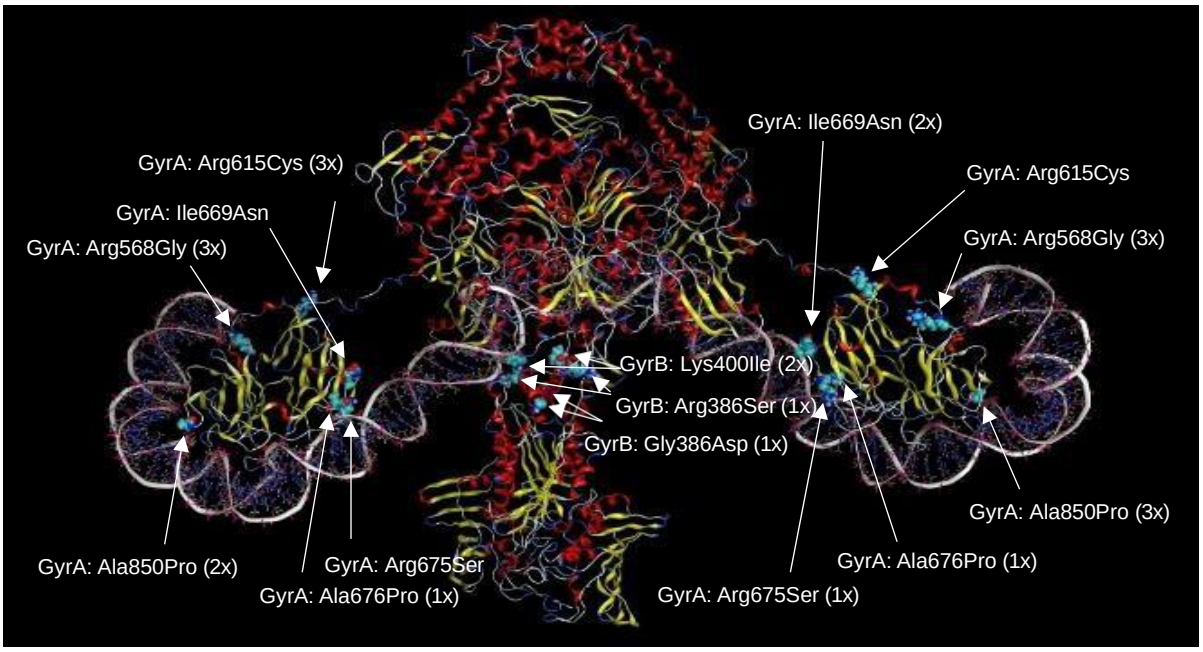

Figure 3.2: Structural homology of *E. coli* wild-type gyrase complex structure mapped with obtained target gene mutations found in Cys^R.

Cross-resistance profile of Cys^R

Analysis of 30 resistant strains' cross-resistance to ciprofloxacin, colistin, zoliflodacin, gepotidacin, levofloxacin and moxifloxacin provided resistance profiles of selected Cys^R. No cross-resistance (larger than four-fold) to colistin (Figure 3.3). Most Cys^R did not show cross-resistance to fluoroquinolones, third generation fluoroquinolones, or NBTI. However, two Cys^R showed a MIC shift of four-fold to gepotidacin and moxiflodacin, while nine Cys^R showed a MIC fould-shift of four-fold to ciprofloxacin. 15 and 11 Cys^R showed a MIC shift of four- to eight-fold to zoliflodacin and levofloxacin, respectively. Cross-resistance to ciprofloxacin was only observed for Cys^R containing a point mutation in *ybdL* (Q354H) and one mutant with a single point mutation within the promotor region of a master antibiotic resistance regulator gene, *gigB* (-35bp T>G) (Figure 3.3; Table S3.3). Cys^R with mutations within *gyrA*, *gyrB*, and *ybdL* caused

high-level resistance (16-128 MIC fold-shift) to cystobactamids, while other gene mutations resulted in low-level resistance (Figure 3.3). One exception of a gene mutation that caused high-level resistance (>128 MIC fold-shift) is the single point mutation within the promotor region of *gigB*.

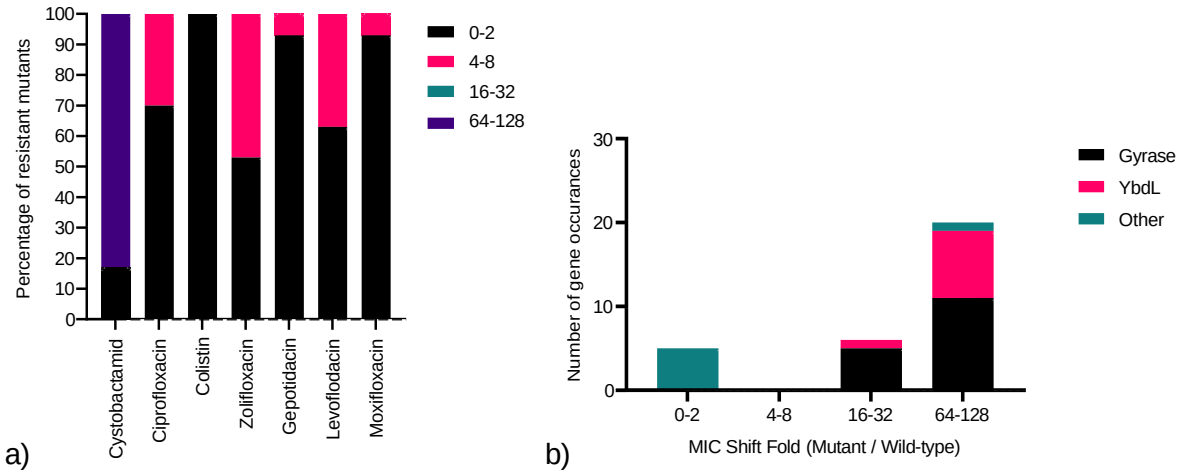

Figure 3.3: a) MIC fold-shift values (MIC of Cys^R/wild-type) in percentage of 30 Cys^R to cystobactamid derivatives, ciprofloxacin, colistin, zoliflodacin, gepotidacin, levofloxacin and moxiflodacin. b) MIC fold-shift of 30 Cys^R for cystobactamid derivatives with gene mutations occurrence of *gyrA*, *gyrB*, *ybdL* and other gene mutations.

Characterization of Cys^R carrying the *ybdL* point mutation

To investigate the role of *ybdL* in resistance to cystobactamid derivatives as well as the reason for the observed cross-resistance to ciprofloxacin, zolifloxacin and levofloxacin, four Cys^R carrying the *ybdL* (Q354H) mutation were assessed. These Cys^R was assessed in terms of fitness cost as well as transcriptomic analysis by means of RNA-sequencing. As mentioned, *ybdL* mutation showed a MIC fold-shift of >64-fold to cystobactamid derivatives (Figure 3.2). All four Cys^R had the *ybdL* (Q354H) point mutation while two Cys^R have additional mutations within *gigA* (Leu89Pro), *rsbP* (Asp90Tyr), and a *hypothetical gene* (TPR repeat containing protein) (His29Leu) (Table 3.4).

The MIC (µg/mL) of the Cys^R differed by one- to two-fold after passaging the selected Cys^R on non-selective agar for 10 days which indicates that the mechanism of the observed resistance is not reversible (Table S3.2). Fitness cost assessment revealed a large difference in metabolic heat flow profiles as well as heat produced by Cys^R compared to the wild-type strain (Figure 3.4). The observed data via isothermal micro-calorimetry is in agreement with the traditional growth curve measurement (OD_{600}) which also in indicates a loss of fitness for Cys^R due to lower OD_{600} values as well as lower heatflow observed (Figure 3.4).

Table 3.4: The genotype and minimum inhibition concentration fold-shift (Cys^R MIC/wild-type strain MIC) of **1** and **5**.

Strain	Genotype	MIC fold-shift			
		1	5	ZOL	LEVO
Wild-type	*A. baumannii* DSM-30007	-	-	-	-
Cys^{R}1	*A. baumannii* DSM-30007 CN-861^R *ybdL*: Q354H	64-128	64	2-4	8
Cys^{R}2	*A. baumannii* DSM-30007 CN-861^R *ybdL*: Q354H	64-128	64	2-4	8
Cys^{R}3	*A. baumannii* DSM-30007 CN-861^R *ybdL:* Q354H*; gigA:* L89P*; rsbP* - D90Y	66	64	-	8
Cys^{R}4	*A. baumannii* DSM-30007 CN-861^R *ybdL:* Q354H*; gigA:* L89P*; rsbP* - D90Y*; Hypothetical gene (TPR repeat containing protein):* H29L	>128	32	-	8

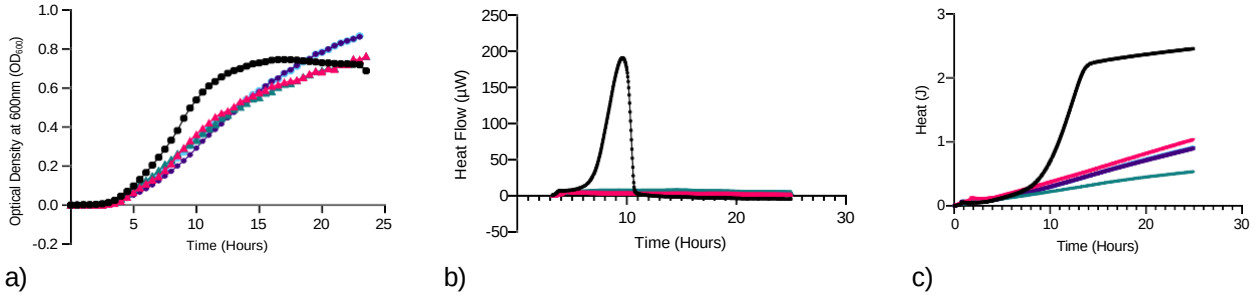

a) b) c)

Figure 3.4: a) Optical density measured by Tecan plate reader at 600nm (OD_{600}) over 24 hours. b) heatflow (µW) and c) Heat (J) and of the Cys^R and respective wild-type during isothermal calorimetry measurement over 24 hours. Black: Wild-type *A. baumannii*, Pink: Cys^{R}1, Green: Cys^{R}2, Purple: Cys^{R}3, and Blue: Cys^{R}4.

Transcriptomic assessment of Cys^R with *ybdL* mutation

The transcriptome of four Cys^R were assessed and the differentially expressed genes (DEGs) were analyzed and compared to the wild-type strains. The total DEGs of each mutant can be seen in Table S3.5. The four Cys^R share 94.44% of DEGs (p-value of ≤0.001 and fold-change o f≤-1.5; ≥1.5) are shared and a total of 34 DEGs are shared between the Cys^R. Interestingly, 33 DEGs are down regulated while only MepA that is upregulated with an average expression level of 2.04-fold. (Table S3.5). Figure 3.5 illustrated the DEGs of all the Cys^R with the DEGs

with a p-value of ≤0.001 and expression level average of ≤-1.5 and ≥1.5 marked in green and blue, respectively. The most upregulated gene is the *mepA* gene, a MATE pump (<0.001; log ratio value: ≥1.5) marked in green. Further, STRING clusters that were enriched within the down-regulated DEGs are capsid and pilus organization, styrene degradation, aromatic hydrocarbons catabolism, cell motility, trehalose metabolic, signal, and phosphopantetheine (Table S3.6).

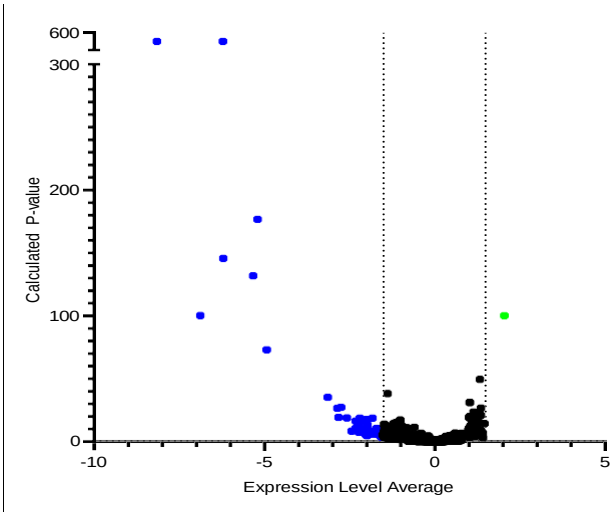

Figure 3.5: Volcano plot of all DEGs (p-value ≤0.001 and fold-change of ≤-1.5; ≥1.5) for all selected Cys^R. Blue: Shared down-regulated genes. Green: Shared up-regulated genes.

Transcriptomic assessment of Cys^R with mutation in *gigB* promotor region

As a single point mutation within the promotor region of *gigB* is the only gene mutation other than *gyrA*, *gyrB* or *ybdL* that caused high-level resistance (≥64 MIC fold-shift) to cystobactamids, we assessed the mutant by RNA-sequencing. Here, six DEGs were found to be differentially up-and down-regulated (p-value ≤0.001 and fold-change of ≤-1.5; ≥1.5) (Figure 3.6). The most upregulated genes are the three components of the AdeIJK (*adeI*, *adeJ* and *adeK*) RND-efflux pump system, D-amino acid dehydrogenase (*dadA*) and two hypothetical genes. The most down-regulated gene is a hypothetical gene (Table S3.7).

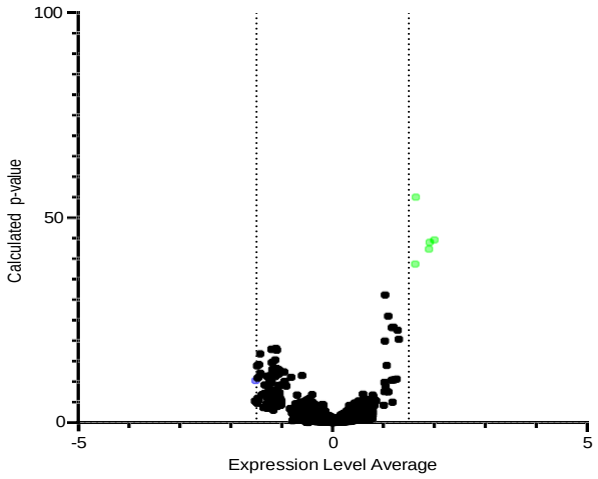

Figure 3.6: Volcano plot of all DEGs (p-value ≤0.001 and fold-change of ≤-1.5; ≥1.5) for selected Cys^R. Blue: Shared down-regulated genes. Green: Shared up-regulated genes.

3.4. Discussion and Conclusion

Colistin is one of the last resort drugs for multidrug resistant *A. baumannii* and carbapenem resistant *A. baumannii* infections (Isler *et al*., 2019). However, cystobactamid derivatives showed a comparable activity profile to colistin, which speaks in favor for the cystobactamid compound class. Derivatives **3** (0.03-1 µL/mL), **5** (0.03-0.5 µL/mL) **6** (0.01-0.5 µL/mL), **7** (0.03-0.5 µL/mL), and **8** (0.01-1 µL/mL) all ranging within low minimum inhibition concentrations. Cystobactamid derivatives, **5**, **6**, **7** and **8** were as assessed against carbapenem resistant *A. baumannii* isolates assessed and showed a smaller susceptibility profile compared to colistin (0.125-0.5 µL/mL).

Topoisomerase inhibitors that include fluoroquinolones and NBTIs (Novel Bacterial Topoisomerase Inhibitors) have all shown activity to several ESKAPE pathogens including *A. baumannii* and CRAB strains, but susceptibility differs between species (Kokot *et al*., 2022; Desai *et al*., 2021). Overall, cystobactamids showed a preferable susceptibility profile to selected *A. baumannii* strains compared to other topoisomerase inhibitors such as ciprofloxacin, zoliflodacin, gepotidacin, levofloxacin, moxifloxacin and had a comparable susceptibility profile to colistin (Table 3.1 and Table 3.2). Compared to ciprofloxacin, cystobactamids show superior inhibition of topoisomerase II and IV, especially topoisomerase IV. These results are of interest as Baumann and co-workers (2014) reported superior inhibition of *E. coli* gyrase compared to *E. coli* topoisomerase IV. This dual mechanism of action which is also commonly observed for all gyrase inhibitor drugs such as zoliflodacin and gepotidacin (Krokot *et al*., 2022; Brandford *et al*., 2020). Colistin is a polycationic polypeptide antibiotic that has been increasingly used in combination with other antibiotics for the treatment of MDR (Multidrug resistant) *Acinetobacter baumannii* infection (Petrosillo *et al*., 2008). Table

S3.1 confirms the synergestic effect of colistin and cystobactamids. The synergistic killing of *Acinetobacter baumannii* was recently demonstrated in many in vitro studies. Various colistin combinations have been explored, including those containing carbapenems, aminoglycosides, fosfomycin, and rifampicin. The reason for the observed synergy is not completely understood, however, it is linked to the outer membrane permeabilizer effect of colistin which permits the entry of larger hydrophobic molecules (Soudeiha *et al*., 2017). Colistin is positively charged and targets the bacterial outer membrane and exhibits its antimicrobial action by binding to the negatively charged lipopolysaccharide that leads to permeabilization of the outer membrane and ultimatly destabilization (Poirel *et al*., 2017).

A. baumannii developed resistance to colistin by altering the lipid A that changes the charge and prevents binding of colistin. The two major mechanisms include the addition of 4-amino-4-deoxy-l-arabinose (l-Ara4N) and/or phospho ethanolamine (PEtn) that reduces the net negative charge of LPS. *A baumannnii* lipid A modification is mainly achieved by point mutations of the *pmrAB* that cause an addition of phospho ethanolamine to LPS (Moffatt *et al*., 2010). Since colistin is one of the last resort drug treatments for CRAB infections, resistance to colistin is considered as a serious medical threat. Here, no cross-resistance to colistin was observed for any of the with Cys^R strains (Figure 3.2). This is expected as 53% of the Cys^R have mutations are target mutations within *gyrA* or *gyrB*, which is different to colistin's target.

Further, no cross-resistance above four-fold MIC shift was observed from the NBTI, gepotidacin, and third generation fluoroquinolones, zolifloxacin and moxifloxacin. According to Spence and Towner (2003), the main resistance mechanism of *A. baumannii* clinical isolates to moxifloxacin are target mutations within binding region Ser-83 in GyrA and ser-80 in ParC. Resistance to zoliflodacin is mostly caused by target mutations within gyrB (Alm *et al*., 2015; Foerster *et al*., 2019; Jacobsson *et al*., 2021). However, Foerster and co-workers (2015) reported that resistance is also caused by the over expression of efflux pumps. Gepotidacin resistant causing mutations are clustered within GyrA (D82N) and ParC (D79N) in *E. coli* and *Klebsiella pneumonia* and GyrA (S91F, D95A, A75S or A92T/V) and ParC (D86N) in *Neisseria gonnorhea* (VanScoy *et al*., 2020). According to Szili *et al.* (2019) the gepotidacin forms a salt bridge to the topoisomerase-DNA complex at Asp82 on *gyrA* and Asp79 on *parC* thus, mutations within this pocket can result alterations in binding and lead to resistance.

The whole genome of 30 strains were assessed and revealed that 53% of the Cys^R had mutations in *gyrA* (43%) (subunit A of the gyrase complex responsible for DNA coiling) or *gyrB* (10%) (subunit B of the gyrase complex responsible for DNA coiling). Cystobactamids are topoisomerase inhibitors therefore the assumption is that the observed gene mutations found within the target interferes with the gyrase-DNA complex binding thus leading to resistance. Figure 3.1 indicates the predicted mutation sites found on the published *E. coli* gyrase

(homolog model made by Timo Risch). The found gyrase mutations do not overlap with known binding sites of fluoroquinolones (ciprofloxacin, levofloxacin, and moxifloxacin) nor NBTIs (zoliflodacin, gepotdacin). Since, there is no overlap with the known fluoroquinolone binding sites, no cross-resistance is expected (Table S3.3). However, the gene mutations are not in a distinct binding pocket and are rather dispersed within the C-terminal domains, Gyrase A-box, and TOPRIM-region of gyrase B (Figure 3.1 and Table S3.4).

Elgaher and co-workers (2020) and Baumann and colleagues (2014) reported that the primary binding site of the cystobactamids is probably located at the gyrase–DNA interface and that cystobactamids interact with the DNA part of the gyrase-DNA complex by binding to DNA utilizing the minor groove without significant intercalation. This was proven by displacement titration experiments using fluorescent dyes that show increased fluorescence upon calf thymus DNA binding: Hoechst 33342 for DNA minor-groove binding and ethidium bromide (EtBr) for intercalation. Interestingly, Michalczyk and co-workers (2023) were able to explain how a structurally similar compound with a gyrase inhibiting mechanism, albicidin, exhibits a dual binding mechanism as once side interacts with the crucial gyrase dimer interface, while the other side intercalates between the fragments of cleaved DNA substrate. This binding in turn locks the complex and prevents further re-ligation of the DNA. As cystobactamids are structurally similar, this opens a door for further investigation of the binding of cystobactamids within the DNA-gyrase complex. Binding and placement are important, and the C-terminal regions play a vital role in DNA binding and stability (Corbet *et al*., 2004). However, the binding mechanism of cystobactamids is still to be confirmed.

Moreover, nine Cys^R with a MIC shift with eight-fold for levofloxacin, all Cys^R with a point mutation within the *ybdL* (Q354H). As in the case of gepotidacin, resistance to levofloxacin is caused to mutations in DNA gyrase or topoisomerase IV, or via alterations to drug efflux (Fabrega *et al*., 2009). The FDA (2022) reported that resistance to levofloxacin is common to occur for fluoroquinolones and NBTI but is unlikely to develop between levofloxacin and other antibiotic classes. Cross-resistance to levofloxacin with a MIC shift of eight-fold and ciprofloxacin with four-fold only occurs for the Cys^R that poses the point mutations within *ybdL* (Q354H) or in the case of a single Cys^R, a point mutation within the promotor region of *gigB* (-35bp T>G). Cross-resistance with zoliflodacin is also observed for Cys^R with point mutations within *ybdL* (Q354H). In addition, the *gyr* and *ybdL* mutations are more associated with high-level resistance (16->128 MIC fold-shift) for cystobactamids compared to no to two-fold MIC fold-shift observed with other gene mutations observed (Figure 3.2). However, other gene mutations that caused high-level resistance (>128 MIC fold-shift) is the mutant with the single point mutation in the promotor region of *gigB*. Therefore, further investigation was done for

Cys^R with the point mutation within *ybdL* (Q354H) and *gigB* (-35bp T>G) by means of transciptomics.

The single point mutation within the *ybdL* (Q354H) is the second most occurring mutation with 27% in all Cys^R. YbdL is a PLP-dependent aminotransferase with a preference for methionine followed by histidine and phenylalanine that catalyze a wide variety of reaction types and usually have a conserved lysine residue in the active site for PLP binding. However, no mechanism has been described how alterations within *ybdL* can confer resistance to antibacterial compounds. To investigate the resistance to cystobactamids as well as observed cross-resistance, selected Cys^R carring the *ybdL* (Q354H) was assessed based on growth kinetics and metabolic activity. All Cys^R showed a loss in fitness (Figure 3.3). Fitness loss is often seen in Cys^R as it play an important role in dynamics of resistance and the success of resistant bacteria (Andersson and Hughes, 2010). It is possible to use the physiological reasoning of fitness costs to aid in the design of novel treatment options that targets the physiological weaknesses associated with a resistance mechanism. Understanding of fitness costs can aid in predicting the rate and trajectory of bacterial resistance. (Schulz zur Wiesch *et al*., 2010).

The transcriptomic analysis of the Cys^R strains with the *ybdL* mutation revealed the up-regulation of MepA (Figure 3.4; Table S3.5). MepA is as a multidrug and toxic compound extrusion (MATE) family efflux transporter and has been previously described to be able to extrude fluoroquinolones. The main role of MATE pumps is to pump compounds such as cationic dyes, fluoroquinolones, and aminoglycosides in the periplasmic space by utilizing the gradient of Na+ and H+ as energy source (Su *et al*., 2005; Freitas *et al*., 2022). MepA is the neighbor gene of *ybdL* thus linking the single point mutation within *ybdL* to over-expression of MepA resulting in the observed resistance being efflux-mediated. MATE efflux pumps in *A. baumannii* have proven to confer more than a four-fold increase in the MICs of ciprofloxacin and other compounds (Su *et al*., 2005). The four-fold increase are in line with the observed cross-resistance to fluoroquinolones of the Cys^R. This is also agreement with Langevin and Dunlop (2018) that states that the over-expression of efflux pumps can have a negative effect on the fitness of bacteria, which is observed within the assessed Cys^R as well as the irreversibility aspect. Antibiotic resistance due to a change in membrane permeability and efflux comes at a significant cost. This is due to the simultaneous expulsion of nutrients and other required factors with the antimicrobial compound (Ferenci, 2005). Moreover, in Gram-negative strains, the MATE efflux pump resistance mechanism has been linked with the induction of SOS response, which is a known to be caused by cystobactamids (Piddock *et al*., 1990; Franke *et al*., 2021). STRING clusters that were significantly enriched were capsid protein, and pilus organization, styrene degradation, aromatic hydrocarbons catabolism, cell

motility, trehalose metabolic process, signal, and phosphopantetheine (Table S3.6). All of these clusters contained genes that were down-regulated and can be associated with antibacterial resistance, stress, and virulence in *A. baumannii* (Vijayakumar *et al*., 2016; Kashyap *et al*., 2021; Eijkelkamp *et al*., 2011; Maria-Neto *et al*., 1848, Gupta *et al*., 2020; De Silva and Kumar, 2019; Crippen and co-workers (2021).

Interestingly, Cys^R with the point mutations within the promotor region also resulted in the up-regulation of an RND-efflux pump, AdeIJK (Figure 3.4; Table S3.7). AdeIJK is present in all strains of *A. baumannii*. It contributes to resistance to a large range of antimicrobial compounds including topoisomerase inhibitors (Xing *et al*., 2014). There is no indication that adeIJK genes are specifically regulated and therefore assumed to be controlled at an integrated level (Xing *et al*., 2014). GigB is a regulator of stress and antibiotic resistance in *A. baumannii* and has been identified as required for the characteristic MDR phenotype of a contemporary *A. baumannii* isolate (AB5075) a (Gebhardt *et al*., 2015; Gebhardt, 2017). However, more information needs to be gathered on GigB as well as the regulators of AdeIJK to be able to make a sound deduction.

In conclusion, cystobactamid derivatives have s an evident susceptibility profile for *A. baumannii* clinical strains, including CRAB strains, comparable to colistin and superior to other topoisomerase II inhibitors and NBTI drugs. The IC_{50} shows pronounced activity for topoisomerase II and IV inhibition. High-level resistance is obtained by target mutations of the GyrA and GyrB, which is in line with the resistance mechanisms of other topoisomerase inhibitors. The precise binding site of cystobactamids has not yet been determined and however, the lack of high-level cross-resistance to other topoisomerase inhibitors excludes known binding sites. Besides mutations of GyrA and GyrB, an additional mutation within YbdL is responsible for high-level resistance as well as a point mutation within the promotor region of a major antibiotic resistant regulator, GigB (-35bp T>G). Here, we were able to assess the transcriptome of Cys^R containing the ybdL point mutation and the point mutation within the gigB promotor site. Cys^R containing the ybdL resulted in the up-regulation of the neighboring gene, *mepA*. MepA is a MATE efflux pump and has been described in resistance to fluoroquinolones and SOS induction. Further, point mutation within the promotor region of a major antibiotic resistant regulator, GigB (-35bp T>G) transcriptome revealed the upregulation of a RND- efflux pump, AdeIJK. The obtained results are preliminary, and mechanisms should be further investigated. However, taken all data together, the main resistance mechanisms of *A. baumannii* against topoisomerase inhibiting cystobactamids are target mutations and efflux-mediated.

3.5. References

Alm, R.A., Lahiri, S.D., Kutschke, A., Otterson, L.G., McLaughlin, R.E., Whiteaker, J.D., Lewis, L.A., Su, X., Huband, M.D., Gardner, H. and Mueller, J.P., 2015. Characterization of the novel DNA gyrase inhibitor AZD0914: low resistance potential and lack of cross-resistance in Neisseria gonorrhoeae. Antimicrobial agents and chemotherapy, 59(3), pp.1478-1486.

Andersson, D.I. and Hughes, D., 2010. Antibiotic resistance and its cost: is it possible to reverse resistance?. Nature Reviews Microbiology, 8(4), pp.260-271.

Baumann, S., Herrmann, J., Raju, R., Steinmetz, H., Mohr, K.I., Hüttel, S., Harmrolfs, K., Stadler, M. and Müller, R., 2014. Cystobactamids: myxobacterial topoisomerase inhibitors exhibiting potent antibacterial activity. Angewandte Chemie International Edition, 53(52), pp.14605-14609.

Beijerinck, M.W., 1911. Pigmenten als oxydatie-producen door bacterien gevormd. Koninklijke Akademie Wetenschappente Amsterdam, 13, pp.1066-1177.

Blair, J.M., Webber, M.A., Baylay, A.J., Ogbolu, D.O. and Piddock, L.J., 2015. Molecular mechanisms of antibiotic resistance. Nature reviews microbiology, 13(1), pp.42-51.

Bradford, P.A., Miller, A.A., O'Donnell, J., and Mueller, J.P., 2020. Zoliflodacin: an oral spiropyrimidinetrione antibiotic for the treatment of Neisseria gonorrheae, including multi-drug-resistant isolates. ACS Infectious Diseases, 6(6), pp.1332-1345.

Corbett, K.D., Shultzaberger, R.K., and Berger, J.M., 2004. The C-terminal domain of DNA gyrase A adopts a DNA-bending β-pinwheel fold. Proceedings of the National Academy of Sciences, 101(19), pp.7293-7298.

Crippen, C.S., Glushka, J., Vinogradov, E., and Szymanski, C.M., 2021. Trehalose-deficient Acinetobacter baumannii exhibits reduced virulence by losing capsular polysaccharide and altering membrane integrity. Glycobiology, 31(11), pp.1520-1530.

De Silva, P.M., and Kumar, A., 2019. Signal transduction proteins in Acinetobacter baumannii: Role in antibiotic resistance, virulence, and potential as drug targets. Frontiers in microbiology, 10, p.49.

Desai, J., Sachchidanand, S., Kumar, S., and Sharma, R., 2021. Novel bacterial topoisomerase inhibitors (NBTIs)–a comprehensive review. European Journal of Medicinal Chemistry Reports, 3, p.100017.

Eijkelkamp, B.A., Hassan, K.A., Paulsen, I.T. and Brown, M.H., 2011. Investigation of the human pathogen Acinetobacter baumannii under iron limiting conditions. BMC genomics, 12, pp.1-14.

Elgaher, W.A., Hamed, M.M., Baumann, S., Herrmann, J., Siebenbürger, L., Krull, J., Cirnski, K., Kirschning, A., Brönstrup, M., Müller, R. and Hartmann, R.W., 2020. Cystobactamid 507: concise synthesis, mode of action, and optimization toward more potent antibiotics. Chemistry–A European Journal, 26(32), pp.7219-7225.

Fàbrega, A., Madurga, S., Giralt, E. and Vila, J., 2009. Mechanism of action of and resistance to quinolones. Microbial biotechnology, 2(1), pp.40-61.

Ferenci, T., 2005. Maintaining a healthy SPANC balance through regulatory and mutational adaptation. Molecular Microbiology, 57(1), pp.1-8.

Foerster, S., Drusano, G., Golparian, D., Neely, M., Piddock, L.J., Alirol, E. and Unemo, M., 2019. In vitro antimicrobial combination testing of and evolution of resistance to the first-in-class spiropyrimidinetrione zoliflodacin combined with six therapeutically relevant antimicrobials for Neisseria gonorrhoeae. Journal of Antimicrobial Chemotherapy, 74(12), pp.3521-3529.

Foerster, S., Golparian, D., Jacobsson, S., Hathaway, L.J., Low, N., Shafer, W.M., Althaus, C.L. and Unemo, M., 2015. Genetic resistance determinants, in vitro time-kill curve analysis and pharmacodynamic functions for the novel topoisomerase II inhibitor ETX0914 (AZD0914) in Neisseria gonorrhoeae. Frontiers in microbiology, 6, p.1377.

Food and Drug Administration (FDA). Approved Drug Products: Levaquin (levofloxacin) oral tablets. https://www.accessdata.fda.gov/drugsatfda_docs/label/2011/021721s033s034lbl.pdf (Accessed 23 March 2023).

Fournier, C., Poirel, L. and Nordmann, P., 2020. Implementation and evaluation of methods for the optimal detection of carbapenem-resistant and colistin-resistant Pseudomonas aeruginosa and Acinetobacter baumannii from stools. Diagnostic microbiology and infectious disease, 98(2), p.115121.

Franke, R., Overwin, H., Häussler, S. and Brönstrup, M., 2021. Targeting Bacterial Gyrase with Cystobactamid, Fluoroquinolone, and Aminocoumarin Antibiotics Induces Distinct Molecular Signatures in Pseudomonas aeruginosa. Msystems, 6(4), pp.e00610-21.

Freitas, P.R., de Araújo, A.C.J., dos Santos Barbosa, C.R., Muniz, D.F., de Almeida, R.S., de Menezes, I.R.A., da Costa, J.G.M., Rodrigues, F.F.G., Rocha, J.E., Pereira-Junior, F.N. and Tintino, S.R., 2022. Inhibition of the MepA efflux pump by limonene demonstrated by in vitro and in silico methods. Folia Microbiologica, 67(1), pp.15-20.

Gebhardt, M.J., 2017. Identification and Characterization of a Novel Stress Response Pathway in Acinetobacter baumannii (Doctoral dissertation, The University of Chicago).

Gebhardt, M.J., Gallagher, L.A., Jacobson, R.K., Usacheva, E.A., Peterson, L.R., Zurawski, D.V. and Shuman, H.A., 2015. Joint transcriptional control of virulence and resistance to antibiotic and environmental stress in Acinetobacter baumannii. MBio, 6(6), pp.e01660-15.

Groß, S., Schnell, B., Haack, P.A., Auerbach, D. and Müller, R., 2021. In vivo and in vitro reconstitution of unique key steps in cystobactamid antibiotic biosynthesis. Nature communications, 12(1), p.1696.

Gupta, A., Singh, P.K., Sharma, P., Kaur, P., Sharma, S., and Singh, T.P., 2020. Structural and biochemical studies of phosphopantetheine adenylyltransferase from Acinetobacter baumannii with dephospho-coenzyme A and coenzyme A. International journal of biological macromolecules, 142, pp.181-190.

Isler, B., Doi, Y., Bonomo, R.A. and Paterson, D.L., 2019. New treatment options against carbapenem-resistant Acinetobacter baumannii infections. Antimicrobial agents and chemotherapy, 63(1), pp.e01110-18.

Jacobsson, S., Golparian, D., Scangarella-Oman, N. and Unemo, M., 2018. In vitro activity of the novel triazaacenaphthylene gepotidacin (GSK2140944) against MDR Neisseria gonorrhoeae. Journal of Antimicrobial Chemotherapy, 73(8), pp.2072-2077.

Kashyap, S., Sharma, P. and Capalash, N., 2021. Potential genes associated with survival of Acinetobacter baumannii under ciprofloxacin stress. Microbes and Infection, 23(9-10), pp.104844.

Kokot, M., Anderluh, M., Hrast, M. and Minovski, N., 2022. The structural features of novel bacterial topoisomerase inhibitors that define their activity on topoisomerase IV. Journal of medicinal chemistry, 65(9), pp.6431-6440.

Kyriakidis, I., Vasileiou, E., Pana, Z.D. and Tragiannidis, A., 2021. Acinetobacter baumannii antibiotic resistance mechanisms. Pathogens, 10(3), p.373.

Langevin, A.M. and Dunlop, M.J., 2018. Stress introduction rate alters the benefit of AcrAB-TolC efflux pumps. Journal of bacteriology, 200(1), pp.e00525-17.

Lupo, A., Haenni, M. and Madec, J.Y., 2018. Antimicrobial resistance in Acinetobacter spp. and Pseudomonas spp. Microbiology spectrum, 6(3), pp.6-3.

Maria-Neto, S., de Almeida, K.C., Macedo, M.L.R. and Franco, O.L., 2015. Understanding bacterial resistance to antimicrobial peptides: From the surface to deep inside. Biochimica et Biophysica Acta (BBA)-Biomembranes, 1848(11), pp.3078-3088.

Michalczyk, E., Hommernick, K., Behroz, I., Kulike, M., Pakosz-Stępień, Z., Mazurek, L., Seidel, M., Kunert, M., Santos, K., von Moeller, H. and Loll, B., 2023. Molecular mechanism of topoisomerase poisoning by the peptide antibiotic albicidin. Nature Catalysis, pp.1-16.

Moffatt, J.H., Harper, M., Harrison, P., Hale, J.D., Vinogradov, E., Seemann, T., Henry, R., Crane, B., St. Michael, F., Cox, A.D. and Adler, B., 2010. Colistin resistance in Acinetobacter baumannii is mediated by complete loss of lipopolysaccharide production. Antimicrobial agents and chemotherapy, 54(12), pp.4971-4977.

Petrosillo, N., Ioannidou, E. and Falagas, M.E., 2008. Colistin monotherapy vs. combination therapy: evidence from microbiological, animal and clinical studies. Clinical Microbiology and Infection, 14(9), pp.816-827.

Piddock, L.J., Walters, R.N., and Diver, J.M., 1990. Correlation of quinolone MIC and inhibition of DNA, RNA, and protein synthesis and induction of the SOS response in Escherichia coli. Antimicrobial agents and chemotherapy, 34(12), pp.2331-2336.

Poirel, L., Jayol, A. and Nordmann, P., 2017. Polymyxins: antibacterial activity, susceptibility testing, and resistance mechanisms encoded by plasmids or chromosomes. Clinical microbiology reviews, 30(2), pp.557-596.

Schulz zur Wiesch, P., Engelstadter, J. and Bonhoeffer, S., 2010. Compensation of fitness costs and reversibility of antibiotic resistance mutations. Antimicrobial agents and chemotherapy, 54(5), pp.2085-2095.

Soudeiha, M.A., Dahdouh, E.A., Azar, E., Sarkis, D.K. and Daoud, Z., 2017. In vitro evaluation of the colistin-carbapenem combination in clinical isolates of A. baumannii using the checkerboard, Etest, and time-kill curve techniques. Frontiers in cellular and infection microbiology, 7, p.209.

Spence, R. P. and Towner, K. J., 2003. Frequencies and mechanisms of resistance to moxifloxacin in nosocomial isolates of Acinetobacter baumannii. Journal of Antimicrobial Chemotherapy, 52(4), pp.687-690.

Su, X.Z., Chen, J., Mizushima, T., Kuroda, T. and Tsuchiya, T.J., 2005. AbeM, an H+-coupled Acinetobacter baumannii multidrug efflux pump belonging to the MATE family of transporters. Antimicrobial Agents and Chemotherapy, 49(10), pp.4362-4364.

Szili, P., Draskovits, G., Révész, T., Bogár, F., Balogh, D., Martinek, T., Daruka, L., Spohn, R., Vásárhelyi, B.M., Czikkely, M. and Kintses, B., 2019. Rapid evolution of reduced susceptibility against a balanced dual-targeting antibiotic through stepping-stone mutations. Antimicrobial Agents and Chemotherapy, 63(9), pp.e00207-19.

Tacconelli, E., 2017. Global Priority List of Antibiotic-Resistant Bacteria to Guide Research, Discovery, and Development.

Tacconelli, E., Carrara, E., Savoldi, A., Harbarth, S., Mendelson, M., Monnet, D.L., Pulcini, C., Kahlmeter, G., Kluytmans, J., Carmeli, Y. and Ouellette, M., 2018. Discovery, research, and

development of new antibiotics: the WHO priority list of antibiotic-resistant bacteria and tuberculosis. The Lancet Infectious Diseases, 18(3), pp. 318-327

VanScoy, B.D., Scangarella-Oman, N.E., Fikes, S., Min, S., Huang, J., Ingraham, K., Bhavnani, S.M., Conde, H., and Ambrose, P.G., 2020. Relationship between gepotidacin exposure and prevention of on-therapy resistance amplification in a Neisseria gonorrhoeae hollow-fiber in vitro infection model. Antimicrobial Agents and Chemotherapy, 64(10), pp.e00521-20.

Vijayakumar, S., Rajenderan, S., Laishram, S., Anandan, S., Balaji, V. and Biswas, I., 2016. Biofilm Formation and Motility Depend on the Nature of the Acinetobacter baumannii Clinical Isolates. Frontiers in Public Health, 4, p.105.

Whiteway, C., Breine, A., Philippe, C. and Van der Henst, C., 2022. Acinetobacter baumannii. Trends in microbiology, 30(2), pp.199-200.

Xing, L., Barnie, P.A., Su, Z. and Xu, H., 2014. Development of efflux pumps and inhibitors (EPIs) in A. baumannii, https://ir.ucc.edu.gh/xmlui/handle/123456789/5514. (Accessed: 15 March 2023).

3.6. Supplemental Figures and Tables

Table S3.1: Synergy of a cystobactamid derivatives and colistin with *A. baumannii* DSM-30008.

Antimicrobial Combination	Synergistic effect (FICI≤0.5)	Indifferent effect (FICI >0.5-4)	Antagonistic effect (FICI >4)
Colistin + 4	Yes (0.38)	-	-
Colistin + 5	-	-	-
Colistin + 6	Yes (0.38)	-	-
Colistin + 7	Yes (0.31)	-	-

Table S3.2: Minimum inhibition concentration fold-shift (Cys^R MIC (µg/mL)/wild-type strain MIC (µg/mL)) of **1** and **5** after 10 times cultivation on non-selective agar.

Strain	MIC shift- fold after streaking out on non-selective agar 10x	
	1	5
Wild-type	-	-
Cys^R1	64	32
Cys^R2	32	16-32
Cys^R3	32	32
Cys^R4	64	32
Cys^R5	32	32

Table S3.3: Minimum Inhibition Concentrations fold-shift of Cys^R for cystobactamid derivatives and clinically relevant antibiotics and mutant genotypes.

Cys^R	Cystobactamid derivative	CIP	COL	ZOL	GEP	LEV	MOXI	Genome information
1	64	4	1	8	1	8	1	*ybdL*: Q354H
2	32	4	1	8	1	8	1	*ybdL*: Q354H
3	64	4	1	8	1	8	1	*ybdL:* Q354H*; gigA:* L89P*; rsbP* - D90Y
4	32	4	1	8	1	8	1	*ybdL:* Q354H*; gigA:* L89P*; rsbP* - D90Y*; Hypothetical gene (TPR repeat containing protein):* H29L
5	64	4	1	2	1	8	1	gigB: -35bp T>G
6	64	4	1	8	1	8	1	ybdL; Gln354His
7	64	4	1	8	1	8	1	ybdL; Gln354His
8	32	4	1	2	1	8	1	Hypothetical gene (Transcriptional regulator. TetR); Arg20Leu; Hypothetical gene (gigB; Putative anti-anti-sigma factor): Met1Ile; ybdL; Gln354His
9	64	4	1	8	1	8	1	Hypothetical gene (gigA; putative tcs - rr; rsbP); Leu89Pro; Asp90Tyr; ybdL; Gln354His
10	1	1	1	1	1	0.25	1	fatty acid desaturase 571bp; GCA->GTA; Arg287His
11	1	1	1	1	1	0.25	1	fatty acid desaturase 571bp; GCA->GTA; Upstream of ligE -78bp A->G
12	1	1	1	1	1	0.25	1	fatty acid desaturase 571bp; GCA->GTA; Arg287His
13	1	1	1	1	1	0.25	1	fatty acid desaturase 571bp; GCA->GTA; Arg287His
14	1	1	1	1	1	0.5	1	fatty acid desaturase 571bp; GCA->GTA; Arg287His
15	133	2	1	4	2	4	<1	GyrA: Ala676Pro
16	17	0.5	<1	2	1	2	<1	GyrA: Arg568Gly
17	67	2	<1	2	1	2	<1	GyrA: Ile669Asn
18	67	1	<1	2	2	2	<1	GyrA: Arg568Gly
19	67	1	<1	4	4	2	<1	GyrA: Ile669Asn
20	67	0	<1	2	1	2	<1	GyrA: Arg568Gly
21	33	0	<1	2	1	2	<1	GyrA: Ala850Pro
22	33	0	<1	2	1	2	<1	GyrA: Ala850Pro
23	33	1	<1	2	1	2	<1	GyrA: Arg675Ser
24	67	2	<1	4	4	2	<1	GyrB: Gly386Asp
25	16	1	1	2	2	0.5	1	GyrA: Ins Leu864

26	32	1	0.5	8	2	1	4	GyrA: Gly566Arg
27	128	1	1	8	2	4	4	GyrA: Leu557Pro
28	64	1	0.5	4	0.5	2	2	GyrB: Arg529His
29	32	1	1	4	1	2	2	GyrA: Arg565Ser
30	32	1	1	4	0.5	1	1	GyrB: Arg529His

Table S3.4: Mutations found within target genes of 30 selected Cys^R.

Gene	Mutation	Repeats	Region
gyrA	Ala676Pro	1	C-terminal
gyrA	Ile669Asn	2	C-terminal
gyrA	Ala850Pro	2	C-terminal
gyrA	Arg568Gly	3	Gyrase-box motif
gyrA	Arg675Ser	1	C-terminal
gyrA	Leu557Pro	1	C-terminal
gyrA	Arg565Ser	1	Gyrase-box motif
gyrA	Gly566Arg	1	Gyrase-box motif
gyrA	Leu864 insert	1	C-terminal
gyrB	Gly386Asp	1	C-terminal
gyrB	Arg529His	2	Toprim region

Table S3.5: DEGs of all selected Cys^R (p-value ≤0.001 and fold-change of ≤-1.5; ≥1.5).

Gene locus tag	Gene name	STRING Annotation	Calculated p-value	Average expression level	Average confidence level	Average p-value
FQU82_03699	mepA	Multidrug transporter mate; Na+ driven multidrug efflux pump; Derived by automated computational analysis using gene prediction method: Protein Homology	100.25	2.04	112.23	5.7E-101
FQU82_00807	otsA	Trehalose-6-phosphate synthase; Alpha, alpha-trehalose-phosphate synthase [UDP-forming]; Derived by automated computational analysis using gene prediction method: Protein Homology	8.62	-1.91	7.68	2.4E-09
FQU82_00808	otsB	Trehalose phosphatase: Removes the phosphate from trehalose 6-phosphate to produce free trehalose	10.64	-2.32	10.52	2.29E-11

FQU82_01580	paaA	Atpase aaa; 1,2-phenylacetyl-CoA epoxidase subunit A; With PaaBCDE catalyzes the hydroxylation of phenylacetyl-CoA; Derived by automated computational analysis using gene prediction method: Protein Homology	3.63	-1.55	3.06	0.00
FQU82_01659	betI 4	TetR family transcriptional regulator; Similar to gene ACICU_01412 in CP000863	13.46	-1.97	14.26	3.49E-14
FQU82_01660	fadD3	Fatty acid--CoA ligase; COG: COG0318	10.63	-1.70	10.79	2.36E-11
FQU82_01667	hypothetical protein	Hypothetical protein; Similar to gene ACICU_01419 in CP000863	6.16	-1.78	5.68	6.96E-07
FQU82_01670	hypothetical protein	Surface antigen 1; Similar to gene ACICU_01422 in CP000863	7.45	-2.23	7.06	3.56E-08
FQU82_01671	hypothetical protein	Not Annotated by String-DB	8.50	-2.44	10.98	3.13E-09
FQU82_01672	hypothetical protein	Competence/damage-inducible protein CinA; COG: COG1546; Belongs to the CinA family.	5.58	-1.64	9.06	2.62E-06
FQU82_01673	hypothetical protein	Iron-containing redox enzyme family protein; Similar to gene ACICU_01425 in CP000863	7.46	-1.51	8.37	3.35E-08
FQU82_01676	hypothetical protein	Uncharacterized protein; Similar to gene ACICU_01428 in CP000863	4.70	-1.98	4.88	1.64E-05
FQU82_02171	ttuB 3	MFS transporter; Derived by automated computational analysis using gene prediction method: Protein Homology	8.47	-1.56	7.28	3.43E-09
FQU82_02391	pliG	Not Annotated by String-DB	6.16	-1.54	6.04	6.85E-07
FQU82_02392	hypothetical protein	Hypothetical protein; Similar to gene ACICU_02270 in CP000863	5.93	-1.63	8.29	1.16E-06
FQU82_02414	hypothetical protein	Uncharacterized protein; Similar to gene ACICU_02289 in CP000863	5.39	-2.02	6.48	4.08E-06
FQU82_02470	mmgC 7	Isovaleryl-CoA dehydrogenase Acyl-	18.84	-1.83	19.55	1.45E-19

		CoA dehydrogenase, short-chain specific; Derived by automated computational analysis using gene prediction method: Protein Homology				
FQU82_02471	putative oxidoreductase	3-hydroxy-2-methylbutyryl-CoA dehydrogenase; Belongs to the short-chain dehydrogenases/reductases (SDR) family	17.56	-2.00	17.54	2.76E-18
FQU82_02548	hypothetical protein	Uncharacterized protein; Similar to gene ACICU_02413 in CP000863	19.34	-2.82	21.10	4.54E-20
FQU82_02549	hypothetical protein	SCPU domain-containing protein; COG: COG5430	176.73	-5.20	193.90	1.9E-177
FQU82_02550	hypothetical protein	Protein CsuD; COG: COG3188	131.83	-5.33	138.67	1.5E-132
FQU82_02551	hypothetical protein	Molecular chaperone; COG: COG3121	500	-6.22	1000	0
FQU82_02552	hypothetical protein	Spore coat protein U domain-containing protein; Similar to gene ACICU_02417 in CP000863	145.76	-6.21	161.43	1.7E-146
FQU82_02553	hypothetical protein	Protein CsuA; Similar to gene ACICU_02418 in CP000863	100.40	-6.88	561.27	4E-101
FQU82_02554	hypothetical protein	Spore coat protein U domain-containing protein; COG: COG5430	500	-8.15	1000	0
FQU82_02556	hypothetical protein	TetR/AcrR family transcriptional regulator; Similar to gene ACICU_02421 in CP000863	73.06	-4.93	82.62	8.76E-74
FQU82_02557	hypothetical protein	Uncharacterized protein; Similar to gene ACICU_02422 in CP000863	16.42	-2.31	15.78	3.79E-17
FQU82_02571	hypothetical protein	DUF2171 domain-containing protein; Similar to gene ACICU_02436 in CP000863	9.89	-2.11	10.04	1.3E-10
FQU82_02807	hypothetical protein	TetR family transcriptional regulator; Derived by automated computational analysis using gene prediction method: Protein Homology	18.78	-2.20	19.63	1.67E-19
FQU82_03735	aroP 4	Aromatic amino acid transport protein AroP; COG: COG1113	14.23	-2.19	13.40	5.84E-15

FQU82_03736	hypothetical protein	Fumarylacetoacetase; Derived by automated computational analysis using gene prediction method: Protein Homology	35.28	-3.14	33.59	5.25E-36
FQU82_03737	nagL	Maleylacetoacetate isomerase; Derived by automated computational analysis using gene prediction method: Protein Homology	26.63	-2.86	25.66	2.33E-27
FQU82_03738	fosB	Glyoxalase/Bleomycin resistance /Dioxygenase superfamily protein; COG: COG0346	27.37	-2.75	27.33	4.22E-28
FQU82_03740	hpd	4-hydroxyphenylpyruvate dioxygenase; COG: COG3185	18.88	-2.58	17.45	1.33E-19

Table S3.6: STRING clustering of DEGs of selected Cys^R (p-value ≤0.001 and fold-change of ≤-1.5; ≥1.5).

Cluster ID	Cluster description	Observed gene count	Background gene count	Strength	False discovery rate
CL:3270	Mixed, incl. Capsid protein, and pilus organization	6	10	1.83	1.60E-06
CL:3273	Capsid protein, and pilus organization	5	5	2.06	3.52E-06
CL:2055	Mixed, incl. Styrene degradation, and Aromatic hydrocarbons catabolism	4	6	1.88	0.00
CL:5332	Mostly uncharacterized, incl. trehalose metabolic process, and cell motility	5	20	1.45	0.00
CL:3191	Mixed, incl. Signal, and Phosphopantetheine	7	76	1.02	0.00

Table S3.7: DEGs of the Cys^R with a point mutation in the promotor region of *gigB* (-35) found up- and down-regulated (p-value of ≤0.001 and fold-change of ≤-1.5; ≥1.5).

Gene locus tag	Gene name	STRING Annotation	Calculated p-value	Average expression level	Average confidence level	Average p-value
FQU82_02298	hypothetical protein	Adenine deaminase; Multidrug efflux RND transporter AdeABC outer membrane channel subunit AdeK; Derived by automated computational analysis using gene prediction method: Protein Homology	5.27	-1.52	4.98	5.42E-06
FQU82_01800	hypothetical protein	Phosphatidylglycerophosphatase; Derived by automated	10.29	-1.51	8.57	5.17E-11

		computational analysis using gene prediction method: Protein Homology				
FQU82_03098	AdeK	D-amino acid dehydrogenase; COG: COG0665	38.68	1.62	35.81	2.09E-39
FQU82_03095	hypothetical protein	AdeA/AdeI family multidrug efflux RND transporter periplasmic adaptor subunit; COG: COG0845; Belongs to the membrane fusion protein (MFP) (TC 8.A.1) family.	54.99	1.63	51.42	1.02E-55
FQU82_02324	dadA	Multidrug transporter; Belongs to the resistance-nodulation-cell division (RND) (TC 2.A.6) family	42.34	1.90	39.37	4.61E-43
FQU82_03096	AdeI	Uncharacterized protein; Similar to gene ACICU_02081 in CP000863	43.99	1.91	40.9	1.01E-44
FQU82_03097	AdeJ	Hypothetical protein	44.59	2.00	41.32	2.58E-45

Chapter 4: Resistance to Myrtucommulones in *Staphylococcus aureus* is Linked to Changes in the Cell Envelope and Reduced Virulence as a Consequence of Disruption of the Two-Component System SaeRS

4.1. Abstract

Natural products cover a vast range of chemical structures that allow for diversity in characteristics such as biological activity. Myrtucommulone, an acylphloroglucinol compound class isolated from myrtle (*Myrtus communis*), has activity on bacteria, parasites, fungi, and cancer cell lines. The mechanism of action is unknown. However, the molecular target is speculated to be located in the cell membrane. Here, we describe a broad characterization of *in vitro* generated myrtucommulone-resistant *Staphylococcus aureus* mutants (Myr^R) that shed further light on the mode of action and mode of resistance of this interesting natural product class. Myr^R were primarily assessed by means of whole genome sequencing, transcriptomics, and electron microscopy. Findings revealed that Myr^R have a vast number of differentially expressed genes and all investigated Myr^R displayed a deletion in the phosphorylation site of the response regulator of a two-component system, SaeRS. The deletion led to down-regulation of two-component system and related virulence factors genes. In addition, genes from the two-component system, VraRS, and FmtA were both found up-regulated in the Myr^R and is involved in the regulation of cell wall biosynthesis. Further, electron microscopy revealed a thickened cell membrane in the Myr^R. This phenotype presumably contributes to the observed cross-resistance with cell wall targeting vancomycin, daptomycin and β-lactams. This study reveals SaeRS as a major contributor to resistance in *S. aureus* whereas downstream effects are similar to those observed in vancomycin, daptomycin and β-lactam resistant bacteria. However, the causal effect is complex and requires further investigation to fully understand the mechanism of resistance.

4.2. Introduction

Myrtus communis is a shrub that belongs to the *Myrtaceae* family, and it is found mainly in the Mediterranean region and Western Asia (Messaoud *et al*., 2012). It is used as part of traditional medicine as the leaves were found to be useful in the treatment of digestive, pulmonary, and skin diseases (Nicoletti *et al.*, 2018; Lounasmaa *et al.*, 1977; Marchini and Maccioni 1998). Previous studies on the *Myrtus communis* plant resulted in the isolation of several interesting compounds such as phenolic acids, flavonoids, volatiles anthocyanins, fatty acids, and organic acids coumarins, myrtucommulone, semimyrtucommulone, galloyl-glucosides, ellagitannins, galloyl-quinic acids, caffeic, gallic and ellagic acids (Messaoud *et al*., 2005; Wannes *et al*., 2010; Messaoud and Boussaid 2011; Alipour *et al*., 2014; Sumbul *et al*., 2011; Akin *et al*., 2012). More recent studies indicate further pharmacological roles of *Myrtus communis* plant

that include antioxidative, anticancer, anti-diabetic, antiviral, antibacterial, antifungal, hepatoprotective and neuroprotective activity (Alipour *et al.*, 2014, Appendino *et al*., 2002; Messaoud *et al*., 2012). The antimicrobial activities have been ascribed to phenolic compounds that cause cell membrane and cell wall damage (Cox *et al*., 2001). In the 1970s, the first isolation of a phloroglucinol antibiotic compound was reported. This compound was named myrtucommulone A, which is structurally related to the phloroglucinol derivatives of dryopteris ferns, kousso flowers and kamala (Appendino *et al.*, 2002, Lounasmaa *et al.*, 1977). Müller and co-workers (2010) were able to fully synthesize myrtucommulone A (1), myrtucommulone F (2) and myrtucommulone C. The synthetic compounds showed the same activity as well as inhibition of inflammation and induction of apoptosis (Hans *et al*., 2015).

Myrtucommulone A has significantly high antimicrobial activity against multidrug resistant Gram-positive bacteria, however, the reason for the antimicrobial activity is not clear (Alipour *et al.*, 2014, Appendino *et al.*, 2002, Lounasmaa *et al.*, 1977, Kashman *et al*., 1974). Owlia *et al*., 2010 postulates that the mechanism of action of myrtucommulone A is due to its hydrophobic nature, which enables it to disturb the cell membrane structure. Transcriptomic studies have been conducted on rhodomyrtone that is a structurally similar compound and classified as an acylphloroglucinol (Nicoletti *et al*., 2018). This study indicated that rhodomyrtone modulates the expression of proteins and genes involved in cell wall biosynthesis, division, stress responses, antigens, virulence factors, and several metabolic pathways (Visutthi *et al*., 2011). According to our knowledge, no information has been published regarding the resistance mechanism of myrtucommulones. Therefore, the aim was to evaluate and compare the transcriptome and genotype profiles of myrtucommulone-resistant *Staphylococcus aureus* against the wild-type strain to shed some light on potential mechanisms of resistance. The findings were validated via pathway enrichment analysis and additional microbiological assessments. Electron microscopy was also conducted to further evaluate and the mutant phenotypes.

4.3. Results

Myrtucommulone derivatives exhibit a bactericidal mechanism

Five derivatives were tested against a panel of pathogens to determine the minimal inhibitory concentrations (MIC) and the cell toxicity (Table 4.1). No antimicrovial activity on Gram-negative bacteria was observed with the exeption of an *E. coli* Δ*tolC*, with the addition of permeability enhancer (PMßN) (Table S4.1). The results therefore indicate that Gram-negative bacteria possess the molecular target, but the uptake is severely hindered. Furthermore, the IC_{50} values on the CHO-K1 cell lines were in the low microgram per milliliter range for all derivatives, with the exception of derivative 3, which was virtually inactive on bacteria.

Derivative 2, 10 and 12 inhibit several Gram-positive pathogens with MIC values in the sub-micrograms per milliliter range. Importantly, derivative 2 showed the most favorable selectivity (MIC of ~0.5 µg/mL *vs.* IC_{50} of ~10 µg/mL). Overall, compound **1** and **2** showed the most promising results with and SI of 6 and 20, respectively, and these compounds were selected for further testing.

Table 4.1: Complete profiling data summarizing antibacterial (MIC), toxicity (IC_{50}) and Selectivity Index (SI) values of five assessed myrtucommulone derivatives.

Cell Line	**IC_{50} (µg/mL)**				
	1	**2**	**3**	**10**	**12**
CHO-K1 (Chinese hamster ovary)	9.1	9.8	>100	2.0	0.4
Strain	**MIC (µg/mL)**				
	1	**2**	**3**	**10**	**12**
B. subtilis DSM-10	4	0.5	32	0.5	0.25
E. faecalis DSM-20478	8	4	64	8	4
E. faecium DSM-20477	8	1	64	2	1
E. faecium DSM-17050 (VRE)	8	2	64	4	1
S. aureus DSM-11822 (MDR)	4	0.5-1	64	0.5-1	0.5
S. aureus N315 (MRSA)	2	0.125	64	1	0.25
S. aureus Mu50 (MRSA/VISA)	4	0.5-1	32-64	0.5	0.25
S. aureus Newman	2	0.5	-	-	-
S. pneumoniae DSM-20566	0.125	0.03	8	0.06	0.06
S. aureus ATCC-29213	4	0.5	-	-	-
S. aureus USA300	4	1	-	-	-
M. smegmatis mc^2155	64	64	>64	32	64
M. marinum	8	4	-	-	-
E. coli DSM-1116	>64	>64	>64	>64	>64
E. coli ΔtolC (TolC-deficient)	>64	>64	64	64	>64
P. aeruginosa PA14	>64	>64	>64	>64	>64
P. aeruginosa PA14 Δ*mexAB*	>64	>64	>64	>64	>64
Selectivity Index (SI)	**1**	**2**	**3**	**10**	**12**
(IC_{50} CHO-K1 *vs.* MIC *S. aureus* N315)	6	20	-	-	-

-: nd

The mechanism of action was determined to be bactericidal based on the determined Minimum Bactericidal Concentration (MBC), being less or equal to four-fold (Table S4.2). It was also determined that the mechanism of action differs from the known bactericidal membrane targeting glycopeptide, vancomycin, as no membrane depolarization occurs when wild-type cells are treated with sub-MIC concentrations (Figure S4.1). These two derivatives also exhibit a large lytic effect on treated cells, even at sub-MIC concentrations (Figure S4.2). Lastly, electron microscopy imaging revealed an alteration in cell shape, cell division, morphology, and cell wall ultrastructure with the treatment at sub-MIC concentrations in accordance with membrane targeting compounds such as vancomycin, daptomycin and ß-lactamase (Figure S4.3 and Figure S4.4).

The minimum inhibitory concentrations (MICs), mutant prevention concentrations (MPCs) and frequency of resistance (FoR) of **1** and **2** were determined for four *S. aureus* strains. Myr^R were successfully obtained for *S. aureus* Newman and *S. aureus* ATCC 29213 at low frequency (Table 4.2). However, after several attempts, no mutants were generated for neither *S. aureus* N315 (MRSA) nor *S. aureus* Mu50 (MRSA/VISA). This might be explained by the MPC values. To determine the FoR, the culture was exposed to a 4x MIC value. However, the MPC values of *S. aureus* N315 and *S. aureus* Mu50 are equivalent or smaller that the 4x MIC values, thus no culture was able to grow on 4x MIC and thus no mutants could be obtained at 4x MIC. The Myr^R of the well-characterized Newman strain were selected for further analyses. A total of 12 Myr^R were selected and revealed a MIC shift of four-fold to **1** and **2** with a MIC of 8 µg/mL and 4 µg/mL, respectively. Following 10 consecutive passaging on non-selective agar, the MIC values remained constant, which indicates that the underlying mutations are non-reversible.

Table 4.2: Minimum inhibitory concentration, mutant prevention concentrations, and frequency of resistance of myrtucommulone A (**1)** and myrtucommulone F (**2)** in different *S. aureus* strains.

Strain	MIC (µg/mL)		MPC (µg/mL)		FoR (at 4x MIC)	
	1	2	1	2	1	2
***S. aureus* Mu50 (MRSA/VISA)**	4	1	≤16	≤4	n. d	n. d
***S. aureus* N315 (MRSA)**	0.5	0.125	≤2	≤0.5	n. d	n. d
***S. aureus* Newman**	2	0.5	16	4	1.1×10^{-5}	8.7×10^{-6}
***S. aureus* ATCC 29213**	4	0.5	>32	>4	1.6×10^{-7}	1.3×10^{-7}

Not determined: n.d

Myr^R show a deletion in the response regulator gene of a two-component system

The genome of the Myr^R were analyzed by whole genome sequencing and all Myr^R displayed a deletion within the receiver domain of the response regulator gene of the two-component system SaeRS (*S. aureus* exoprotein expression) (Table 4.3 and Table S4.3). All Myr^R display a five amino acid deletion in response region Δ*saeR*:Val49_Met53 deletion, whereas 25% have an additional mutation within the intergenic region, upstream from *sarA* (g.-92C>A) and other 25% have an additional mutation in a *hypothetical gene* (Val48Tyr). The fitness of Myr^R were determined and compared to *S. aureus* Newman wild-type with the use of isothermal calorimetry as well as optical density over time. Figure 4.1 and Figure 4.2 shows the optical density and the heat flow for the Myr^R compared to the wild-type as well as the time to activity and metabolic rate observed by isothermal calorimetry. No change in optical density and time to activity was observed between the strains, however, isothermal calorimetry revealed a slight decrease in heat flow and metabolic rate when comparing the Myr^R to the wild-type strain. In

particular, a larger decrease is observed for Myr^{R}1 and Myr^{R}3, while Myr^{R}2 showed a similar metabolic rate as the wild-type**.**

Table 4.3: Summary of genotypes and frequency of genotype occurrence for Myr^R. Strains were mapped to *S. aureus* Newman strain (NC_009641).

Genotype Representative	Genotype	Frequency of occurrence of genotype
Myr^{R}1	*S. aureus* Newman 1^R Δ*saeR*:Val49_Met53	6/12
Myr^{R}2	*S. aureus* Newman 1^R Δ*saeR*:Val49_Met53; *sarA*: g.-92C>A	3/12
Myr^{R}3	*S. aureus* Newman 2^R Δ*saeR*:Val49_Met53; *hypothetical protein*: Val48Tyr	3/12

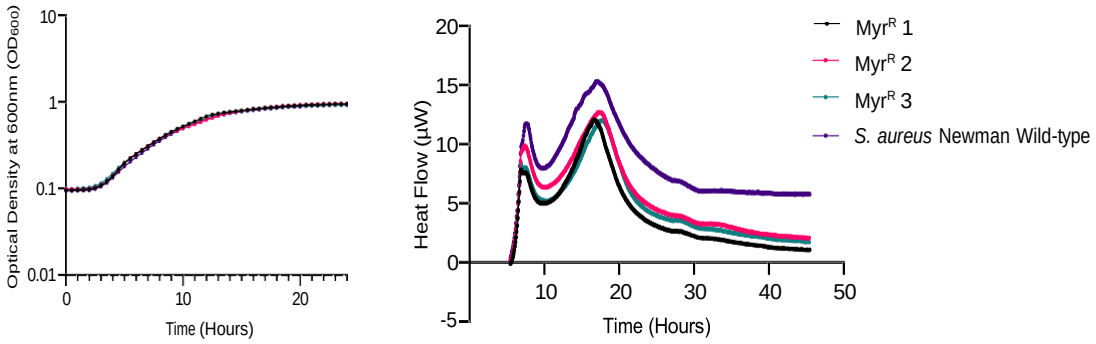

a) b)

Figure 4.1: a) Optical density (OD_{600}) measured by Tecan plate reader and b) Heatflow (µW) observed by isothermal calorimetry for wild-type *S. aureus* Newman and selected Myr^R over 24 hours.

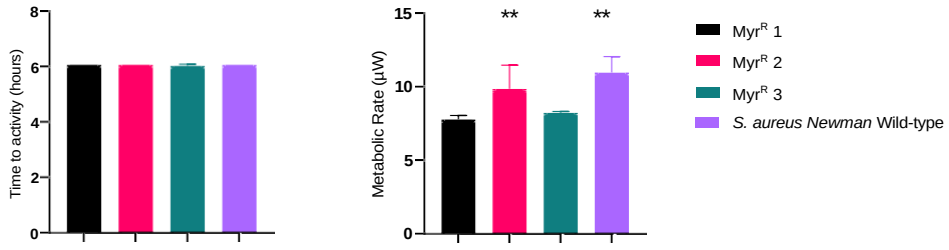

a) b)

Figure 4.2 a) Calculated time to activity (hours) and b) metabolic heat flow (µW) observed by isothermal calorimetry for selected myr^R and wild-type *S. aureus* Newman. p-value in comparison to wild-type: *<0.05,** <0.01,****<0.001.

Transcriptomic analysis reveals the down-regulation of *saeRS* and related genes

Transcriptomic analysis was performed by RNA-sequencing on the *S. aureus* Newman wild-type and the representative Myr^R. cDNA libraries were constructed, sequenced, and mapped

to the reference genome of *S. aureus* Newman (Accession number NC_009641). A total of 2341 genes were identified to be differentially expressed in Myr^R1, Myr^R2 and Myr^R3. The list of differentially expressed genes adjusted by a fold-change of ≤-2.5 and ≥2.5 and a p-value of ≤0.001 which resulted in a total of 196 genes that were down-regulated (82 hypothetical and uncharacterized genes) and 122 genes were up-regulated (58 hypothetical and uncharacterized genes) (Figure 4.3; Table S4.4; Table S4.5). Figure 4.4 represents the observed linkes between the most up-and down-regulated genes in all Myr^R.To investigate the function of the DEGs responsible for the resistance on Myr^R, GO enrichment analysis was performed with the up-and down- regulated DEGs, excluding the hypothetical and uncharacterized genes. Based on sequence homology, DEGs were assigned to one or more GO terms and categorized into secondary level GO terms in the three main categories (biological process, molecular function, and cellular component).

Upon GO functional enrichment a total of 61, 8, and 3 specific GO terms in biological process, molecular function and cellular component were identified, respectively (Table S4.6). A total of 61 GO terms were enriched in the category of biological process, including “Threonine, Valine, Isoleucine, Diaminopimelate, Branched-chain amino acid, Threonine, Leucine and Lysine biosynthetic process”, “De novo imp biosynthetic process”, “De novo ump biosynthetic process”. A total of eight GO terms that included several binding functions was enriched in the category “Cellular function”. Three GO terms were enriched in the GO Component which included “Cellular anatomical entity”, “Cytoplasm” and “Cytosol”. To identify the involved pathways, DEGs were mapped to the KEGG database, followed by KEGG pathway enrichment analysis (Table S4.7).

KEGG pathways “Monobactam biosynthesis”, “Valine, leucine and isoleucine biosynthesis”, “C5-Branched dibasic acid metabolism”, “2-Oxocarboxylic acid metabolism”, “O-Antigen nucleotide sugar biosynthesis” and “Vancomycin resistance” were significantly enriched. Further, a total of 29 clusters were identified which included “Nickel cation binding”, “De novo imp biosynthetic process”, “Antiport”, “De novo ump biosynthetic process”, “O-Antigen nucleotide sugar biosynthesis”, “Branched-chain amino acid biosynthesis”, “protein tyrosine kinase activity” and “Lysine biosynthesis” (Table S4.7; Figure S4.5).

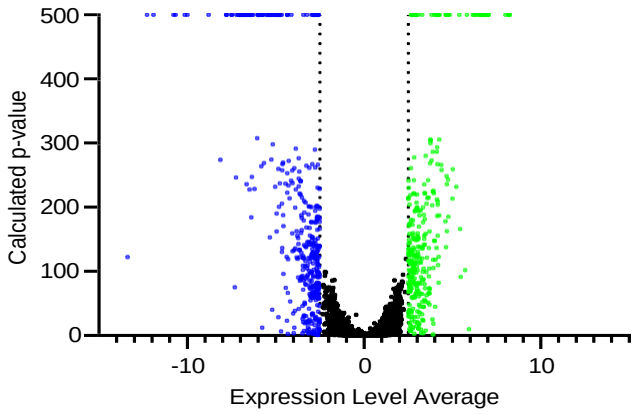

Figure 4.3: a) Volcano plot illustrating the overlapping DEGs of Myr^R that were up- and down-regulated (p-value of ≤0.001 and fold-change of ≤-2; ≥2). Note-worthy up-regulated genes are highlighted in green and important down-regulated genes are highlighted in blue. Generated by “Geneious2String” (not published - Haeckl, 2022)**.**

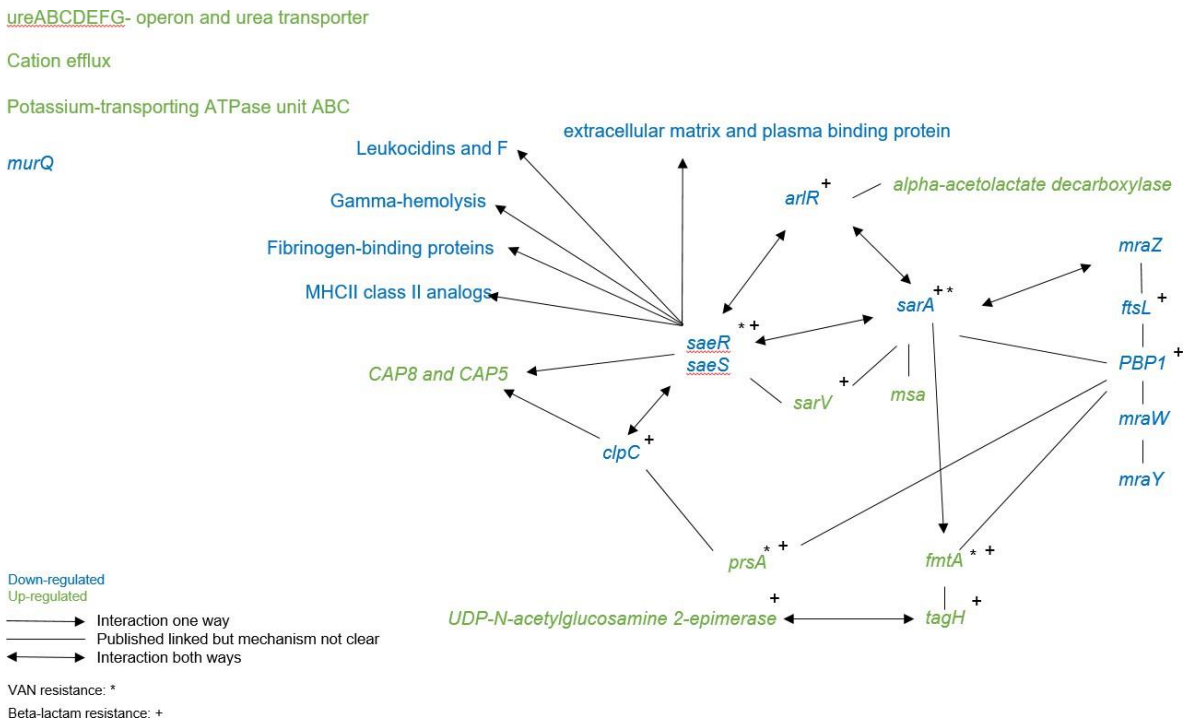

Figure 4.4: Proposed connections between most significant DEGs that are influenced by and connected to the SaeRS- two component system based on literature and String clustering (Jensen *et al*., 2009). Blue: down-regulated genes; green: up-regulated genes; -> reported one-way interaction; - published link with unknown mechanism; <-> two-way interaction; *genes involved in vancomycin/daptomycin resistance; +genes involved in ß-lactam resistance.

Myr^R show intermediate cross-resistance to vancomycin, daptomycin and ß-lactams

The obtained Myr^R were tested for resistance to **1** and **2** and cross-resistance to vancomycin, daptomycin, several ß-lactam antibiotics and a structurally similar compound originally isolated from *Rhodomyrtus tomentosa* (Wunnoo *et al*., 2021), rhodomyrtone (Table 4.4). Myr^R showed a MIC shift of four-fold to **1** and **2**. The Myr^R all showed intermediate resistance to vancomycin and daptomycin. Further, all Myr^R were cross-resistance to penicillin G, ampicillin, oxicillin and meropenem. No MIC shift was observed for amoxicillin or rhodomyrtone.

Table 4.4: The minimum inhibition concentration of selected Myr^R to myrtucommulone A (**1)** and myrtucommulone F (**2),** vancomycin, daptomycin, penicillin, amoxicillin, oxicillin, meropenem and rhodomyrtone.

Strain	MIC (µg/mL)									
	1	**2**	**VAN**	**DAP**	**PG**	**AMO**	**AMP**	**OXI**	**MER**	**RHO**
***S. aureus* Newman**	2	0.5	2	0.5	4	0.25	0.5	0.25	1	0.5
Myr^{R}1	8	2	16	2	16	0.5	1-2	0.5-1	2-4	0.5
Myr^{R}2	8	2	8	1	16	0.5	4	1	4	0.5
Myr^{R}3	8	2	4-8	2	16	0.5	1-2	1	4	0.5

VAN: Vancomycin; DAP: Daptomycin; PG: Penicillin G; AMO: Amoxicillin, Amp: Ampicillin; OXI: Oxicillin; MER: Meropenem; RHO: Rhodomyrtone

Deletion in *saeR* resulted in a change of biofilm production and cell wall

The obtained Myr^R and *S. aureus* Newman wild-type were imaged by scanning electron microscopy (SEM) and transmission electron microscopy (TEM) alongside the wild-type strain. The SEM images revealed a reduction of clustering for all Myr^R which was confirmed to be a reduction in biofilm production for all Myr^R compared to the wild-type which is linked to the down-regulation of SaeRS (Figure 4.5). The TEM imaging revealed an unusual (thickened and non-centered) septa appearance for Myr^{R}3, which is reportedly linked to membrane dysregulation and down-regulation of cell division genes. An increase of “fuzzy” and irregular surfaces appearance is apparent on all Myr^R compared to the wild-type strain (Figure 4.6). Electron microscopy revealed an increase of cell diameter for Myr^{R}1 and Myr^{R}2 and cell wall thickness (Figure 4.7).

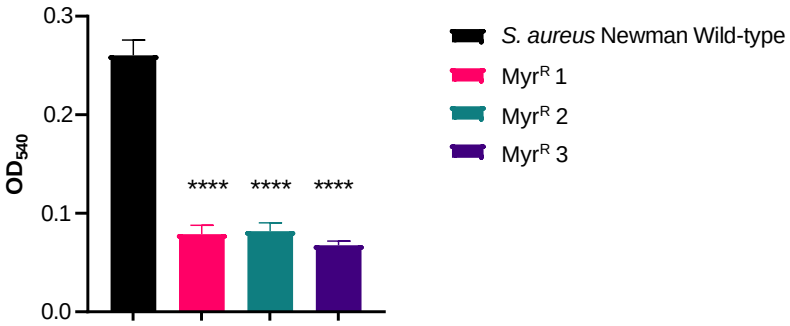

Figure 4.5: Observed biofilm formation of wild-type *S. aureus* Newman and selected Myr^R after 48 hours determined by a crystal violet assay.

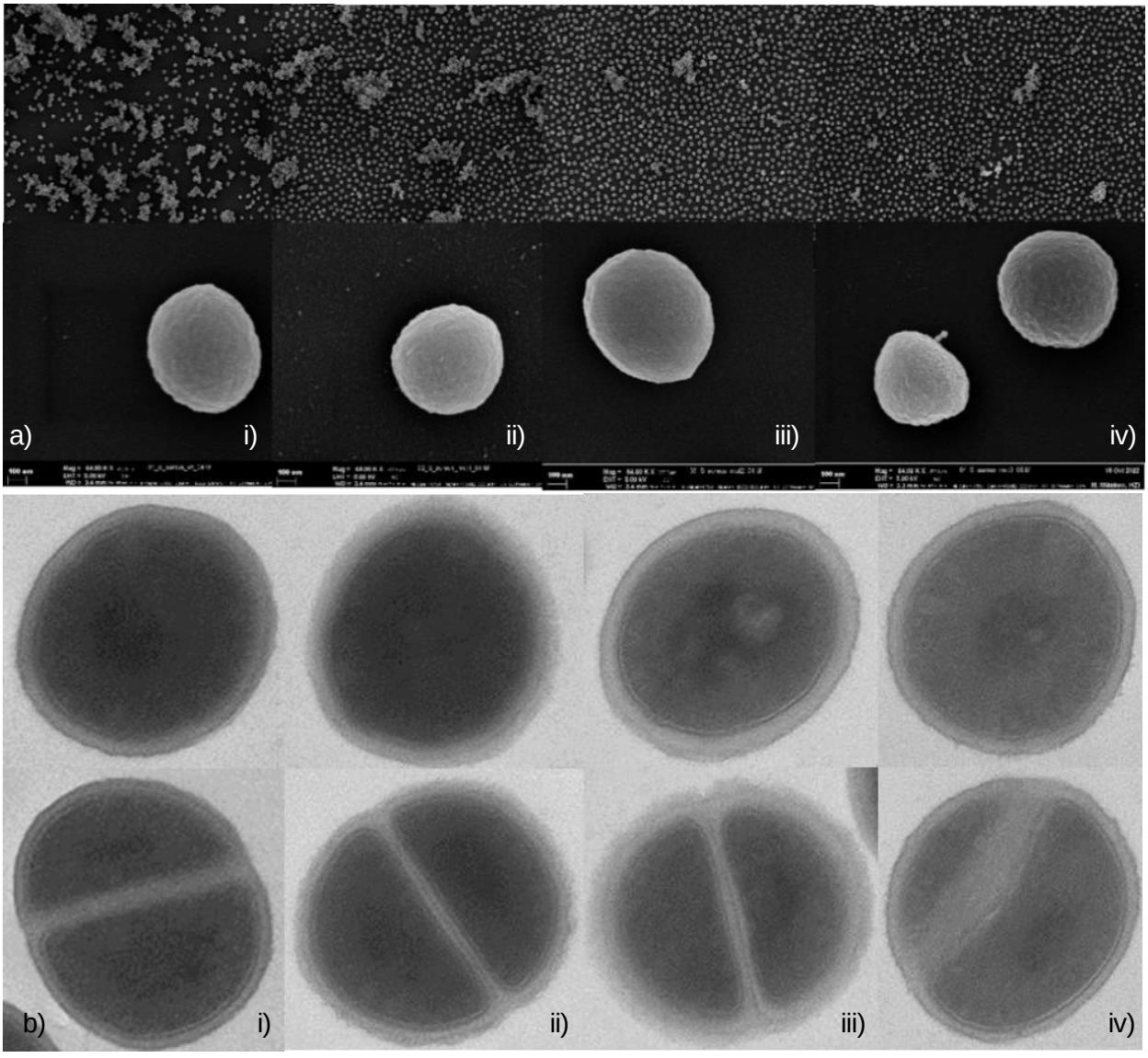

Figure 4.6: Wild-type *S. aureus* Newman strain (i), Myr^{R}1 (ii), Myr^{R}2, (iii) and Myr^{R}3 (iv) cultivated for 24 hours a) SEM of the wild-type *S. aureus* Newman strain, and Myr^R cultivated for 24 hours. b) TEM of the wild-type *S. aureus* Newman strain, and Myr^R cultivated for 24 hours. Large septa formation observed in Myr^{R}3 (red arrow).

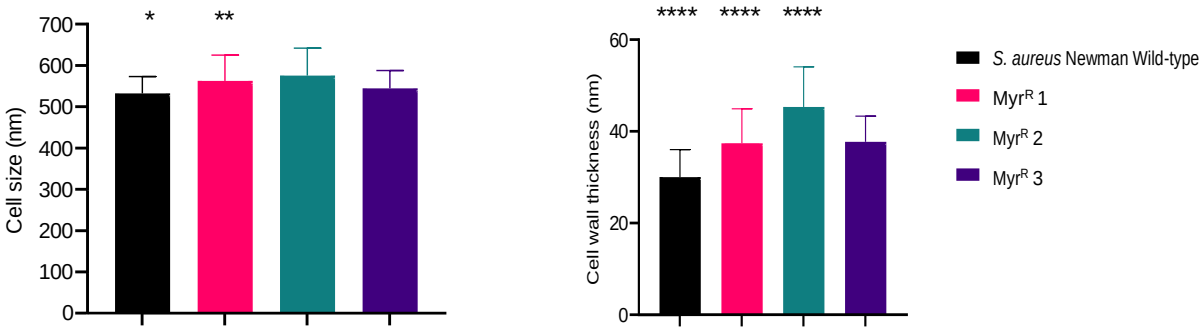

Figure 4.7: a) Cell diameter (nm) of the wild-type and Myr^R measured by ImageJ. b) Cell wall thickness (nm) of the wild-type and Myr^R measured by ImageJ (Schneider *et al.*, 2012). p-value in comparison to wild-type: *<0.05,** <0.01,****<0.001.

Down-regulation of SaeRS resulted in down-regulation of virulence genes

Myr^R strains showed a visual reduction of hemolysis on blood agar plates observed for all Myr^R compared to the wild-type which is in line with the down-regulation of SaeRS linked to hemolysis (Figure 4.8). The lysis ability of the selected Myr^R and *S. aureus* Newman wild-type was determined by the cultivation of the stains in media containing Trixton-100X, a lytic agent. All three Myr^R showed reduction in lysis compared to the wild-type strain (Figure 4.9 (a). Further, the extracellular protease production was assessed due to the down-regulation of *sarA* and up-regulation of *sarV* all Myr^R that is involved with extracellular protease production. The protease production for all the Myr^R was plotted on the standard curve and were all higher than that of the wild-type strain, which had a lower level than detected by the standard trypsin curve (Figure 4.9 (b)).

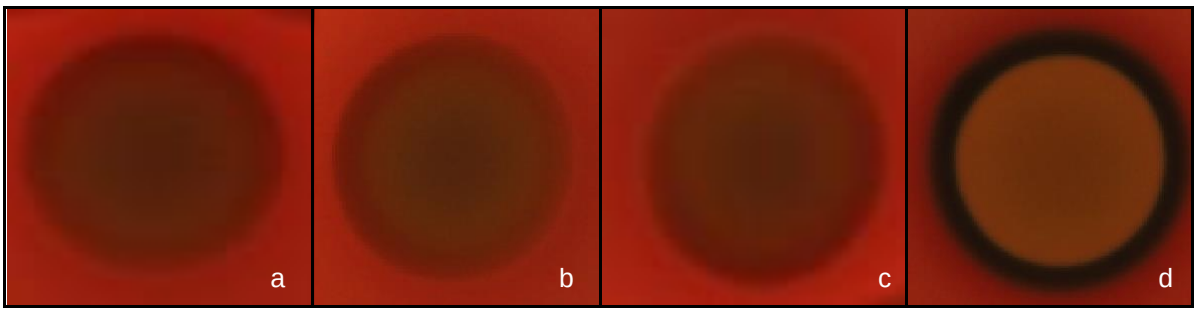

Figure 4.8: Observed hemolysis plated on blood agar plates placed against a black surface of a) Myr^{R}1 b) Myr^{R}2, c) Myr^{R}3 and d) *S. aureus* Newman wild-type.

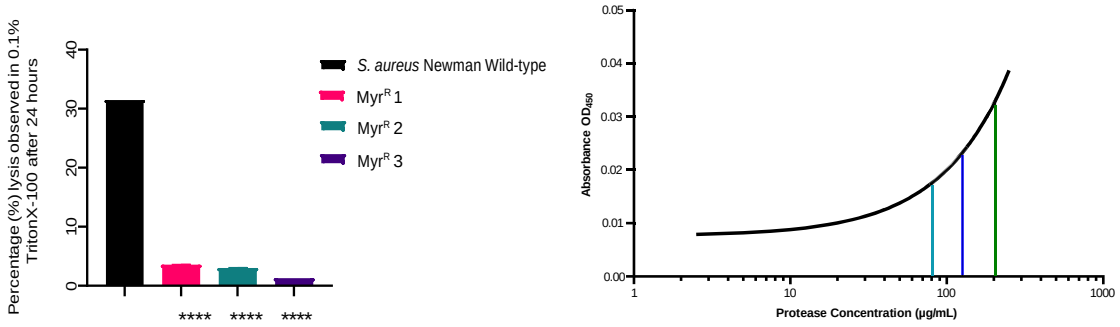

Figure 4.9: Percentage (%) lysis of wild-type and Myr^R observed after a time period of 24 hours in the presence of 0.1% triton-X 100. III: Protease production of wild-type *S. aureus* Newman and Myr^R determined by ThermoScientific colorimetric protease kit. Standard curve was done with trypsin (black line). Dark blue (126.14 µg/mL for Myr^{R}1), light blue (80.79 µg/mL for Myr^{R}2) and green (205.20 µg/mL for Myr^{R}3) lines indicate values for Myr^R, while the wild-type protease could not be estimated as the amount is lower than detection limit of assay.

4.4. Discussion and Conclusion

Myrtucommulone A (**1**) is the best-studied derivative of myrtucommulones. Myrtucommulone A (**1)** and Myrtucommulones F (**2**) are grouped together based on the hexanoyl residue on the phloroglucinol ring are characterized by a trimeric structure. Comparing **1** and **2**, **2** displayed a superior activity against the assessed strains that might be explained by the longer lipophilic side chain of **2**, which might interfere with biological membranes of the bacteria more efficiently (Tan *et al*., 2017). The observed activity of **1** and **2** on Gram-positive bacteria, in particular MRSA and VISA (Vancomycin Intermediate *Staphylococcus aureus*) strains, are in line with what has been reported previously for these and closely related compounds. Rotstein and co-workers (1974) reported Gram-positive activity for *Staphylococcus aureus*, *Bacillus* species, *Streptococcus faecalis* and *Corynebacterium diphtheriae*. Other related compounds were also reported to show Gram-positive activity such as Eucalyptone G, Nortriketones, Myrtucommulone B-E and Usnone-A (Mohamed and Ibrahim, 2007; Killeen and Larsen *et al*., 2016).

Phloroglucinols are known for their activity against Gram-positive bacteria, however, activity on Gram-negative bacterial has been reported in rare cases such as Eucalyptone G and rhodomyrtone (Mohamed and Ibrahim, 2007; Liu *et al*., 2016). With the exception of the inactive derivative 3, the panel of derivatives target Gram-positive bacteria including methicillin resistant strains (MRSA/VISA) but not Gram-negative bacteria. Our investigation revealed that **1** and **2** does exhibit a Gram-negative activity for an *E. coli* strain with a deletion of the Δ*tolC*, rendering the RND ineffective and increasing the permeability. However, the activity was only observed in *E. coli* Δ*tolC* with already increased permeability and with the addition of

permeability enhancer (PMßN) (Table S4.1). The results therefore indicate that Gram-negative bacteria possess the molecular target, but the uptake is severely hindered.

The Myr^R were sent for whole-genome sequencing and 12 out of the 12 Myr^R showed a deletion in the phosphorylation site of a response regulator of SaeRS, a two-component system, (Δ*saeR*: Val49_Met53). Another single nucleotide point mutation occurred in the intergenic region upstream from the *sarA* gene (g.-92C>A) for 3 out of 12 Myr^R. Another three Myr^R had a single nucleotide point mutation in a hypothetical gene (Val48Tyr) (Table 4.3 and Table S4.3). A similar *saeR* deletion mutation was observed in a study conducted by Miller and co-workers (2021) with the deletion in D46 to L55 leading to intermediate resistant development to vancomycin that is in accordance with the intermediate and resistant isolates in this study Table 4.4). Furthermore, it has been reported that the SaeRS system showed down-regulation in daptomycin, and up-regulation with the treatment of photonophore, CCCP (Carbonyl cyanide m-chlorophenyl hydrazone), ß-lactams and vancomycin (Kuroda *et al*., 2007; Joo *et al*., 2015; Bayer *et al*., 2013). The fitness cost was assessed for the Myr^R by OD_{600} measurements and isothermal calorimetry. Here, no shift of time to activity was observed for the tested Myr^R indicating no significant change in bacterial growth fitness; however, a significant decrease in metabolic rate can be seen for the Myr^R compared to the wild-type (Figure 4.1 and Figure 4.2). Since the SaeRS two-component has been reported to be involved in several cell functions thus a metabolic activity difference of the genotypes can be expected (Liu *et al*., 2015).

The SaeRS two-component system genes were down-regulated alongside several other genes that has been reported to have SaeR binding sites (Figure 4.4). The deletion led to the deactivation of the two-component system that was further confirmed by decrease in hemolysis in the Myr^R compared to the wild-type strain on blood agar and a decrease in biofilm formation of the Myr^R compared to the wild-type strain (Figure 4.5 and 4.8). The SaeRS is responsible for regulation over 22 virulence factors including, but not exclusively, hemolysins, leukocidins, antigens, surface proteins, binding protein, and proteases (Liu *et al*., 2015). Sun *et al*. (2010) found more than 150 genes to contain at least one *SaeR* binding site. According to Mrak and co-workers (2012) phosphorylation is essential for the DNA binding activity of *saeR,* and the regulation of target genes are divided into two classes. Class I (high-affinity) promoters regulate factors such as hemolysins and can bind *SaeR* regardless of phosphorylation status. In contrast, Class II (low-affinity) promoters regulate factors such as coagulase and fibronectin binding protein and require phosphorylated *SaeR* (Cho *et al*., 2012). Based on the observed reduction in hemolysis activity as well as the down-regulation of *saeS*, fibronectin binding proteins and capsular genes the *saeR* deletion mutation found present in the mutant strains

can not maintain regulation of Class I nor Class II genes leading to the decrease alongside *saeR* gene.

Genes that form part of the lysine biosynthesis pathway (8 out of the 23 genes) showed differential expression and enrichment (Figure S4.5). The genes encoding aspartate kinase I and II (EC: 2.7.2.4 - SAOUHSC_01319; SAOUHSC_01394), aspartate semialdehyde dehydrogenase (EC: 1.2.1.11- *asd*), 4-hydroxy-tetrahydrodipicolinate synthase (EC: 4.3.3.7- *dapA*), and 4-hydroxy-tetrahydrodipicolinate reductase (EC:1.17.1.8 - *dapB*). Lysine biosynthesis occurs in two pathways, the diaminopimelate and α-aminoadipate pathway. In this study, *asd*, *dapA* and *dapB* genes are shown to be down-regulated resulting in the down regulation of biosynthesis of monobactam, methionine, threonine, isoleucine, and lysine. Diaminopimelate (DAP) is a metabolite for lysine biosynthesis that is essential for peptidoglycan biosynthesis. The DAP biosynthetic pathway produces not only the precursors for methionine, homoserine, threonine, and lysine, but also for the other amino acids such as arginine and proline, all of which are essential for cell cycle and metabolism and which explains the significant enriched pathways (Pavelka *et al*., 1996, Sianglum *et al*., 2012). Interestingly, the DAP biosynthesis operon was highlighted to be important in the mechanism of action for rhodomyrtone, a structurally similar compound that also exhibits cell lysis on *S. aureus* (Sianglum *et al*., 2011). However, as there was no cross-resistance observed with rhodomyrtone, further investigations are necessary concerning the mechanism of action for both rhodomyrtone and myrtucommulones (Table 4.4).

The Myr^R showed cross-resistance to vancomycin, daptomycin, and penicillin G with a four-fold MIC shift, and there was an increase in cross-resistance observed for the Myr^R for, ampicillin, oxicillin and meropenem (Table 4.4). Resistance to vancomycin is a complex process with several key players, the main being the VAN operon which we do not see significantly up-regulated within the transcriptomic profile. Full vancomycin resistance in *S. aureus* (MIC ≥64 μg/ml) is conferred by the vanA operon and is well understood; however, intermediate resistance (MIC ≥4-32 μg/ml) is ill-defined (McGuinness *et al*., 2017). Genes encoding for the global regulator *sarA* and two-component regulatory systems, such as *vraRS*, graRS and walKR, have been linked to the intermediate vancomycin resistant *S. aureus* (VISA) phenotype as well as a gene deletion in *saeR* (D46 to L55) (Meehl *et al*., 2007, McEvoy *et al*., 2013, Trotonda *et al*., 2009; Miller *et al*., 2021). Interestingly, Cui and co-workers (2003) reported that cell wall thickening is a common feature in strains with resistance to vancomycin and other cell wall targeting compounds (Figure 4.7). Resistance to daptomycin has also been ascribed to the increase of cell wall thickness, however, Yang and colleagues (2010) showed that thickening of the cell wall is not necessarily linked to all daptomycin resistant phenotypes.

Interestingly, the saeRS showed to be down-regulated within daptomycin resistant mutants (Bayer *et al*., 2013) which explains the intermediate cross-resistance with daptomycin observed in the Myr^R.

Upregulated *vraRS*, *sarA*, *msa* (putative membrane protein and modulator of sarA), and *prsA* has been reported to be involved with ß-lactam resistance in methicillin resistant *S. aureus* strains (MRSA) and other cell wall targeting antibiotics (Fujimoto and Bayles, 1998; Duran *et al*., 1996; Liu *et al.*, 2016; Sambanthamoorthy *et al*., 2006, Gardete *et al*., 2006; Jousselin *et al*., 2012). The loss of *sarA* and the acquisition of mutations leading to the VISA phenotype leads to altered regulation of capsular and fibronectin-binding proteins (Dunman *et al*., 2001, McAleese *et al*., 2006). We also observe this within the transcriptome data set, as *sarA* is down-regulated in the Myr^R strains, and several capsular and fibronectin-binding genes are upregulated (Figure 4.4). Furthermore, *fmtA* gene was significantly upregulated (fold-change of 4.39) and has a low binding affinity for ß-lactams (Table S4.4). Studies show that FmtA plays a role as a penicillin-binding protein and contributes to ß-lactam resistance and is directly linked to the two-component system, *vraRS* (Fan *et al*., 2007; Komatsuzawa *et al*., 1999).

Focusing on the up-regulated DEGs, we see alpha-acetolactate decarboxylase is the most up-regulated. that has been shown to be repressed by the global regulator MgrA (Table S4.4). MgrA is a major controlling factor for autolysis, negatively regulating autolytic genes and positively regulating anti-autolytic factors (Luong *et al.*, 2006). The *sarV* gene was up-regulated by five-fold which is part of the pathway by which MgrA and SarA control autolysis (Trotonda *et al*., 2009). Previous study conducted by Manna *et al*. (2004) showed that the *sarV* regulates extracellular and intracellular murein hydrolase and protease activity. Additionally, (Manna *et al.*, 2006) showed that both SarA and MgrA specifically down-regulate SarV, which can serve as a marker of murein hydrolase activity. However, because SarV does not regulate MgrA or SarA, but is influenced by MgrA and SarA, SarV constitutes an important “hub” for the control of lysis. The *msa* gene was also up-regulated and encodes for a putative membrane protein accessory element involved in the expression of SarA. However, the function and precise role of *msa* is still unclear and open for investigation (Sambanthamoorthy *et al*., 2006).

Besides *sarV* and *sarA*, PBP1 gene has also been reported to contribute to autolysis (Pereira *et al*., 2009). A study conducted by Duran and co-workers (1996) reported that with the deactivation of the SarA in a MRSA *S. aureus* strain, the high and constitutive production of PBP2 was not affected, but the membrane protein pattern was altered and unexpectedly the PBP1 and PBP3 content seemed to be reduced. Further observations by Pereira and co-workers (2007) suggest that PBP1 does not contribute to the cross-linking of peptidoglycan

and that it is expected to contribute to cell division. Within this study, the transcriptome revealed the down-regulation of the PBP1 gene and TEM imaging reported irregular large septa occurring in resistant strains (Table S4.5; Figure 4.6). Besides PBP1, Kuroda *et al*., 2007 reported the SaeRS two-component system regulates that Clp protease ATPase subunits which in turn influences the cell division, the transcriptome is in agreement with this due to the down regulation of *clpP*. Further, Massidda and co-workers (1998) reported the peptidoglycan synthesis operon consists of (mraZ-mraW-ftsL-pbpa) which all form part of cell division regulation. Within this study, we see a dysregulation of septa formation and the transcriptome revealed a down regulation of all mraZ-mraW-ftsL-pbpa genes indicating a possible contribution. In conjunction with the observed dysregulation of cell division, the cell wall thickness is increased in the Myr^R compared to the wild-type (Figure 4.6). TEM imaging revealed an increase in the "fuzzy" appearance possibly linked to an increase in wall teichoic acids and resistance to cell wall targeting antibiotic (Yang *et al*., 2010). Wall teichoic acids makes up to 60% of the cell mass and acts as a barrier for entrance and influences cell division, biofilm formation, lysis, and bacterial resistance (Rahman *et al.*, 2016; Romaniuk and Cegelski, 2018).

Besides peptidoglycan, the *S. aureus* cell wall contains polymers called teichoic acids. These chains are either covalently connected to the peptidoglycan (wall teichoic acids) or to membrane glycolipids (lipoteichoic acids) (Ward, 1981). Teichoic acids are charged and involved in the control of autolysin, cross-linking and peptidoglycan (PGN) turnover (Wecke *et al* 1997; Atilano *et al*., 2010; Qamar *et al*., 2012). Furthermore, WTA are required for β-lactam resistance and vancomycin (Brown *et al*., 2012; Brown *et al*., 2013). An increase in positively charged d-alanine residues allows for vancomycin resistance by preventing the ionic interaction of the cationic vancomycin with the negatively charged teichoic acids thus a change in the d-alanine amount will result in modulation of their charge (Rahman *et al.*, 2016). This charge-dependent decrease in binding of vancomycin plays a role in the *S. aureus* VISA phenotype. Common characteristics for VISA phenotype and also shared with the Myr^R strains include (i) a thickened cell wall based on the electron imaging; (ii) a decreased virulence due the down-regulation of the SaeRS, observed genotypes and decrease in hemolysis and biofilm productions which are all virulence factors (Figure 4.5; Figure 4.6; Figure 4.7; Figure 4.8 Table 4.4); and (iii) a reduced lysis in presence of an lytic agent (Figure 4.9).

Transcriptomic data further revealed an up-regulation of the *vraSR*, *tagG*, *fmtA* and *mnaA* genes (Table S4.4). *tagG* forms part of the late-stage biosynthesis of wall teichoic acids as it facilitates translocation across the membrane while *mnaA* is an epimerase that interconverts UDP-GlcNAc and UDP-ManNAc, thus providing substrates for TarO and TarA for the initial

biosynthesis process (Schirner *et al*., 2011; Mann *et al*., 2016; McAleese, *et al*. 2006). FmtA and the two-component system, VraSR, forms part of the cell wall stimulon which has been reported to be involved with methicillin and vancomycin resistance, cell wall biosynthesis and wall teichoic acids charge and VISA-phenotype (Bernal *et al*., 2010; McAleese *et al*., 2006; Rahman *et al*., 2016; Howden *et al*., 2008). Boles and colleagues (2010) showed the cell wall of the *S. aureus ΔfmtA* mutant to lack wall teichoic acids (WTAs) highlighting the importance of the stimulon. Further, Rahman and mentioned co-workers 2016 proved that FmtA acts by removing the d-alanine from the lipoteichoic acids to make it available to wall teichoic acid thus influencing the d-alanine amount and cell wall charge. Within the transcriptome, genotype, and phenotype we observe several hints to the change in cell wall composition and possibly charge which can then lead to intermediate resistant and cross-resistance to vancomycin and ß-lactams. The observed resistance has several contributors is not only caused by one facet but is rather a combination of contributors.

Interestingly, SarA has been reported to act synergistically with SaeRS two-component system to repress the production of extracellular proteases as well as the production of alpha toxins, proteases, cysteine proteases, secretory antigens, and glycerophosphodiester (Mrak *et al*., 2012; Baroja *et al*., 2016). According to Joo and Otto (2015) SaeRS regulate antimicrobial peptides resistance by secreted proteases. It was also found that the proteolytic defense mechanisms via SaeRS can be stimulated by antimicrobial peptides regardless of their charge and is likely a result of a general disturbance of membrane function which resembles a general stress response (Joo and Otto, 2015).

In this study, the Myr^R showed an increase in extracellular protease compared to the wild-type (Figure 4.9, (b)) and transcriptome indicates the down regulation of *sarA*, however, the described proteolytic inactivation seems unlikely to interfere with the structures of **1** and **2**, thus leading to the increase of extracellular protease to rather be a general stress response to the cell membrane targeting antibiotic than the resistance mechanism. The Myr^R 1R Δ*saeR*:Val49_Met53, *sarA*: g-92C>A did produce the least amount of calculated protease compared to the other strains and the fitness assessment indicated a “closer-to-wild-type” metabolic rate (Figure 4.1 and Figure 4.2). A current observation indicates that the additional mutation within the intergenic region of the *sarA* gene, lead to a slight increase production of SarA compared to the other Myr^R strains which lead to less protease production and a more normal metabolic profile compared to the wild-type (Figure 4.9, (b)).

The integrity of the cell wall is generally maintained by two competing processes: cell wall synthesis and cell wall lytic activity. The enzymes involved in the synthesis of peptidoglycan, the major component in the cell wall of *S. aureus*, are penicillin-binding proteins. Autolysis, on

the other hand, is mediated by autolytic enzymes (also called “autolysins” or “murein hydrolases”), which cleave the covalent bonds that confer stability to the cross-linked peptidoglycan chain in order to form the rigid cell wall. An imbalance between synthesis and lysis leads to cell death, as e.g., in penicillin-induced lysis, wherein cell wall synthesis is disrupted while lytic activity remains unchanged. Within this study, Myr^R showed a reduction in lysis compared to the wild-type. Triton X-100 is a commonly used detergent in laboratories that disrupts the hydrogen bonding in lipid bilayer as it becomes inserted in the lipid bilayer and ultimately demolishing the integrity of the of the lipid membrane. The observed difference in lysis along with the transcriptome profile between the wild-type and Myr^R strains indicates a clear change in cell wall structure (Figure 4.7; Figure 4.9, (a)).

We conclude our investigation on the mechanism of resistance of *S. aureus* Newman to **1** and **2**. Whole genome sequencing identified the deletion in the *saeR* response regulation of the virulence controlling SaeRS, two-component system. RNA-sequencing provided a platform to investigate the resistance mechanism and by utilizing the most up-and down-regulated genes a complex network of two-component systems and cross-resistance was revealed. Several role-players were identified to contribute to the observed intermediate and cross-resistance to vancomycin and ß-lactams which allowed the Myr^R strains to share characteristics with a VISA phenotype. The mutant characterization revealed a down-regulation of several virulence factors and the transcriptome profile, genotype and phenotype were in line and provided evidence of lysis resistant in the Myr^R strains which lead to the electron imaging confirming an increase in cell wall thickness and structure. The transcriptome provided hints towards the biosynthesis and export of wall teichoic acids which increase the thickness and alters the change of the cell wall. In conclusion, the transcriptome analysis revealed and lead the investigation to narrow and to better understand the mechanism of resistance of *S. aureus* strains to the acylphloroglucinol derivatives, **1** and **2**. Based on all experimental results and literature the resistance mechanism of the *S. aureus* Myr^R is related to the increase of cell wall thickness and change of membrane charge, most likely by the increased production and exportation of wall teichoic acids, which in turn leads to a VISA-like phenotype.

4.5. References

Akin, M., Aktumsek, A. and Nostro, A., 2010. Antibacterial activity and composition of the essential oils of Eucalyptus camaldulensis Dehn. and Myrtus communis L. growing in Northern Cyprus. African journal of biotechnology, 9(4).

Alipour, G., Dashti, S. and Hosseinzadeh, H., 2014. Review of pharmacological effects of Myrtus communis L. and its active constituents. Phytotherapy research, 28(8), pp.1125-1136.

Appendino, G., Bianchi, F., Minassi, A., Sterner, O., Ballero, M. and Gibbons, S., 2002. Oligomeric acylphloroglucinols from myrtle (Myrtus communis). Journal of natural products, 65(3), pp.334-338.

Atilano, M.L., Pereira, P.M., Yates, J., Reed, P., Veiga, H., Pinho, M.G. and Filipe, S.R., 2010. Teichoic acids are temporal and spatial regulators of peptidoglycan cross-linking in Staphylococcus aureus. Proceedings of the National Academy of Sciences, 107(44), pp.18991-18996.

Baroja, M.L., Herfst, C.A., Kasper, K.J., Xu, S.X., Gillett, D.A., Li, J., Reid, G., and McCormick, J.K., 2016. The SaeRS two-component system is a direct and dominant transcriptional activator of toxic shock syndrome toxin 1 in Staphylococcus aureus. Journal of Bacteriology, 198(19), pp.2732-2742.

Bayer, A.S., Schneider, T., and Sahl, H.G., 2013. Mechanisms of daptomycin resistance in Staphylococcus aureus: role of the cell membrane and cell wall. Annals of the New York Academy of Sciences, 1277(1), pp.139-158.

Bernal, P., Lemaire, S., Pinho, M.G., Mobashery, S., Hinds, J., and Taylor, P.W., 2010. Insertion of epicatechin gallate into the cytoplasmic membrane of methicillin-resistant Staphylococcus aureus disrupts penicillin-binding protein (PBP) 2a-mediated β-lactam resistance by delocalizing PBP2. Journal of Biological Chemistry, 285(31), pp.24055-24065.

Boles, B.R., Thoendel, M., Roth, A.J. and Horswill, A.R., 2010. Identification of genes involved in polysaccharide-independent Staphylococcus aureus biofilm formation. PloS one, 5(4), p.e10146.

Brown, S., Santa Maria Jr, J.P. and Walker, S., 2013. Wall teichoic acids of Gram-positive bacteria. Annual review of microbiology, 67, pp.313-336.

Brown, S., Xia, G., Luhachack, L.G., Campbell, J., Meredith, T.C., Chen, C., Winstel, V., Gekeler, C., Irazoqui, J.E., Peschel, A. and Walker, S., 2012. Methicillin resistance in Staphylococcus aureus requires glycosylated wall teichoic acids. Proceedings of the National Academy of Sciences, 109(46), pp.18909-18914.

Cho, H., Jeong, D.W., Li, C. and Bae, T., 2012. Organizational requirements of the SaeR binding sites for a functional P1 promoter of the sae operon in Staphylococcus aureus. Journal of bacteriology, 194(11), pp.2865-2876.

Cox, S.D., Mann, C.M., Markham, J.L., Gustafson, J.E., Warmington, J.R. and Wyllie, S.G., 2001. Determining the antimicrobial actions of tea tree oil. Molecules, 6(2), pp.87-91.

Cui, L., Ma, X., Sato, K., Okuma, K., Tenover, F.C., Mamizuka, E.M., Gemmell, C.G., Kim, M.N., Ploy, M.C., El Solh, N. and Ferraz, V., 2003. Cell wall thickening is a common feature of

vancomycin resistance in Staphylococcus aureus. Journal of clinical microbiology, 41(1), pp.5-14.

Dunman, P.Á., Murphy, E., Haney, S., Palacios, D., Tucker-Kellogg, G., Wu, S., Brown, E.L., Zagursky, R.J., Shlaes, D. and Projan, S.J., 2001. Transcription profiling-based identification of Staphylococcus aureus genes regulated by the agr and/or sarA loci.

Duran, S.P., Kayser, F.H. and Berger-Bächi, B., 1996. Impact of sar and agr on methicillin resistance in Staphylococcus aureus. FEMS microbiology letters, 141(2-3), pp.255-260.

Fan, X., Liu, Y., Smith, D., Konermann, L., Siu, K.M. and Golemi-Kotra, D., 2007. Diversity of penicillin-binding proteins. Journal of Biological Chemistry, 282(48), pp.35143-35152.

Fujimoto, D.F., and Bayles, K.W., 1998. Opposing roles of the Staphylococcus aureus virulence regulators, Agr and Sar, in Triton X-100-and penicillin-induced autolysis. Journal of bacteriology, 180(14), pp.3724-3726.

Gardete, S., Wu, S.W., Gill, S. and Tomasz, A., 2006. Role of VraSR in antibiotic resistance and antibiotic-induced stress response in Staphylococcus aureus. Antimicrobial agents and chemotherapy, 50(10), pp.3424-3434.

Hans, M., Charpentier, M., Huch, V., Jauch, J., Bruhn, T., Bringmann, G. and Quandt, D., 2015. Stereoisomeric composition of natural myrtucommulone A. Journal of natural products, 78(10), pp.2381-2389.

Howden, B.P., Smith, D.J., Mansell, A., Johnson, P.D., Ward, P.B., Stinear, T.P. and Davies, J.K., 2008. Different bacterial gene expression patterns and attenuated host immune responses are associated with the evolution of low-level vancomycin resistance during persistent methicillin-resistant Staphylococcus aureusbacteraemia. BMC microbiology, 8(1), pp.1-14.

Jensen, L.J., Kuhn, M., Stark, M., Chaffron, S., Creevey, C., Muller, J., Doerks, T., Julien, P., Roth, A., Simonovic, M. and Bork, P., 2009. STRING 8—a global view on proteins and their functional interactions in 630 organisms. Nucleic acids research, 37(suppl_1), pp.D412-D416.

Joo, H.S. and Otto, M., 2015. Mechanisms of resistance to antimicrobial peptides in staphylococci. Biochimica et Biophysica Acta (BBA)-Biomembranes, 1848(11), pp.3055-3061.

Jousselin, A., Renzoni, A., Andrey, D.O., Monod, A., Lew, D.P., and Kelley, W.L., 2012. The posttranslocational chaperone lipoprotein PrsA is involved in both glycopeptide and oxacillin resistance in Staphylococcus aureus. Antimicrobial agents and chemotherapy, 56(7), pp.3629-3640.

Kashman, Y., Rotstein, A. and Lifshitz, A., 1974. The structure determination of two new acylphloroglucinols from Myrtus communis L. Tetrahedron, 30(8), pp.991-997.

Killeen, D.P., Larsen, L., Dayan, F.E., Gordon, K.C., Perry, N.B., and van Klink, J.W., 2016. Nortriketones: Antimicrobial trimethylated acylphloroglucinols from manuka (Leptospermum scoparium). Journal of natural products, 79(3), pp.564-569.

Komatsuzawa, H., Ohta, K., Labischinski, H., Sugai, M. and Suginaka, H., 1999. Characterization of fmtA, a gene that modulates the expression of methicillin resistance in Staphylococcus aureus. Antimicrobial Agents and Chemotherapy, 43(9), pp.2121-2125.

Kuroda, H., Kuroda, M., Cui, L. and Hiramatsu, K., 2007. Subinhibitory concentrations of β-lactam induce haemolytic activity in Staphylococcus aureus through the SaeRS two-component system. FEMS microbiology letters, 268(1), pp.98-105.

Liu, Q., Cho, H., Yeo, W.S. and Bae, T., 2015. The extracytoplasmic linker peptide of the sensor protein SaeS tunes the kinase activity required for staphylococcal virulence in response to host signals. PLoS pathogens, 11(4), p.e1004799.

Liu, X., Zhang, S. and Sun, B., 2016. SpoVG regulates cell wall metabolism and oxacillin resistance in methicillin-resistant Staphylococcus aureus strain N315. Antimicrobial Agents and Chemotherapy, 60(6), pp.3455-3461.

Lounasmaa, M., Pri, S. and Widen, C. 1977. Phloroglucinol derivatives of Callistemon lanceolatus leaves. Phytochemistry (UK), 16(11), pp.1851-1852.

Luong, T.T., Dunman, P.M., Murphy, E., Projan, S.J. and Lee, C.Y., 2006. Transcription profiling of the mgrA regulon in Staphylococcus aureus. Journal of bacteriology, 188(5), pp.1899-1910.

Mann, P.A., Müller, A., Wolff, K.A., Fischmann, T., Wang, H., Reed, P., Hou, Y., Li, W., Müller, C.E., Xiao, J. and Murgolo, N., 2016. Chemical genetic analysis and functional characterization of staphylococcal wall teichoic acid 2-epimerases reveals unconventional antibiotic drug targets. PLoS pathogens, 12(5), p.e1005585.

Manna, A.C. and Cheung, A.L., 2006. Transcriptional regulation of the agr locus and the identification of DNA binding residues of the global regulatory protein SarR in Staphylococcus aureus. Molecular microbiology, 60(5), pp.1289-1301.

Manna, A.C., Ingavale, S.S., Maloney, M., Van Wamel, W., and Cheung, A.L., 2004. Identification of sarV (SA2062), a new transcriptional regulator, is repressed by SarA and MgrA (SA0641) and involved in the regulation of autolysis in Staphylococcus aureus. Journal of bacteriology, 186(16), pp.5267-5280.

Marchini, G. and Maccioni, S., 1998. Liguria in parole povere. La bassa Val di Magra. Sagep Libri Ed., Genova, p.159.

Massidda, O., Anderluzzi, D., Friedli, L. and Feger, G., 1998. Unconventional organization of the division and cell wall gene cluster of Streptococcus pneumoniae. Microbiology, 144(11), pp.3069-3078.

McAleese, F., Wu, S.W., Sieradzki, K., Dunman, P., Murphy, E., Projan, S. and Tomasz, A., 2006. Overexpression of genes of the cell wall stimulon in clinical isolates of Staphylococcus aureus exhibiting vancomycin-intermediate-S. aureus-type resistance to vancomycin. Journal of bacteriology, 188(3), pp.1120-1133.

McEvoy, C.R., Tsuji, B., Gao, W., Seemann, T., Porter, J.L., Doig, K., Ngo, D., Howden, B.P. and Stinear, T.P., 2013. Decreased vancomycin susceptibility in Staphylococcus aureus caused by IS 256 tempering of WalKR expression. Antimicrobial Agents and Chemotherapy, 57(7), pp.3240-3249.

McGuinness, W.A., Malachowa, N. and DeLeo, F.R., 2017. Focus: infectious diseases: vancomycin resistance in Staphylococcus aureus. The Yale journal of biology and medicine, 90(2), p.269.

Meehl, M., Herbert, S., Götz, F. and Cheung, A., 2007. Interaction of the GraRS two-component system with the VraFG ABC transporter to support vancomycin-intermediate resistance in Staphylococcus aureus. Antimicrobial agents and chemotherapy, 51(8), pp.2679-2689.

Messaoud, C. and Boussaid, M., 2011. Myrtus communis berry color morphs: A comparative analysis of essential oils, fatty acids, phenolic compounds, and antioxidant activities. Chemistry & biodiversity, 8(2), pp.300-310.

Messaoud, C., Laabidi, A. and Boussaid, M., 2012. Myrtus communis L. infusions: the effect of infusion time on phytochemical composition, antioxidant, and antimicrobial activities. Journal of food science, 77(9), pp.C941-C947.

Messaoud, C., Zaouali, Y., Salah, A.B., Khoudja, M.L. and Boussaid, M., 2005. Myrtus communis in Tunisia: variability of the essential oil composition in natural populations. Flavour and Fragrance Journal, 20(6), pp.577-582.

Miller, C.R., Monk, J.M., Szubin, R. and Berti, A.D., 2021. Rapid resistance development to three antistaphylococcal therapies in antibiotic-tolerant staphylococcus aureus bacteremia. Plos one, 16(10), p.e0258592.

Mohamed, G.A. and Ibrahim, S.R., 2007. Eucalyptone G, a new phloroglucinol derivative and other constituents from Eucalyptus globulus Labill. Arkivoc, 15, pp.281-291.

Mrak, L.N., Zielinska, A.K., Beenken, K.E., Mrak, I.N., Atwood, D.N., Griffin, L.M., Lee, C.Y. and Smeltzer, M.S., 2012. saeRS and sarA act synergistically to repress protease production and promote biofilm formation in Staphylococcus aureus. PloS one, 7(6), p.e38453.

Müller, H., Paul, M., Hartmann, D., Huch, V., Blaesius, D., Koeberle, A., Werz, O. and Jauch, J., 2010. Total synthesis of myrtucommulone A. Angewandte Chemie International Edition, 49(11), pp.2045-2049.

Nicoletti, R., Salvatore, M.M., Ferranti, P. and Andolfi, A., 2018. Structures and bioactive properties of myrtucommulones and related acylphloroglucinols from Myrtaceae. Molecules, 23(12), p.3370.

Owlia, P., Saderi, H., Rasooli, I. and Sefidkon, F., 2010. Antimicrobial c haracteristics of some herbal oils on. Pseudomonas aeruginosa, pp.107-14.

Pavelka Jr, M.S., Weisbrod, T.R. and Jacobs Jr, W.R., 1997. Cloning of the dapB gene, encoding dihydrodipicolinate reductase, from Mycobacterium tuberculosis. Journal of bacteriology, 179(8), pp.2777-2782.

Pereira SF, Henriques AO, Pinho MG, de Lencastre H, Tomasz A. 2007. Role of PBP1 in cell division of Staphylococcus aureus. *Journal of Bacteriology*, 189(9), pp.3525-3531.

Pereira, S.F., Henriques, A.O., Pinho, M.G., De Lencastre, H. and Tomasz, A., 2009. Evidence for a dual role of PBP1 in the cell division and cell separation of Staphylococcus aureus. Molecular microbiology, 72(4), pp.895-904.

Qamar, A. and Golemi-Kotra, D., 2012. Dual roles of FmtA in Staphylococcus aureus cell wall biosynthesis and autolysis. Antimicrobial agents and chemotherapy, 56(7), pp.3797-3805.

Rahman, M.M., Hunter, H.N., Prova, S., Verma, V., Qamar, A. and Golemi-Kotra, D., 2016. The Staphylococcus aureus methicillin resistance factor FmtA is a d-amino esterase that acts on teichoic acids. MBio, 7(1), pp.e02070-15.

Romaniuk, J.A. and Cegelski, L., 2018. Peptidoglycan and teichoic acid levels and alterations in Staphylococcus aureus by cell-wall and whole-cell nuclear magnetic resonance. Biochemistry, 57(26), pp.3966-3975.

Rotstein, A., Lifshitz, A. and Kashman, Y., 1974. Isolation and antibacterial activity of acylphloroglucinols from Myrtus communis. Antimicrobial agents and chemotherapy, 6(5), pp.539-542.

Sambanthamoorthy, K., Smeltzer, M.S. and Elasri, M.O., 2006. Identification and characterization of msa (SA1233), a gene involved in expression of SarA and several virulence factors in Staphylococcus aureus. Microbiology, 152(9), pp.2559-2572.

Schirner, K., Stone, L.K. and Walker, S., 2011. ABC transporters required for export of wall teichoic acids do not discriminate between different main chain polymers. ACS chemical biology, 6(5), pp.407-412.

Schneider, C.A., Rasband, W.S. and Eliceiri, K.W., 2012. NIH Image to ImageJ: 25 years of image analysis. Nature methods, 9(7), pp.671-675.

Sianglum, W., Srimanote, P., Taylor, P.W., Rosado, H. and Voravuthikunchai, S.P., 2012. Transcriptome analysis of responses to rhodomyrtone in methicillin-resistant Staphylococcus aureus.

Sianglum, W., Srimanote, P., Wonglumsom, W., Kittiniyom, K. and Voravuthikunchai, S.P., 2011. Proteome analyses of cellular proteins in methicillin-resistant Staphylococcus aureus treated with rhodomyrtone, a novel antibiotic candidate. Plos one, 6(2), p.e16628.

Sumbul, S., Ahmad, M.A., Asif, M. and Akhtar, M., 2011. Myrtus communis Linn.-A review. https://nopr.niscpr.res.in/handle/123456789/13336. (Access: 4 February 2023).

Sun, F., Li, C., Jeong, D., Sohn, C., He, C. and Bae, T., 2010. In the Staphylococcus aureus two-component system sae, the response regulator SaeR binds to a direct repeat sequence and DNA binding requires phosphorylation by the sensor kinase SaeS. Journal of bacteriology, 192(8), pp.2111-2127.

Tan, H., Liu, H., Zhao, L., Yuan, Y., Li, B., Jiang, Y., Gong, L. and Qiu, S., 2017. Structure-activity relationships and optimization of acyclic acylphloroglucinol analogues as novel antimicrobial agents. European Journal of Medicinal Chemistry, 125, pp.492-499.

Trotonda, M.P., Xiong, Y.Q., Memmi, G., Bayer, A.S. and Cheung, A.L., 2009. The Role of mgrA and sarA in Autolysis and Resistance to Cell Wall-Active Antibiotics in Methicillin-Resistant Staphylococcus aureus. The Journal of infectious diseases, 199(2), p.209.

Visutthi, M., Srimanote, P. and Voravuthikunchai, S.P., 2011. Responses in the expression of extracellular proteins in methicillin-resistant Staphylococcus aureus treated with rhodomyrtone. The Journal of Microbiology, 49, pp.956-964.

Wannes, W.A., Mhamdi, B., Sriti, J., Jemia, M.B., Ouchikh, O., Hamdaoui, G., Kchouk, M.E. and Marzouk, B., 2010. Antioxidant activities of the essential oils and methanol extracts from myrtle (Myrtus communis var. italica L.) leaf, stem and flower. Food and chemical toxicology, 48(5), pp.1362-1370.

Ward, J.B., 1981. Teichoic and teichuronic acids: biosynthesis, assembly, and location. Microbiological reviews, 45(2), pp.211-243.

Wecke, J., Madela, K. and Fischer, W., 1997. The absence of D-alanine from lipoteichoic acid and wall teichoic acid alters surface charge, enhances autolysis and increases susceptibility to methicillin in Bacillus subtilis. Microbiology, 143(9), pp.2953-2960.

Wunnoo, S., Bilhman, S., Amnuaikit, T., Ontong, J.C., Singh, S., Auepemkiate, S. and Voravuthikunchai, S.P., 2021. Rhodomyrtone as a New Natural Antibiotic Isolated from Rhodomyrtus tomentosa Leaf Extract: A Clinical Application in the Management of Acne Vulgaris. Antibiotics, 10(2), p.108.

Yang, S.J., Nast, C.C., Mishra, N.N., Yeaman, M.R., Fey, P.D. and Bayer, A.S., 2010. Cell wall thickening is not a universal accompaniment of the daptomycin nonsusceptibility phenotype in Staphylococcus aureus: evidence for multiple resistance mechanisms. Antimicrobial agents and chemotherapy, 54(8), pp.3079-3085.

4.5. Supplementary Information

Table S4.1: Minimum Inhibition Concentration of Gram-negative *E. coli* strains with the addition of Polymyxin B nonapeptide (PMBN) and phenylalanine-arginine beta-naphthylamide (PAβN).

Strain	MIC (µg/mL)		MIC (µg/mL) + 20µg/mL PMBN		MIC (µg/mL) + 3µg/mL PAβA	
	1	2	1	2	1	2
***E. coli* DSM-1116**	>64	>64	>64	>64	>64	>64
***E. coli* BW25113**	>64	>64	>64	>64	>64	>64
***E. coli* ΔtolC**	>64	>64	>64	>64	4	2
***E. coli* ΔarcB**	>64	>64	>64	>64	>64	>64

Table S4.2: Minimum Bactericidal Concentration of Gram-positive *S. aureus* and *E. faecium* strains.

Strain	MIC (µg/mL)		MBC (µg/mL)	
	1	2	1	2
***S. aureus* Newman**	2	0.5	4	1
***S. aureus* N315**	2	0.125	4	0.25
***E. faecium* DSM 20477**	8	1	8	1

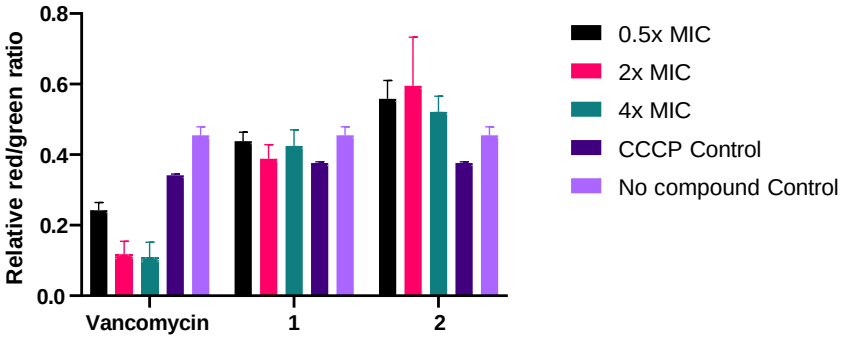

Figure S4.1: The relative red/green ratio of *S. aureus* N315 using DIOC2(3) stained cells after 1 hour of exposure to vancomycin, myrtucommulone A (**1**) and myrtucommulone F (**2**) with ½ x MIC, MIC and 2x MIC. Green fluorescence corresponds to the depolarized cells; red fluorescence corresponds to the polarized cells. The changes in the fluorescence were measured at an excitation wavelength of 488 nm and 525 nm (emission) for green and 675 nm (emission) for red.

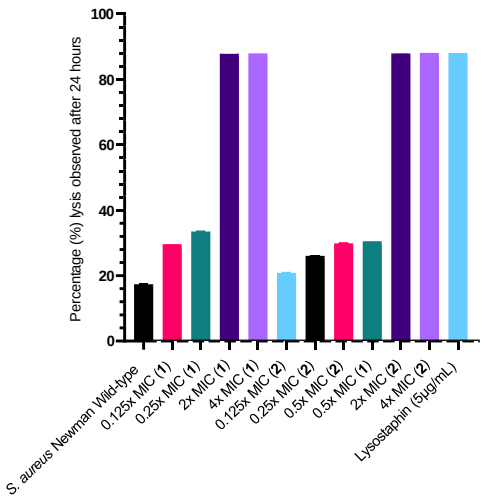

Figure S4.2: Percentage (%) cell lysis observed with the addition of myrtucommulone A (**1)** and myrtucommulone F (**2**) with *S. aureus* Newman in TritonX-100 after 24 hours.

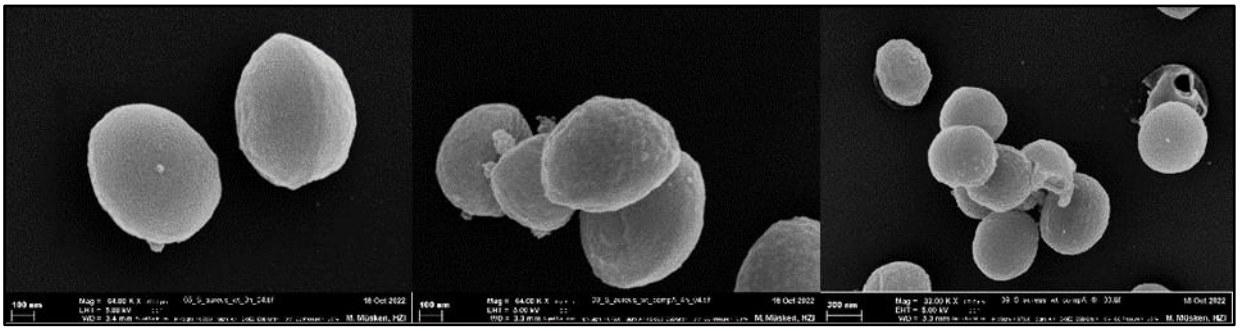

Figure S4.3: Scanning electron microscope (SEM) imaging of wild-type *S. aureus* Newman a) in the presence of sub-MIC concentrations of myrtucommulone A (**1)** and myrtucommulone F (**2**) (1 µg/ml for 1; and 0.5 µg/ml for 2) for 4 hours (b and c). Mag: 64.00 K X, EHT: 5.00 kV, WD: 3.3 mm. Scale bar: 100nm.

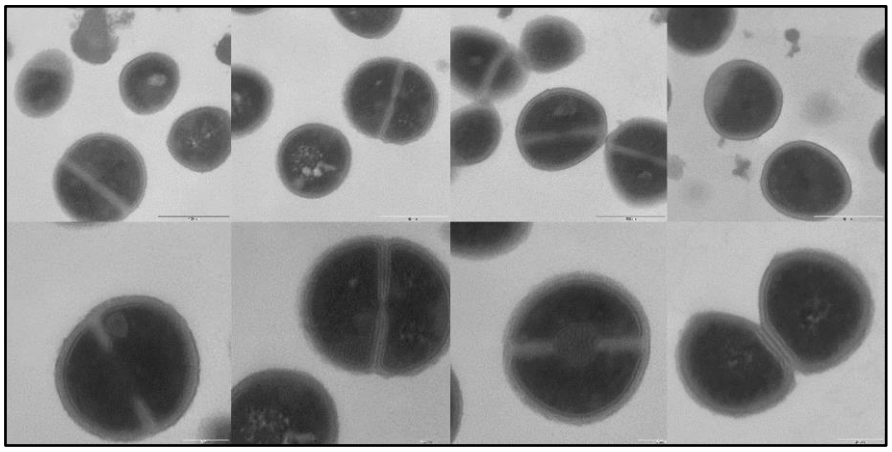

Figure S4.4: Transmission electron microscope (TEM) imaging of wild-type *S. aureus* Newman a) in the presence of sub-MIC concentrations of myrtucommulone A (**1)** and myrtucommulone F (**2**) (1 µg/ml for 1; and 0.5 µg/ml for 2) for 4 hours (b and c). Scale bar: 500nm (a-d) and 200nm (e-h).

Table S4.3: Gene mutations found in all selected Myr^R.

Strain	Intergenic region upstream from ***sarA***	***saeR***	**Hypothetical protein** (Gene interval: 2085795 -> 2085649)
Myr^R 1		Val49_Met53del	
Myr^R 2	g.-92C>A	Val49_Met53del	
Myr^R 3		Val49_Met53del	Val48Tyr
Myr^R 4		Val49_Met53del	
Myr^R 5	g.-92C>A	Val49_Met53del	
Myr^R 6	g.-92C>A	Val49_Met53del	
Myr^R 7		Val49_Met53del	
Myr^R 8		Val49_Met53del	
Myr^R 9		Val49_Met53del	Val48Tyr
Myr^R 10		Val49_Met53del	Val48Tyr
Myr^R 11		Val49_Met53del	
Myr^R 12		Val49_Met53del	

Table S4.4: Differentially expressed up-regulated genes with fold-change of ≤2.5; ≥2.5 and p-value ≤0.001 in all selected Myr^R.

Gene locus tag	Gene	Calculated p-value	Expression level average	Average confidence	Average p-value
SAOUHSC_02467	alpha-acetolactate decarboxylase	500	8.24	1000	0
SAOUHSC_02558	urease subunit gamma	500	8.20	1000	0
SAOUHSC_02559	urease subunit beta	500	8.18	1000	0
SAOUHSC_02468	acetolactate synthase	500	8.01	1000	0
SAOUHSC_02561	urease subunit alpha	500	7.06	1000	0
SAOUHSC_02312	potassium-transporting ATPase subunit A	500	7.00	1000	0
SAOUHSC_02562	urease accessory protein UreE	500	6.88	1000	0
SAOUHSC_02563	urease accessory protein UreF	500	6.77	1000	0
SAOUHSC_02311	potassium-transporting ATPase subunit B	500	6.67	1000	0
SAOUHSC_02310	potassium-transporting ATPase subunit C	500	6.57	1000	0
SAOUHSC_01761a	membrane protein	500	6.37	1000	0
SAOUHSC_02565	urease accessory protein UreD	500	6.26	1000	0
SAOUHSC_02564	urease accessory protein UreG	500	6.16	1000	0
SAOUHSC_02389	cation efflux family protein	500	5.89	1000	0
SAOUHSC_02557	urea transporter	500	5.39	1000	0

SAOUHSC_02532	sarV	213.60	5.01	628.92	2.5E-214
SAOUHSC_01166	aspartate carbamoyltransferase catalytic subunit	185.40	4.77	795.92	4E-186
SAOUHSC_01165	uracil permease	236.13	4.69	808.57	7.4E-237
SAOUHSC_00129	UDP-N-acetylglucosamine 2-epimerase	500	4.63	1000	0
SAOUHSC_00998	methicillin resistance protein FmtA	257.99	4.39	638.14	1E-258
SAOUHSC_02306	4'-phosphopantetheinyl transferase	500	4.27	1000	0
SAOUHSC_00126	capsular polysaccharide biosynthesis protein Cap8M	187.22	4.26	619.74	6.1E-188
SAOUHSC_02947	sulfite reductase (NADPH) flavoprotein subunit alpha	500	4.20	1000	0
SAOUHSC_01972	protein export protein PrsA	203.86	4.17	800.53	1.4E-204
SAOUHSC_00128	cap5O protein/UDP-N-acetyl-D-mannosaminuronic acid dehydrogenase	293.65	4.15	822.91	2.3E-294
SAOUHSC_00127	cap5N protein/UDP-glucose 4-epimerase	212.18	4.12	802.60	6.7E-213
SAOUHSC_01172	orotate phosphoribosyltransferase	286.42	4.12	646.07	3.8E-287
SAOUHSC_00412	NADH dehydrogenase subunit 5	136.48	4.10	579.02	3.3E-137
SAOUHSC_02614	aldose 1-epimerase	500	4.08	1000	0
SAOUHSC_02840	L-serine dehydratase iron-sulfur-dependent subunit beta	147.89	4.02	786.58	1.3E-148
SAOUHSC_01171	orotidine 5'-phosphate decarboxylase	221.79	3.97	805	1.6E-222
SAOUHSC_02550	formate dehydrogenase accessory protein	225.54	3.93	805.93	2.9E-226
SAOUHSC_01168	dihydroorotase	117.94	3.91	779.10	1.1E-118
SAOUHSC_00721	7-cyano-7-deazaguanine synthase QueC	273.31	3.83	817.86	4.8E-274
SAOUHSC_02316	DEAD-box ATP dependent DNA helicase	299.60	3.76	824.40	2.5E-300
SAOUHSC_00173	azoreductase	305.59	3.76	825.89	2.6E-306
SAOUHSC_00119	capsular polysaccharide biosynthesis protein Cap8F	72.35	3.72	415.50	4.48E-73
SAOUHSC_00109	replication initiation protein	48.30	3.70	55.58	4.97E-49
SAOUHSC_00118	capsular polysaccharide biosynthesis protein Cap5E	74.01	3.68	591.53	9.72E-75
SAOUHSC_02641	permease domain-containing protein	104.37	3.70	153.62	4.3E-105
SAOUHSC_00125	cap5L protein/glycosyltransferase	136.34	3.68	605.69	4.5E-137
SAOUHSC_02945	precorrin-2 dehydrogenase	121.44	3.56	415.94	3.6E-122

SAOUHSC_02305	alanine racemase	205.55	3.55	625.46	2.8E-206
SAOUHSC_00124	capsular polysaccharide biosynthesis protein Cap5K	62.87	3.55	347.73	1.33E-63
SAOUHSC_01169	carbamoyl phosphate synthase small subunit	98.76	3.52	395.46	1.7E-99
SAOUHSC_02074	phi PVL orf 39-like protein	7.66	3.49	12.75	2.2E-08
SAOUHSC_00120	UDP-N-acetylglucosamine 2-epimerase	53.23	3.48	582.04	5.89E-54
SAOUHSC_01504	ferredoxin	73.45	3.46	104.21	3.57E-74
SAOUHSC_00123	capsular polysaccharide biosynthesis protein Cap5J	55.69	3.43	544.12	2.06E-56
SAOUHSC_02544	molybdopterin precursor biosynthesis MoaB	150.42	3.40	580.89	3.8E-151
SAOUHSC_02541	molybdopterin-guanine dinucleotide biosynthesis protein MobB	141.27	3.39	784.92	5.3E-142
SAOUHSC_00122	capsular polysaccharide biosynthesis protein Cap5I	44.66	3.39	350.24	2.17E-45
SAOUHSC_01170	carbamoyl phosphate synthase large subunit	104.26	3.38	594.26	5.5E-105
SAOUHSC_00121	capsular polysaccharide biosynthesis protein O-acetyl transferase Cap5H	44.90	3.34	350.55	1.25E-45
SAOUHSC_02829	NAD(P)H-flavin oxidoreductase	135.56	3.28	571.60	2.8E-136
SAOUHSC_00117	capsular polysaccharide biosynthesis protein Cap5D	90.87	3.23	593.33	1.35E-91
SAOUHSC_02542	molybdopterin biosynthesis protein MoeA	138.63	3.16	571.86	2.3E-139
SAOUHSC_01684	heat shock protein GrpE	113.87	3.14	567.65	1.3E-114
SAOUHSC_00116	capsular polysaccharide biosynthesis protein Cap8C	61.13	3.10	147.67	7.44E-62
SAOUHSC_01267	2-oxoglutarate ferredoxin oxidoreductase subunitbeta	221.95	2.81	611.56	1.1E-222
SAOUHSC_01380	oligopeptide transporter permease	106.72	2.80	136.63	1.9E-107
SAOUHSC_02962	tributyrin esterase	132.79	2.71	200.56	1.6E-133
SAOUHSC_01379	oligopeptide transporter permease	115.25	2.67	152.16	5.6E-116
SAOUHSC_00641	teichoic acids export protein ATP-binding subunit	144.99	2.60	582.58	1E-145

Table S4.5: Differentially expressed down-regulated genes with a fold-change of ≤2.5; ≥2.5 and p-value ≤0.001 in all selected Myr^R.

Gene locus tag	Gene	Calculated p-value	Expression level average	Average confidence	Average p-value
SAOUHSC_02161	MHC class II analog protein	500	-12.28	1000	0
SAOUHSC_02708	gamma-hemolysin h-gamma-II subunit	500	-10.66	1000	0
SAOUHSC_02709	leukocidin s subunit	500	-10.14	1000	0
SAOUHSC_02710	leukocidin f subunit	500	-8.79	1000	0
SAOUHSC_02284	ketol-acid reductoisomerase	273.97	-8.13	818.09	1.1E-274
SAOUHSC_00816	extracellular matrix and plasma binding protein	500	-7.80	1000	0
SAOUHSC_00715	response regulator	500	-7.51	1000	0
SAOUHSC_02285	2-isopropylmalate synthase	500	-7.46	1000	0
SAOUHSC_02283	acetolactate synthase 1 regulatory subunit	75.29	-7.30	129.65	5.13E-76
SAOUHSC_02281	dihydroxy-acid dehydratase	246.55	-7.25	811.25	2.8E-247
SAOUHSC_01322	homoserine kinase	500	-7.20	1000	0
SAOUHSC_00199	acyl CoA: acetate/3-ketoacid CoA transferase	500	-7.10	1000	0
SAOUHSC_00714	sensor histidine kinase SaeS	500	-7.06	1000	0
SAOUHSC_00608	alcohol dehydrogenase	500	-7.01	1000	0
SAOUHSC_01114	fibrinogen-binding protein	500	-6.97	1000	0
SAOUHSC_02282	acetolactate synthase large subunit	500	-6.91	1000	0
SAOUHSC_02706	immunoglobulin G-binding protein Sbi	500	-6.85	1000	0
SAOUHSC_01110	fibrinogen-binding protein-like protein	500	-6.82	1000	0
SAOUHSC_01321	threonine synthase	500	-6.73	1000	0
SAOUHSC_01320	homoserine dehydrogenase	500	-6.68	1000	0
SAOUHSC_00157	N-acetylmuramic acid-6-phosphate etherase	236.22	-6.65	623.27	6E-237
SAOUHSC_01121	alpha-hemolysin	500	-6.64	1000	0
SAOUHSC_02287	isopropylmalate isomerase large subunit	500	-6.52	1000	0
SAOUHSC_01395	aspartate semialdehyde dehydrogenase	227.78	-6.48	806.56	1.7E-228
SAOUHSC_01451	threonine dehydratase	500	-6.47	1000	0
SAOUHSC_02286	3-isopropylmalate dehydrogenase	500	-6.37	1000	0
SAOUHSC_02288	3-isopropylmalate dehydratase small subunit	500	-6.27	1000	0
SAOUHSC_00158	PTS system transporter	228.51	-6.19	806.67	3.1E-229
SAOUHSC_01452	alanine dehydrogenase	307.90	-6.04	826.56	0
SAOUHSC_02803	fibronectin-binding protein	500	-5.90	1000	0

SAOUHSC_01396	4-hydroxy-tetrahydrodipicolinate synthase	500	-5.98	1000	0
SAOUHSC_02444	BCCT family osmoprotectant transporter	500	-5.97	1000	0
SAOUHSC_02289	threonine dehydratase	500	-5.93	1000	0
SAOUHSC_00926	oligopeptide ABC transporter ATP-binding protein	500	-5.79	1000	0
SAOUHSC_00625	monovalent cation/H+ antiporter subunit A	500	-5.36	1000	0
SAOUHSC_01319	aspartate kinase	153.16	-5.33	787.89	7E-154
SAOUHSC_02773	transporter	500	-5.20	1000	0
SAOUHSC_02441	alkaline shock protein 23	500	-5.12	1000	0
SAOUHSC_00927	oligopeptide ABC transporter substrate-binding protein	500	-5.02	1000	0
SAOUHSC_02712	6-carboxyhexanoate--CoA ligase	231.81	-5.02	430.06	1.5E-232
SAOUHSC_00624	integrase/recombinase	190.15	-4.93	231.08	7E-191
SAOUHSC_01397	4-hydroxy-tetrahydrodipicolinate reductase	500	-4.87	1000	0
SAOUHSC_00626	monovalent cation/H+ antiporter subunit B	259.71	-4.85	446.04	2E-260
SAOUHSC_01125	superantigen-like protein	200.66	-4.80	410.57	2.2E-201
SAOUHSC_02174	phage phi LC3 family holin	6.60	-4.69	8.30	2.54E-07
SAOUHSC_01013	phosphoribosylformylglycin amidine synthase II	500	-4.66	1000	0
SAOUHSC_01846	acetate--CoA ligase	205.58	-4.64	620.46	2.6E-206
SAOUHSC_01394	aspartate kinase	130.38	-4.63	138.95	4.2E-131
SAOUHSC_01012	phosphoribosylformylglycin amidine synthase I	257.73	-4.63	632.25	1.9E-258
SAOUHSC_00340	trans-sulfuration enzyme family protein	136.43	-4.62	164.11	3.7E-137
SAOUHSC_01398	2,3,4,5-tetrahydropyridine-2,6-dicarboxylate N-acetyltransferase	267.15	-4.60	639.84	7.1E-268
SAOUHSC_01011	phosphoribosylformylglycin amidine synthase PurS	96.13	-4.56	124.70	7.37E-97
SAOUHSC_00195	acetyl-CoA acetyltransferase	74.46	-4.427	564.70	3.5E-75
SAOUHSC_00627	monovalent cation/H+ antiporter subunit C	122.77	-4.37	158.21	1.7E-123
SAOUHSC_01369	indole-3-glycerol-phosphate synthase	23.07	-4.35	31.95	8.46E-24
SAOUHSC_02244	succinyl-diaminopimelate desuccinylase	500	-4.35	1000	0
SAOUHSC_00206	L-lactate dehydrogenase	253.14	-4.33	628.55	7.3E-254
SAOUHSC_02802	fibronectin binding protein B	233.97	-4.27	626.49	1.1E-234
SAOUHSC_01366	anthranilate synthase component I	53.15	-4.18	71.18	7.12E-54
SAOUHSC_01014	amidophosphoribosyltransferase	500	-4.11	1000	0

SAOUHSC_02573	Na+/H+ antiporter NhaC	257.13	-4.04	813.8	7.5E-258
SAOUHSC_01948	ABC transporter	237.65	-4.04	440.99	2.2E-238
SAOUHSC_02729	amino acid ABC transporter-like protein	133.13	-3.95	782.89	7.5E-134
SAOUHSC_01370	N-(5'-phosphoribosyl) anthranilate isomerase	12.22	-3.94	16.655	6.02E-13
SAOUHSC_01368	anthranilate phosphoribosyltransferase	38.60	-3.90	54.34	2.51E-39
SAOUHSC_01124	superantigen-like protein	199.45	-3.89	411.27	3.5E-200
SAOUHSC_01015	phosphoribosylaminoimidazole synthetase	227.84	-3.86	438.47	1.4E-228
SAOUHSC_00628	monovalent cation/H+ antiporter subunit D	291.51	-3.856	645	3.1E-292
SAOUHSC_00339	bifunctional homocysteine S-methyltransferase/5,10-methylenetetrahydrofolate reductase	162.91	-3.80	213.18	1.2E-163
SAOUHSC_00282	branched-chain amino acid transport system II carrier protein	155.69	-3.78	600.09	2E-156
SAOUHSC_02879	squalene desaturase	142.59	-3.70	413.61	2.6E-143
SAOUHSC_01143	16S rRNA (cytosine (1402)-N (4))-methyltransferase	276.58	-3.69	818.68	2.6E-277
SAOUHSC_02922	L-lactate dehydrogenase	133.84	-3.65	140.61	1.4E-134
SAOUHSC_01016	phosphoribosylglycinamide formyltransferase	221.58	-3.65	267.31	2.6E-222
SAOUHSC_02924	4-aminobutyrate aminotransferase	85.31	-3.62	186.06	4.93E-86
SAOUHSC_01112	formyl peptide receptor-like 1 inhibitory protein	159.91	-3.56	588.63	1.2E-160
SAOUHSC_01146	phospho-N-acetylmuramoyl-pentapeptide- transferase	187.62	-3.54	400.28	2.4E-188
SAOUHSC_01666	glycyl-tRNA synthetase	129.11	-3.54	590.49	7.7E-130
SAOUHSC_02043	phage head protein	164.37	-3.53	233.35	4.3E-165
SAOUHSC_01833	D-3-phosphoglycerate dehydrogenase	183.69	-3.52	608.42	2E-184
SAOUHSC_01145	penicillin-binding protein 1	215.08	-3.54	803.32	8.3E-216
SAOUHSC_01367	anthranilate synthase component II	26.00	-3.467	33.59	9.98E-27
SAOUHSC_02740	drug transporter	102.09	-3.46	200.9	8.1E-103
SAOUHSC_02862	ATP-dependent Clp protease ATP-binding subunit ClpC	500	-3.43	1000	0
SAOUHSC_01144	cell division protein	121.10	-3.42	176.55	7.9E-122
SAOUHSC_01435	thymidylate synthase	179.57	-3.41	617.77	2.7E-180
SAOUHSC_00620	accessory regulator A	86.18	-3.41	184.57	6.54E-87
SAOUHSC_01064	pyruvate carboxylase	209.64	-3.39	625.80	2.3E-210
SAOUHSC_01009	5-(carboxyamino)imidazole ribonucleotide synthase	138.78	-3.32	184.49	1.7E-139
SAOUHSC_01127	superantigen-like protein	115.95	-3.31	151.33	1.1E-116

SAOUHSC_00632	monovalent cation/H+ antiporter subunit G	137.83	-3.28	589.00	1.5E-138
SAOUHSC_00818	thermonuclease	30.14	-3.27	35.25	7.24E-31
SAOUHSC_00389	superantigen-like protein	79.04	-3.27	121.85	9.13E-80
SAOUHSC_02173	amidase	20.32	-3.19	30.38	4.84E-21
SAOUHSC_01017	bifunctional phosphoribosylaminoimidazolecarboxamide formyltransferase/IMP cyclohydrolase	188.77	-3.14	417.66	1.7E-189
SAOUHSC_02042	phi Mu50B-like protein	100.94	-3.12	133.39	1.1E-101
SAOUHSC_01010	phosphoribosylaminoimidazole-succinocarboxamide synthase	64.77	-3.067	98.69	1.69E-65
SAOUHSC_02610	formimidoylglutamase	156.10	-3.05	581.74	8E-157
SAOUHSC_01008	5-(carboxyamino)imidazole ribonucleotide mutase	60.90	-3.04	76.31	1.26E-61
SAOUHSC_00733	histidinol-phosphate aminotransferase	97.26	-3.02	138.83	5.54E-98
SAOUHSC_01142	cell division protein MraZ	176.84	-3	207.45	1.4E-177
SAOUHSC_00629	monovalent cation/H+ antiporter subunit E	62.32	-3	116.39	4.81E-63
SAOUHSC_02494	30S ribosomal protein S5	58.85	-2.94	156.42	1.4E-59
SAOUHSC_00424	ABC transporter permease	34	-2.93	46.66	1E-34
SAOUHSC_02038	HK97 family phage protein	128.41	-2.92	145.12	3.9E-129
SAOUHSC_01420	DNA-binding response regulator	134.92	-2.92	380.97	1.2E-135
SAOUHSC_02877	squalene synthase	141.86	-2.88	210.70	1.4E-142
SAOUHSC_02041	phi Mu50B-like protein	112.49	-2.87	121	3.2E-113
SAOUHSC_02502	50S ribosomal protein L14	59.19	-2.82	137	6.46E-60
SAOUHSC_01903	camphor resistance protein CrcB	29.24	-2.73	36.19	5.73E-30
SAOUHSC_02932	choline dehydrogenase	62.18	-2.70	89.39	6.6E-63
SAOUHSC_01400	alanine racemase	105.65	-2.68	123.67	2.2E-106
SAOUHSC_01018	phosphoribosylamine--glycine ligase	123	-2.64	390.56	1E-123
SAOUHSC_00192	staphylocoagulase	92.35	-2.63	137.38	4.48E-93

Table S4.6: Significantly enriched GO Process, GO Function, and GO Component of DEGs in all selected Myr^R.

GO term ID	Description	Observed gene count	Background gene count	Strength	False discovery rate
GO:0009088	Threonine biosynthetic process	6	6	1.22	0.00
GO:0043419	Urea catabolic process	3	3	1.22	0.04
GO:0006189	De novo imp biosynthetic process	11	12	1.18	6.89E-07
GO:0044205	De novo ump biosynthetic process	6	7	1.15	0.00
GO:0009099	Valine biosynthetic process	5	6	1.14	0.00
GO:0009097	Isoleucine biosynthetic process	8	10	1.12	7.89E-05

GO:0019877	Diaminopimelate biosynthetic process	7	9	1.11	0.00
GO:0009082	Branched-chain amino acid biosynthetic process	12	16	1.09	6.89E-07
GO:0006566	Threonine metabolic process	8	11	1.08	0.00
GO:0009098	Leucine biosynthetic process	4	6	1.04	0.02
GO:0019627	Urea metabolic process	4	6	1.04	0.02
GO:0009089	Lysine biosynthetic process via diaminopimelate	7	12	0.98	0.00
GO:0009156	Ribonucleoside monophosphate biosynthetic process	17	30	0.97	1.74E-08
GO:0009130	Pyrimidine nucleoside monophosphate biosynthetic process	7	13	0.95	0.00
GO:0009067	Aspartate family amino acid biosynthetic process	12	23	0.93	8.96E-06
GO:0046112	Nucleobase biosynthetic process	6	12	0.91	0.01
GO:0000162	Tryptophan biosynthetic process	4	8	0.91	0.05
GO:0009124	Nucleoside monophosphate biosynthetic process	18	37	0.90	2.86E-08
GO:0009066	Aspartate family amino acid metabolic process	14	30	0.88	2.80E-06
GO:0042401	Cellular biogenic amine biosynthetic process	5	11	0.87	0.02
GO:0006221	Pyrimidine nucleotide biosynthetic process	7	17	0.83	0.01
GO:1901607	Alpha-amino acid biosynthetic process	33	92	0.77	7.73E-12
GO:0009260	Ribonucleotide biosynthetic process	18	57	0.72	4.44E-06
GO:1901605	Alpha-amino acid metabolic process	38	128	0.69	7.73E-12
GO:0009152	Purine ribonucleotide biosynthetic process	12	45	0.64	0.00
GO:0006520	Cellular amino acid metabolic process	41	163	0.62	1.81E-11
GO:0046394	Carboxylic acid biosynthetic process	37	148	0.61	2.96E-10
GO:0009165	Nucleotide biosynthetic process	19	76	0.61	3.15E-05
GO:0009259	Ribonucleotide metabolic process	21	91	0.58	2.60E-05
GO:0016053	Organic acid biosynthetic process	38	170	0.57	2.19E-09
GO:0043648	Dicarboxylic acid metabolic process	8	37	0.55	0.05
GO:0019752	Carboxylic acid metabolic process	52	269	0.50	4.20E-11
GO:0090407	Organophosphate biosynthetic process	23	119	0.50	9.37E-05
GO:0009150	Purine ribonucleotide metabolic process	15	78	0.50	0.00
GO:0009405	Pathogenesis	17	93	0.48	0.00
GO:0044283	Small molecule biosynthetic process	44	243	0.47	1.82E-08
GO:0006082	Organic acid metabolic process	53	304	0.46	6.43E-10
GO:0009117	Nucleotide metabolic process	22	125	0.46	0.00
GO:1901137	Carbohydrate derivative biosynthetic process	29	168	0.45	3.70E-05
GO:1901566	Organonitrogen compound biosynthetic process	66	392	0.44	7.73E-12
GO:0044419	Interspecies interaction between organisms	18	109	0.43	0.00
GO:0044281	Small molecule metabolic process	76	493	0.40	7.22E-12
GO:0019637	Organophosphate metabolic process	26	180	0.38	0.00

GO:0055086	Nucleobase-containing small molecule metabolic process	24	165	0.38	0.00
GO:0034654	Nucleobase-containing compound biosynthetic process	21	145	0.38	0.01
GO:0018130	Heterocycle biosynthetic process	33	229	0.37	0.00
GO:1901576	Organic substance biosynthetic process	85	619	0.35	7.73E-12
GO:1901362	Organic cyclic compound biosynthetic process	33	241	0.35	0.00
GO:0044249	Cellular biosynthetic process	80	606	0.34	2.26E-10
GO:1901135	Carbohydrate derivative metabolic process	33	249	0.34	0.00
GO:0019438	Aromatic compound biosynthetic process	28	210	0.34	0.00
GO:1901564	Organonitrogen compound metabolic process	80	632	0.32	1.49E-09
GO:0006796	Phosphate-containing compound metabolic process	33	286	0.28	0.01
GO:0006793	Phosphorus metabolic process	34	301	0.27	0.01
GO:0006807	Nitrogen compound metabolic process	90	890	0.22	1.88E-06
GO:0044271	Cellular nitrogen compound biosynthetic process	33	327	0.22	0.05
GO:0071704	Organic substance metabolic process	108	1132	0.20	3.85E-07
GO:0044238	Primary metabolic process	91	943	0.20	1.17E-05
GO:0044237	Cellular metabolic process	106	1117	0.19	8.33E-07
GO:0009987	Cellular process	145	1569	0.18	7.73E-12
GO:0008152	Metabolic process	116	1328	0.16	6.79E-06
GO:0016151	Nickel cation binding	6	8	1.09	0.01
GO:0016854	Racemase and epimerase activity	6	13	0.88	0.04
GO:0019842	Vitamin binding	12	46	0.63	0.01
GO:0016829	Lyase activity	16	91	0.46	0.03
GO:0036094	Small molecule binding	54	510	0.24	0.01
GO:0043167	Ion binding	71	752	0.19	0.01
GO:0003824	Catalytic activity	113	1324	0.15	0.00
GO:0005488	Binding	93	1121	0.13	0.02
GO:0005829	Cytosol	40	353	0.27	0.00
GO:0005737	Cytoplasm	89	1000	0.17	0.00
GO:0110165	Cellular anatomical entity	155	1931	0.12	2.37E-08

Table S4.7: Significantly enriched KEGG pathways of DEGs in all selected Myr^{R}.

KEGG ID	Description	Observed gene count	Background gene count	Strength	False discovery rate
sao00261	Monobactam biosynthesis	5	5	1.22	0.00
sao00290	Valine, leucine, and isoleucine biosynthesis	11	13	1.14	5.77E-07
sao00660	C5-Branched dibasic acid metabolism	7	10	1.06	0.00
sao01210	2-Oxocarboxylic acid metabolism	12	23	0.93	5.00E-06
sao00541	O-Antigen nucleotide sugar biosynthesis	8	18	0.86	0.00
sao01502	Vancomycin resistance	4	11	0.78	0.05

sao00250	Alanine, aspartate, and glutamate metabolism	8	23	0.76	0.00
sao00300	Lysine biosynthesis	8	23	0.76	0.00
sao00270	Cysteine and methionine metabolism	10	29	0.75	0.00
sao00260	Glycine, serine, and threonine metabolism	11	33	0.74	0.00
sao00400	Phenylalanine, tyrosine, and tryptophan biosynthesis	6	20	0.69	0.02
sao00650	Butanoate metabolism	6	20	0.69	0.02
sao01230	Biosynthesis of amino acids	34	122	0.66	1.39E-10
sao00220	Arginine biosynthesis	6	22	0.65	0.03
sao00770	Pantothenate and CoA biosynthesis	6	23	0.63	0.03
sao00230	Purine metabolism	15	67	0.57	0.00
sao01120	Microbial metabolism in diverse environments	28	182	0.40	0.00
sao01110	Biosynthesis of secondary metabolites	52	351	0.39	9.57E-08
sao01100	Metabolic pathways	99	859	0.28	1.39E-10

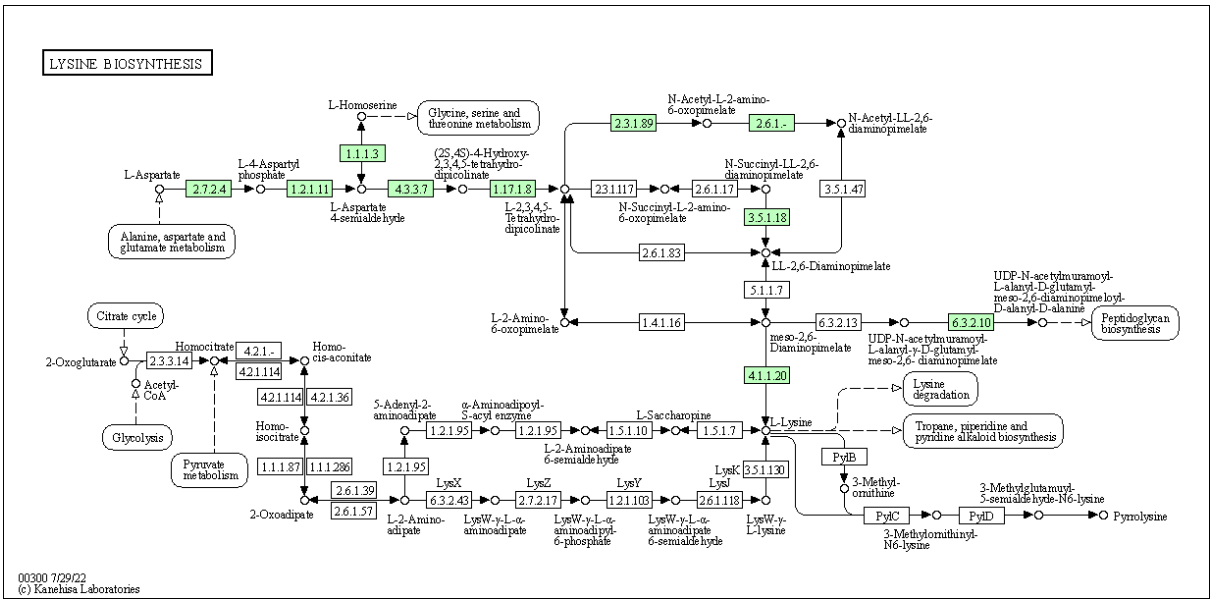

Figure S4.5: Lysine biosynthesis KEGG pathway. Genes highlighted in green were found to be significantly down-regulated in all assessed Myr^R.

Chapter 5: General Discussion and Conclusion

The discovery of the world's first three antimicrobials namely, salvarsan, prontosil, and penicillin was followed by the so-called golden era of discovery of novel antibiotics classes then a dramatic decline in discovery (Gottfried, 2005; Chopra *et al*., 2002). The golden era was possible due to natural products from soil-dwelling actinomycetales and their potential to produce antibiotic natural products (Chopra *et al*., 2002; Waksman *et al.*, 2010). Therefore, the discovery and development of antimicrobial compounds that can combat resistant pathogens is of great importance and natural product–based drugs are a reliable source of novel antimicrobial compounds. This is exemplified within the thesis, where three individual natural products with unique structures inhibits antimicrobial growth of ESKAPE pathogens at low concentrations. The overall aim of the thesis was the investigation of selected Gram-positive and Gram-negative ESKAPE pathogen's resistance mechanisms by means of next-generation sequencing, transcriptomic analysis, and microbial techniques such as antibacterial activity, resistant development, cross-resistance determination, and fitness cost assessment by isothermal micro-isothermal calorimetry. Understanding the mechanisms of resistance is necessary to propose appropriate treatments for resistant strains in a clinical setting and to aid in future antimicrobial drug-development strategies.

5.1. Understanding resistance mechanisms for compound development and contributing technologies

The rise of antimicrobial resistance and the lack of effective antibiotic drugs highlights the need to optimize current drug therapies to limit the spread of multidrug resistance (Frieri *et al*., 2017). It is imperative to understand bacterial resistance mechanisms to optimize current and future therapies to overcome these mechanisms (Alvaro, 2022). Understanding the mechanisms of resistance has helped in the development of several inhibitors that includes gene silencers, using the CRISPR-Cas system, ribosomal inhibitors that alters protein production, and efflux pump inhibitors that can be used in combination therapy. For combinational therapy to be successful, two or more antibiotics are employed simultaneously, with the goal of obtaining synergistic activity. The term 'antibiotic synergy' is defined as the enhanced effect of one antibiotic with another when combined at the optimal ratio (Coates, 2020). For example, the β-lactams in combination with a fluoroquinolone is successful as the impairment of peptidoglycan synthesis by β-lactams leads to the increase of fluoroquinolones intracellular concentration (Giamarellou, 1986). Besides difference drug-classes, combinational therapy is also seen to be successful with the combination of β-lactams and β-lactam inhibitors and biocides that aids in the treatment of multidrug resistant ESKAPE pathogens (Murugaiyan *et al*., 2022).

Genome-focused technologies, such as next-generation sequencing, enable the investigation of resistance on a genome level and in combination with RNA-sequencing the transcriptome profiles can be compared to provide an overview of changes of biological processes with high accuracy (Chernov et al., 2019). Hong and co-workers (2016) utilized RNA-sequencing to better understand the mechanism of resistance of *P. aeruginosa* to tachyplesin I. Here, the comparison of a resistant mutant to the wild-type transcriptome revealed changes of outer membrane porins which provided information that is useful for structural relation studies of optimized compounds. RNA-sequencing is also frequently applied in clinical research studies. In a study by Khaledi and colleagues (2016) RNA-sequencing alongside machine learning technologies provided a direct correlation to resistance, global resistance patterns of phenotype-associated gene expression and sequence variations.

In general, RNA sequencing in combination with whole-genome sequencing and other techniques made sense of observations with regards to resistance mechanisms of ESKAPE pathogens and provided a pathway for further investigation. RNA-sequencing was used as the transcriptome assessment within all three chapters. Here, the data provided insight into larger metabolic and cellular processes that are connected with resistance mechanisms. Chapter 1 focuses on armeniaspirols with a membrane depolarization effect and protonophore mechanism of action in Gram-positive and Gram-negative bacteria. Gram-negative, *E. coli*, has an efflux-mediated mechanism of resistance mainly caused by the RND-efflux ArcAB-tolC. Arm^R of *E. coli* with a deletion of TolC resulted in different point mutations and large gene deletions resulting in the up-regulation of another MdtNOP RND-efflux pump that compensated for the loss of TolC and allowed full resistance to armeniaspirols. The transcriptome profile confirmed the upregulation of the RND-efflux pump and distinguesed between two different mutations leading to the up-regulation of the RND-efflux pump. Further information was obstained by the transcriptome linking armeniaspirol resistance to protonophore resistance and a putative role of the propionate pathway in response to protonophore resistance.

Chapter 2 investigates, topoisomerase inhibitors, cystobactamids with antimicrobial activity against CRAB strains and revealed target mutations to be the main resistance mechanism. In addition, the transcriptome provided information regarding the additional resistance mechanisms linking mutations within *ybdL* and the promotor site of *gigB* that resulted in the up-regulation of MepA and AdeIJK efflux pumps. Chapter 3 explores the mechanism of resistance of a Gram-positive ESKAPE pathogen, *S. aureus*, in response to myrtucommulone derivatives. A deletion within the response regulator of SaeRS that is normally associated with virulence was present in all Myr^R. All Myr^R showed significant in reduction of several virulence factors as well as alteration of the Gram-positive cell wall, which allowed for the observed resistance to myrtucommulones and cross-resistance to vancomycin and daptomycin. The

transcriptome analysis revealed a plausible link of the lysine biosynthesis pathway, and wall teichoic acid to a VISA-like phenotype resistant strain.

5.2. Armeniaspirols

Chapter 2 discusses the mechanisms of armeniaspirol-resistance in bacterial strains in detail, particularly related to the MdtNOP efflux pump and the deletion of specific genes. Here, armeniaspirol-resistance was obtained through spontaneous resistant development, resulting in a low frequency of resistance, which is consistent with mechanisms that alter the proton motive force of bacterial membranes (Feng *et al*., 2015). The genome analysis of Arm^R showed that 50% of strains had gene mutations related to the MdtNOP efflux pump, while the other 50% seemed unrelated to it. Whole genome sequencing and transcriptomic analysis showed that Arm^R16 and Arm^R17 contained a large gene deletion that could be similar to the observed resistance mechanism of the pyrrolomycin-resistant *E. coli* ΔtolC mutant (Valderrama *et al*., 2019). Arisetti *et al.* (2021) provided evidence indicating a similar mechanism of antimicrobial activity for several chloropyrrole-containing compounds. As a similar resistance mechanism is observed for both pyrrolomycin and armeniaspirols, it might indicate a common resistance mechanism for chloropyrrole-containing compounds (Valderrama *et al*., 2019; Arisetti *et al*., 2021). Chelocardins, with a similar dual mechanism as armeniaspirols, reported the increased expression of the *acrAB-tolC* efflux pump to be the main mechanism of resistance, as observed for armeniaspirols (Stepanek *et al*., 2016; Hennessen *et al.,* 2020; Arisetti *et al*., 2021; Darnownski *et al*., 2023). This not only provides information for future optimization of compounds with chloropyrrole-containing moyieties but also for compounds with a similar dual mechanism.

However, as this has only been observed in two compounds, and it is dangerous to assume that it is the same for all chloropyrrole -containing compound, especially as only 50% of Arm^R possessed gene mutations linked to MdtNOP. It is important to investigate the other 50% and understand all of the mutations contributing to resistance. Future investigation within this compound class involves the precise understanding of mechanism of action, which will aid in the understanding of the observed antimicrobial activity in Gram-positive bacteria. Investigation of the resistance mechanism of protonophores might additionally shed light to the current observed resistance and persister formation. As mutations in *cvpA* are linked to protonophore resistance and *plsB* that is linked to persister cell formation and stringent response resistances (Poole *et al*., 2012; Warr *et al*., 2021). In addition, understanding the RND efflux pump, MdtNOP, and the exact link to ArcAB-TolC would aid in to elucidate the large gene deletion and mutations that effected the MdtNOP expression which led to the observed resistant phenotypes.

In conclusion, chapter 2 provides important information on the mechanisms of resistance to armeniaspirols, which could be useful in developing new strategies to optimize armeniaspirols to overcome or the bacterial resistance. The finding that the efflux is the main contributer to resistance can shead light on alternative strategies, especially combination therapies with efflux inhibitors as well as membrane permeabiling agents (Murugaiyan *et al*., 2022). However, the protonophore mechanism of armeniaspriols are also operative in mammalian cells thus posing an additional optimization challenge to assure selection of antibacterial activity over mammalian cell toxicity (Arisetti *et al*., 2021). Whole-genome sequencing and transcriptome analysis provided a clear picture which linked the observed resistance of the selected phenotype, to the genotype and the transcriptome profile. In addition to the highlighting that the resistance mechanism is efflux-mediated, the transcriptome analysis provided information regarding other resistance contributors such as acid resistance, propionate metabolism and phage shock operon that might aid in the understanding of protonophore resistance, persister formation and other chloropyrrole-containing compounds.

5.3. Cystobactamids

As mentioned in chapter 1, various antibacterial targets are described and well-understood. Bacterial topoisomerases, such as DNA gyrase and topoisomerase IV, have been distinguished as well-established and clinically important targets for antibacterial agents. There is an urgent need to develop new topoisomerase-targeting antibacterial agents that lack cross-resistance to the existing topoisomerase inhibitors (Kokot *et al*., 2022). Chapter 3 described that cystobactamid derivatives have pronounced activity for topoisomerase II and IV inhibition and evident susceptibility profiles for *A. baumannii* clinical strains, including CRAB strains. High-level resistance is linked to target mutations as reported for topoisomerase inhibitors (Nayar *et al*., 2015). The main resistance mechanisms of *A. baumannii* to topoisomerase inhibiting cystobactamids are target mutations and efflux-mediated. Target mutations dispersed and not in a distinct binding pocket and therefore it is more difficult to pinpoint the precise binding site of cystobactamids to the DNA-gyrase complex. However, as mentioned in chapter 3, Michaelczyk and co-workers (2023) recently published the binding mechanism of a structurally similar compound, albicidin, that interacts with the DNA-gyrase in a novel manner, which can potentially be applied to cystobactamids. Understanding the binding mechanism would explain the observed mutations within the C-terminal and the low-level cross-resistance that is observed for NBTIs and fluoroquinolones for Cys^R with GyrA and GyrB mutations. Besides target mutations, a point mutation within an aminotransferase gene (*ybdL)* is responsible for high-level resistance. In addition, a point mutation within the promotor region of a major antibiotic resistant regulator, GigB (-35bp T>G) also lead to high level-resistance. Both of these mutations lead to a secondary mecnhism of resistance that is efflux-mediated.

The transcriptome of Cys^R containing the *ybdL* point mutation revealed the up-regulation of the neighboring gene, *mepA*. MepA is a MATE efflux pump and has been described in resistance to fluoroquinolones, in line with the observed cross-resistance. Further, the point mutation within the *gigB* promotor site revealed the upregulation of a RND- efflux pump, AdeIJK.

Further studies are necessary to understand the reason why the point mutation within *ybdL* caused the upregulation of the MATE efflux pump, MepA. Understanding the MATE efflux pump in more detail will aid in understanding the role of MATE efflux pumps in Gram-negative bacteria as MATE efflux pumps have been been move readily described in Gram-positives strains. Moreover, the GigAB major antibiotic two-component system should be investigated as there are only limited data available on the two-component system. In conclusion, investigating how to overcome target-based resistance mechanism and combination therapies should continue as the obtained results are preliminary, and mechanisms should be further investigated alongside the elucidation of the binding complex within the DNA-gyrase complex.

5.4. Myrtucommulones

S. aureus occupies a special place among the above-mentioned ESKAPE species due to its relatively high virulence and great plasticity it can adapt and survive various conditions (Cheung *et al*., 2021). *S. aureus* strains have evolved resistance mechanisms to almost all antimicrobial drugs used in treatment (Mukherjee *et al*., 2021). The findings of this investigation provide valuable insights into the resistance mechanism of *S. aureus* to acylphloroglucinol derivatives **1** and **2**. All Myr^R had a 5 amino acid deletion within the *saeR* response regulation of the virulence controlling SaeRS, two-component system (Δ*saeR*:Val49_Met53 deletion). Further mutations found in 25% have an additional mutation within the intergenic region, upstream from *sarA* (g.-92C>A) and other 25% have an additional mutation in a *hypothetical gene* (Val48Tyr). Isothermal calorimetry revealed a fitness cost in terms of heat and metabolic rate for all Myr^R. Intermediate cross-resistance of MyrR was observed for vancomycin, daptomycin, several ß-lactam antibiotics and these results were further investigated by RNA-sequencing. Several role-players were identified to contribute to the observed intermediate and cross-resistance to vancomycin and ß-lactams which allowed the Myr^R strains to share characteristics with a VISA phenotype. The mutant characterization revealed a down-regulation of several virulence factors and the transcriptome profile, genotype and phenotype were in line and provided evidence of lysis resistance in the Myr^R strains which lead to the electron imaging confirming an increase in cell wall thickness. Moreover, the transcriptome provided hints towards the biosynthesis and export of wall teichoic acids which could be the main cause of increase in cell wall thickness. In conclusion, the transcriptome analysis revealed and lead the investigation to narrow and to better understand the mechanism of resistance of *S. aureus* strains to the acylphloroglucinol derivatives, **1** and **2**. Based on all

experimental results and literature the resistance mechanism of the *S. aureus* Myr^R is related to the increase of cell wall thickness, most likely by the increased production and exportation of wall teichoic acids, which in turn lead to a VISA-like phenotype.

The identification of the complex network of two-component systems and cross-resistance highlights the importance of studying the transcriptome to better understand the resistance mechanism. The increase in cell wall thickness is a critical mechanism of resistance and provides a valuable target for the development of new therapeutic strategies. Alternative drug delivery systems such as biodegradable nanoparticles that have proven to increase antimicrobial efficacy by protecting molecules from degradation, enhancing the targeting accuracy, and generally increasing cellular uptake (Kumari *et al*., 2014).

In conclusion, the investigation on the mechanism of resistance of *S. aureus* Newman has revealed a complex network of two-component systems and cross-resistance that contribute to intermediate and cross-resistance to vancomycin, daptomycin and ß-lactams. The change of thickness of the cell wall is a critical mechanism for resistance, leading to a VISA-like phenotype. However, further investigation is needed concerning the composition and charge of the bacterial cell wall, especially focusing on the abundance of the wall teichoic acids. Nonetheless, the findings provide valuable insights into the resistance mechanism of *S. aureus* to acylphloroglucinol derivatives for optimization and development of new therapeutic strategies within the compound class.

5.5. Conclusion

In conclusion, three unique natural compounds with different molecular targets on ESKAPE pathogens were used as examples to better understand bacterial resistance and resistance mechanisms by means of culture-based, biochemical-based, molecular-based and bio-informatic-based methodologies. Next-generation sequencing linked chromosomal mutations to the observed resistance phenotype. In combination with transcriptome analysis, additional information provided a broader overview on the metabolic and genomic consequences that resulted in the observed resistance by means of STRING clustering, GO processes, and KEGG assessments. Culture-based, biochemical-based methods and isothermal micro-calorimetry confirmed transcriptome analysis and provided more information of the observed resistant phenotype. We were able to identify the major resistance mechanism for two cell wall and membrane-targeting natural compounds, armeniaspirols and myrtucummulones, and one topoisomerase-inhibiting compound, cystobactamids. Understanding the resistance mechanism provides additional information for the structural related studies for further development. Overcoming bacterial resistance is an unceasing and difficult task. However, with continuous improvement and combination of different technologies, identification of

bacterial resistance mechanisms and the prevention of development could be fast-tracked before the problem of resistance peaks.

5.7. References

Arisetti, N., Fuchs, H.L., Coetzee, J., Orozco, M., Ruppelt, D., Bauer, A., Heimann, D., Kuhnert, E., Bhamidimarri, S.P., Bafna, J.A. and Hinkelmann, B., 2021. Total synthesis and mechanism of action of the antibiotic armeniaspirol A. Chemical Science, 12(48), pp.16023-16034.

Alvaro, D., 2022. Antivioitivv Resistance: advances in Understanding and Drug development. Pharma's Almanac, October 11, 2022. https://www.pharmasalmanac.com/articles/antibiotic-resistance-advances-in-understanding-and-drug-development (Accessed: 28 March 2023).

Chernov, V.M., Chernova, O.A., Mouzykantov, A.A., Lopukhov, L.L. and Aminov, R.I., 2019. Omics of antimicrobials and antimicrobial resistance. Expert opinion on drug discovery, 14(5), pp.455-468.

Cheung, G.Y., Bae, J.S. and Otto, M., 2021. Pathogenicity and virulence of Staphylococcus aureus. Virulence, 12(1), pp.547-569.

Chopra, I., 2002. New developments in tetracycline antibiotics: glycylcyclines and tetracycline efflux pump inhibitors. Drug Resistance Updates, 5(3-4), pp.119-125.

Coates, A.R., Hu, Y., Holt, J. and Yeh, P., 2020. Antibiotic combination therapy against resistant bacterial infections: synergy, rejuvenation and resistance reduction. Expert review of Anti-infective therapy, 18(1), pp.5-15.

Darnowski, M.G., Lanosky, T.D., Paquette, A.R. and Boddy, C.N., 2023. Armeniaspirol analogues disrupt the electrical potential (ΔΨ) of the proton motive force. Bioorganic & Medicinal Chemistry Letters, p.129210.

Feng, X., Zhu, W., Schurig-Briccio, L.A., Lindert, S., Shoen, C., Hitchings, R., Li, J., Wang, Y., Baig, N., Zhou, T., and Kim, B.K., 2015. Antiinfectives targeting enzymes and the proton motive force. Proceedings of the National Academy of Sciences, 112(51), pp.E7073-E7082.

Frieri, M., Kumar, K. and Boutin, A., 2017. Antibiotic resistance. Journal of Infection and Public Health, 10(4), pp.369-378.

Giamarellou, H., 1986. Aminoglycosides plus beta-lactams against Gram-negative organisms: Evaluation of in vitro synergy and chemical interactions. The American journal of medicine, 80(6), pp.126-137.

Gottfried, J., 2005. History Repeating? Avoiding a Return to the Pre-Antibiotic Age. Harvard Law School, Class of 2005, April 17, 2005.

Hennessen, F., Miethke, M., Zaburannyi, N., Loose, M., Lukežič, T., Bernecker, S., Hüttel, S., Jansen, R., Schmiedel, J., Fritzenwanker, M. and Imirzalioglu, C. *et al*., 2020. Amidochelocardin Overcomes Resistance Mechanisms Exerted on Tetracyclines and Natural Chelocardin. Antibiotics (Basel), 9(9), p.619.

Hong, J., Hu, J. and Ke, F. 2016. Experimental induction of bacterial resistance to the antimicrobial peptide tachyplesin I and investigation of the resistance mechanisms. Antimicrobial Agents and Chemotherapy, 60(10), pp.6067-6075.

Khaledi, A., Schniederjans, M., Pohl, S., Rainer, R., Bodenhofer, U., Xia, B., Klawonn, F., Bruchmann, S., Preusse, M., Eckweiler, D. and Dötsch, A. 2016. Transcriptome profiling of antimicrobial resistance in Pseudomonas aeruginosa. Antimicrobial Agents and Chemotherapy, 60(8), pp.4722-4733.

Kokot, M., Anderluh, M., Hrast, M. and Minovski, N. 2022. The structural features of novel bacterial topoisomerase inhibitors that define their activity on topoisomerase IV. Journal of Medicinal Chemistry, 65(9), pp.6431-6440.

Kumari, A., Singla, R., Guliani, A., and Yadav, S.K. 2014. Nanoencapsulation for drug delivery. EXCLI Journal, 13, p.265.

Michalczyk, E., Hommernick, K., Behroz, I., Kulike, M., Pakosz-Stępień, Z., Mazurek, L., Seidel, M., Kunert, M., Santos, K., von Moeller, H. and Loll, B., 2023. Molecular mechanism of topoisomerase poisoning by the peptide antibiotic albicidin. Nature Catalysis, pp.1-16.

Mukherjee, R., Priyadarshini, A., Pandey, R.P., and Raj, V.S. 2021. Antimicrobial resistance in Staphylococcus aureus. In Insights into Drug Resistance in Staphylococcus Aureus (pp. 85-107). Academic Press.

Murugaiyan J., Kumar P.A., Rao G.S., Iskandar K., Hawser S., Hays J.P., Mohsen Y., Adukkadukkam S., Awuah W.A., Jose R.A.M., Sylvia N., Nansubuga E.P., Tilocca B., Roncada P., Roson-Calero N., Moreno-Morales J., Amin R., Kumar B.K., Kumar A., Toufik A-R., Zaw T.N., Akinwotu O.O., Satyaseela M.P., van Dongen M.B.M. 2022. Progress in alternative strategies to combat antimicrobial resistance: focus on antibiotics. Antibiotics, 11(2), 200.

Nayar, A.S., Dougherty, T.J., Reck, F., Thresher, J., Gao, N., Shapiro, A.B. and Ehmann, D.E. 2015. Target-based resistance in Pseudomonas aeruginosa and Escherichia coli to NBTI 5463, a novel bacterial type II topoisomerase inhibitor. Antimicrobial Agents and Chemotherapy, 59(1), pp.331-337.

Poole, K., 2008. Bacterial multidrug efflux pumps serve other functions. Microbe-American Society for Microbiology, 3(4), p.179.

Stepanek, J.J., Lukežič, T., Teichert, I., Petković, H. and Bandow, J.E., 2016. Dual mechanism of action of the atypical tetracycline chelocardin. Biochimica et Biophysica Acta (BBA)-Proteins and Proteomics, 1864(6), pp.645-654.

Valderrama, K., Pradel, E., Firsov, A.M., Drobecq, H., Bauderlique-le Roy, H., Villemagne, B., Antonenko, Y.N. and Hartkoorn, R.C., 2019. Pyrrolomycins are potent natural protonophores. Antimicrobial agents and chemotherapy, 63(10), pp.e01450-19.

Waksman, S.A., Schatz, A., and Reynolds, D.M., 2010. Production of antibiotic substances by actinomycetes. Annals of the New York Academy of Sciences, 1213(1), p.112.

Warr, A.R., Giorgio, R.T. and Waldor, M.K., 2021. Genetic analysis of the role of the conserved inner membrane protein CvpA in enterohemorrhagic Escherichia coli resistance to deoxycholate. Journal of Bacteriology, 203(6), pp.e00661-20.

Material and Methods

Materials

Compounds

Armeniaspirol **A** and **B** were synthesized and purified as described previously by Fu and co-workers (2018). Cystobactamid derivatives were synthesized and provided by the lab of the corresponding author according to Testolin *et al*. (2020). Myrtucommulone compound **1** and **2** were synthesized and provided by Prof. Dr. Johann Jauch and Prof. Dr. Alexander Titz. All compounds were stored under protected from light at −20 °C. Stock solutions were made in dimethyl sulfoxide (DMSO) and were diluted as required. The maximum concentration of DMSO present in bioactivity assays was 2%. Other compounds and reagents used in these projects were all obtained from Sigma Aldrich (Merck KGaA, Darmstadt, Germany) unless stated otherwise.

Buffer and Media

All buffers and media used during these projects were prepared following the manufacturer's instructions and recommendations unless otherwise stated.

Microorganisms and Cell Lines

All bacterial strains were obtained from the Deutsche Sammlung für Mikroorganismen und Zellkulturen (DSMZ), American Type Culture Collection (ATCC), Medizinische Hochschule

Hannover (MHH) or were part of our in-house collection. The *P. aeruginosa* PA14Δ*mexAB* strain was kindly provided by Prof. S. Häußler from the Helmholtz-Zentrum für Infektionsforschung (HZI) and TWINCORE in Hannover. Dr Ruben Hartkoorn from Institut Pasteur de Lille provided the pyrrolomycin-resistant mutant strains of *E. coli*. The CHO-K1 (chinese hamster ovary) cell line was obtained from DSMZ.

Methods

Bacterial Cultivation of *Streptomyces armeniacus* and HPLC-MS Analysis.

For the small-scale fermentations, 50 mL of ARM medium (4.0 g/L glucose, 4.0°g/L yeast extract, 10.0 g/L malt extract, 2.0 g/L CaCO3, pH 7.0) (Merck KGaA, Darmstadt, Germany) in 300 mL Erlenmeyer flasks was inoculated with 10% of 3 days old seed culture of *S. armeniacus* DSM19369 wild-type strain on ISP2 medium (4.0 g/L yeast extract, 4.0 g/L dextrose extract, 10.0 g/L malt extract, 20.0 g/L agar, pH 7.2) (Difco Laboratories, Maryland USA). The cultures were incubated for 14 days at 30 ˚C and 160 rpm on a rotary shaker (Infors Multitron Pro, Switzerland). Fermentation broth was harvested by centrifugation at 8,000 rpm for 10 min. The supernatant products were absorbed by 2% (v/v) XAD16N beads with 24 h stirring followed by extraction with 50 mL methanol. The pelleted cells were resuspended in 50 mL methanol and agitated for 24 h. All the fractions were evaporated to dryness *in vacuo* and then dissolved in 1 mL methanol to produce the crude extracts for analysis. The crude extract was analyzed using HPLC-MS (LC: Ultimate 3000 RS; MS: Bruker Maxis II (4Generation) oq-TOF; Column: ACQUITY UPLC BEH C18 Column, 130Å, 1.7 µm, 2.1 mmX 100 mm). Double distilled water supplemented with 0.1% formic acid and distilled acetonitrile supplemented with 0.1% formic acid were used as eluents. The flow rate of the gradient elution was 0.6 mL/min; and the gradient changed from 5 to 95 % acetonitrile in 18.5 min and maintained at 95% acetonitrile for 2 min.

Biofilm formation

Wild-type and resistant strains were cultivated overnight in MHBII (Mueller Hinton Broth cation adjusted) media. The overnight culture was re-suspended 1:100 and cultivated in fresh MHBII media until early exponential. The cultures were added to a 96-well plate with fresh MHBII media. After which the plates were incubated at 37°C under static conditions. After 48-hours the media was gently removed, and wells were rinsed with PBS (phosphate buffer solution) to remove non-adherent bacteria. The plates were air dried for 20 minutes and wells were then stained with 0.1% crystal violet for 10 minutes. After staining, the wells were washed for four executive times with PBS to remove additional strain and planktonic bacteria. After the plates

were air dried once more, absolute ethanol was added to the wells to reconstitute the remaining crystal violet from the attached bacterial cells. The OD_{540} of wells were recorded. Untreated media served as a negative control while the wild-type strain served as the positive control. The change in OD_{540} of the resistant mutant strains was compared to that the wild-type strain.

Compound Isolation (Armeniaspirol A and B)

For isolation of armeniaspirol derivatives from *S. armeniacus*, the XAD16N resin harvested from 16-liter fermentation broth was lyophilized, followed by extracting with 1.5-liter ethyl acetate. The ethyl acetate was evaporated in vacuo and was dissolved in 4 mL methanol for compounds purification. Armeniaspirol derivatives were purified using Ultimate 3000 RS equipped with XBridge Peptide BEH C18 OBD Prep Column (130Å, 5 µm, 10 mm X 250 mm) with acetonitrile gradient elution in the presence of 0.1% formic acid (flow rate: 7 mL/min; the gradient increased from 5% to 56% in the first 20 min and further increased to 62.5% in the following 32 min).

Cytotoxicity Testing in Chinese Hamster Ovary CHO-K1 Cell Line (ACC-110)

Chinese hamster ovary CHO-K1 cells (ACC-110) were cultured in Ham's F12 medium (Merck KGaA, Darmstadt, Germany) supplemented with 10 % FBS (fetal bovine serum) at 37°C with 5 % CO_2. Cells were seeded at 6 x 10^3 cells per well of 96-well plates (Corning CellBind®) in 180 µL complete medium and were directly treated with compound dissolved in DMSO with a serial dilution. Treated cells were incubated for 5 days and for the assessment of viability in comparison to the internal solvent control, 20 µl of 5 mg/mL MTT (thiazolyl blue tetrazolium bromide) in PBS was added per well and it was further incubated for 2 hours at 37 °C. The medium was then discarded, and cells were washed with PBS (100 µL) before adding 2-propanol/10 N HCl (Hydrocloric acid) (250:1, v/v; 100 µL) in order to dissolve formazan granules. The absorbance at 570 nm was measured using a microplate reader (Infinite 200 PRO, Perkin Elmer) and IC_{50} values were determined by sigmoidal curve fitting.

Electron Microscopy

Overnight cultures of resistant mutant strains and wild-type strains were cultivated at 37°C in MHBII medium with and without the presence of the respective compound. The OD_{600} was adjusted to 0.5 in fresh MHBII with and without the presence of sub-MIC test compound and cultivated for 4 hours. A final concentration of 5% formaldehyde and 2% glutaraldehyde was added to the respective samples and stored in the fridge at 4°C until the Electron Microscopy was performed. The Electron Microscopy was performed by ZEIM (Germany, Braunschweig).

Images were then assessed by ImageJ following user guided instructions (Schneider *et al*., 2012).

Extracellular protease activity

The quantitation of protease activity of the wild-type and resistant mutant strains was assessed by the Thermo Scientific™ Pierce™ Protease Assay Kit. Briefly, the filter sterilized supernatant of overnight cultures from the wild-type and resistant mutant strains and the standard trypsin protease samples were added to the relative wells in the 96-well plate. The plated contained wells with succinylated casein solution as well as duplicate wells that contains the blank control assay buffer. The plate was incubated at room temperature for 20 minutes after which the TNBSA (2,4,6-trinitrobenzene sulfonic acid) Working Solution was added to all wells. The plate was again incubated at room temperature for 20 minutes. After the incubation step, the absorbance of wells was read at 450nm. The calculated the change in absorbance at 450nm (ΔA_{450}) of each well was done by subtracting the A_{450} of the blank from that of the corresponding succinylated casein well. The Δ_{A450} is the absorbance generated by the proteolytic activity of the protease. A standard curve was determined with the use of the standards trypsin protease concentrations and the proteolytic activity of the wild-type and resistant mutant strains were determined by plotting the recorded A_{450} values onto the standard curve.

Isothermal micro-calorimetry

Heat flow measurements were performed using a pre-production instrument calScreener™ microcalorimeter (SymCel, Sweden) with its corresponding 48-well plate (calPlate™). Data was collected with the corresponding calView™ software (Version 1.0.28.0, © 2014 SymCel). For our assays, the machine was set and calibrated at 37 °C. General handling and device manipulation was done according to manufacturer's recommendations.

Relative fitness of resistant mutant strains

Relative fitness cost of mutated strains was manually assessed by cultivation overnight cultures and sub-cultivation of the culture to obtain a starting OD_{600} of 0.01 units. The culture was pipetted into the respective wells of a 96-well plate and placed in a TECAN Pro200 plate reader (Tecan Trading AG, Switzerland) where the OD_{600} measurement were measured every hour for 24 hours. Further, isothermal micro-calorimetry was also used to assess the fitness cost of strains. Heat flow measurements were performed using a pre-production instrument calScreener microcalorimeter (SymCel, Sweden AB).

Genomic DNA Isolation

Total DNA of wild-type and selected resistant mutants and wild-type control samples were subjected to whole-genome sequencing on Illumina MiSeq platform at the Helmholtz Centre for Infection Research (Braunschweig, Germany). Libraries were constructed from isolated genomic DNA according to paired-end protocol and sub-sequently sequenced to a total read length of 2 x 300bp. The raw data was then mapped to a reference sequence. Geneious Prime version 2021.1.1 with default settings was used for reference-guided sequence assembly and data analysis.

STRING clustering, KEGG Pathway Enrichment and GO Functional Enrichment

Further analysis was done on the overlapping list of up-and down-regulated genes of the two derivatives that were assessed by in-house Geneious2String Pipeline (*not published* Haeckl *et al*., 2022). GO Functional Enrichment Analysis, KEGG Pathway Enrichment and STRING clustering were obtained from STRING database (Jensen *et al*., 2009).

Hemolysis

Hemolysis was assessed visually by cultivating a strain suspension with a rough estimate of $5x10^6$ bacterial load onto a blood agar plate. The plate was allowed to dry and then incubated at 37°C and after 24 hours the hemolysis ability of the strain was observed.

Homology

The homology model was completed by loading the complete *E. coli* cryoEM gyrase structure in Molecular Operating Environment MOE software (6RKW at PDB) and protonizing structure at pH 7.4. After the structural preparation was corrected and energy was minimized, protein builder was used to import, align, and export *A. baumannii* gyrase sequence to obtain a template for *A. baumannii* sequences. Further, the sequences were aligned according to best model and protonated in 3D where the energy was minimized, and the selected mutations were marked accordingly. (Work was done by M.Sc. Timo Risch).

Topoisomerase assays

The topoisomerases assay was performed following the protocols from Inspiralis (Norwich, UK). Briefly, a mixture of assay buffer, relaxed pBR322 and water was prepared and dispensed within the sample tubes. Solvents and test compounds were added, and the mixture was gently vortexed. The dilution buffer and enzyme dituons were added to appropriate samples followed by vortexing and incubation. The process was stopped by adding sodium tetraethylborate and chloroform/isoamyl alcohol. Followed by vortexing and phase separation.

The upper phase was then loaded onto a 1% agarose gel and ran for 2 hours. The gel was stained and visualized by a gel documentation system. The decantination assay utilized a different substrate, namely, kinetoplast DNA (kDNA) from Crithidia fasciculate. Analysis of the gel was done by means of ImageJ (Schneider *et al*., 2012). To determine the IC_{50} values, all intensities were normalized (% enzyme activity = SC / (SC + relaxed)). Plotting of these values versus the compound concentration yielded sigmoidal shaped curves, which were fitted using GraphPad Prism version 8.0.0 for Windows, GraphPad Software, San Diego, California USA, www.graphpad.com. All determined IC_{50} values are the averages of three independent experiments.

In vitro resistance development, frequency of resistance, and MIC shift

Overnight cultures were prepared from cryo-preserved cultures and were cultivated in liquid media to achieve a final inoculum of 10^9-10^{10} cfu/mL. The cells were confluently spread over CASO agar (Merck KGaA, Darmstadt, Germany) containing 4x MIC for the respective compound and culture. Plates were incubated at appropriate conditions for 24 hours. The obtained resistant mutants were counted to determine the frequency of resistance (number of resistant colonies divided by the number of viable colonies of the initial inoculum), and the resistant mutants were further assessed by determining their MIC shift compared to the wild-type MIC value.

Membrane Potential Determination

An overnight culture was re-inoculated into fresh media to obtain an OD600 of 0.05 (approximately 2.5 x 10^7 CFU/ml), and bacteria were cultivated until they reached exponential phase. Bacterial cells were harvested by centrifugation (4000 g, 10 min). The bacterial pellets were resuspended in phosphate buffered saline (PBS, pH 7.4) and the OD600 was adjusted to 0.2 units. The bacterial suspension was labelled by addition of the potential-sensitive dye 3,3'- diethyloxacarbocyanine iodide (DiOC2(3)) to a final concentration of 30 µM. The labelling was performed for 20 min at room temperature under protection from direct light. The test compounds and controls were added the respective wells of a 96-well black-walled, clear-bottom microtiter plate. One hundred microliters of the labeled cell suspension were dispensed into each of the wells. The change in membrane potential was assessed by the Baclight assay in 96-well format by monitoring the fluorescence shift of DiOC2(3). Fluorescence was measured with the use of a microplate reader (Tecan Infinite M200 Pro) using an excitation at 488 nm, detect red fluorescence at an emission wavelength of 675 nm and green fluorescence at 525 nm after 30 minutes. All measurements were done in triplicate. The membrane potential, expressed as the red/green fluorescence ratio, was calculated with respect to the DMSO-treated control.

Susceptibility tests

The Minimum inhibitory concentrations (MIC) and minimum bactericidal concentrations (MBC) were determined using the broth microdilution methods recommended by the Clinical and Laboratory Standards Institute (CLSI). In short, *o*vernight cultures were prepared from cryopreserved cultures and were diluted to achieve a final inoculum of 10^6 cfu/mL. Serial dilutions of compounds were prepared in sterile 96-well plates in the respective test medium. The cell suspension was added, and microorganisms were grown for 24 hours at or 37 °C. The growth inhibition was assessed visually. Suseptibility with the addition was conducted as above with the addition of within the medium with a final concentration of 20 µg/mL PMBN and 3 µg/mL for PAβN. In addition, MIC done for daptomycin was done with cation adjusted MHB II media to a final concentration of 50 mg/L. MBC were determined by sub-culturing 10 µL volumes from non-turbid wells, spot-inoculating onto CASO plates followed by incubation for 24 hours. The MBC was determined as the lowest concentration of antibacterial with no resultant growth in the sub-culture. Each strain was assessed in triplicate. The MIC shift was determined by dividing the MIC for the resistant mutant to MIC value of the wild-type strain. A MIC shift of ≥4 was considered relevant.

Synergy

Synergy of colistin was assessed against cystobactamid derivatives by means of the checkerboard assay in 96-well plate format as described in Almutairi (2022). Colistin and the tested derivatives were diluted using the two-dilution method ranging from of 0.006X MIC to 4XMIC, repectively. After dilution, the respective bacterial strain was added (approximately $5x10^5$ CFU/ml). The 96-well plate was inculated at appropriate temperature for 24 hours and assessed visually. The fractional inhibitory concentration (FIC) was determined by dividing each drug's MIC when used in combination by each drug's MIC when used alone. FIC of ≤0.5 was synergism; FIC between 0.5 and 1 was considered to have partial synergism; FIC of ≥1 but <4 was indicated as indifference; FIC of ≥4 is indicated as antagonism The experiment was performed in duplicate for each combination.

Mutation Prevention Concentration

Overnight cultures were prepared from cryopreserved cultures and were diluted to achieve a final inoculum of 1 x 10^6 cfu/mL. The cell culture was added to Mueller Hinton Agar (MHA) (Merck KGaA, Darmstadt, Germany) plates containing 4 x MIC to 8 x MIC of respective cultures. The plates were incubated for 16-24 hours at 30 °C. Colonies were counted and the MPC was determined. The MPC was defined as the lowest concentration of test compound that resulted in a 99.9 % reduction in the colony count.

Reversibility of Resistant Phenotype

Selected resistant phenotype strains were streaked out on non-selective agar and incubated at appropriate temperature for 24 hours for ten consecutive days. MIC determination was done on day 3 and 10.

RNA Sampling and Total RNA Isolation

Overnight cultures were collected at pre-determined time points and mixed with RNA protect reagent (Qiagen) (1:2). The samples were vortexed and incubated at room temperature followed by centrifugation at 5000 g for 10 minutes. The pellet was stored at -80 °C until RNA purification. For RNA isolation, the pellet was thawed and resuspended in TE buffer (100mM Tris, 1mM EDTA, pH 8.0) containing 15 mg/mL lysozyme and 20 µL proteinase K. The suspension was vortexed and incubated for two hours at 30°C with 1000rpm shaking. This was followed by a modified method of RNA isolation using the RNeasy mini-Kit (Qiagen). In short, lysis regent was added, and the suspension was vortexed and incubated for 5 minutes at 30 °C and 1000 rpm. Phase separation was done by the addition of chloroform. After phase separation the RNA was eluted with ethanol and washed with the provided wash buffer diluted with isopropanol. DNase digestion followed by using the RNase-free DNase set (Qiagen). Briefly, DNase stock solution was added to the washed solution and incubated at 30 °C for 30 minutes. The RNA was then washed consecutively for three times. The RNA was dried and eluted with RNase free water. The secondary RNA structure was dissolved by inculation the RNA at 70 °C for 2 min. RNA concentration was quality determination using the Nanodrop. The final quality determination was done by determining the RNA Integrity number (RIN) with use of the Agilent 2100 Bioanalyzer, and the respective Agilent RNA 6000 Nano reagents and Agilent 2100 Expert Software version B.02.11.SI811.

RNA Sequencing and Differential Gene Expression Analysis

The samples that passed all quality criteria were sent to a Eurofins, a commercial provider of next-generation sequencing. RNA-sequencing was performed by Eurofins by their commercial set-up. In short, a library was prepared where the mRNA was fragmented, and cDNA was synthesized. Illumina sequencing was performed with single read sequencing (2 x 150 bp) to achieve at least 10 M reads per sample. The reads from were further processed by Geneious Prime 2022.0.1 software package (Biomatters). The raw read files were first imported, followed by mapping against the relevent reference genome. Following this step, the expression levels (RPKM and TPM values) for the mapped genes were calculated and compared using the DEseq2 plugin. Venn diaGrams were drawn using “BioVenn” (Hulsen *et al*., 2008).

Triton X-100-induced autolytic assay

Wild-type and resistant strains were cultivated in antibiotic-free MHBII media, centrifuged, washed, and resuspended in phosphate saline buffer (PBS) containing 0.1% Triton X-100 to an OD_{600} of 0.8. Samples were measured spectrophotometrically hourly for 24 hours. Results were expressed graphically as percent OD_{600} remaining versus time zero.